UNIVERSITY OF THESSALY
SCHOOL OF ENGINEERING
DEPARTMENT OF MECHANICAL ENGINEERING

SIMULATION AND ANALYSIS OF THREE SOLAR ASSISTED GROUND SOURCE HEAT PUMP SYSTEMS

by

GEORGIOS-FILIPPOS ASPETAKIS

Submitted in partial fulfillment of the requirements for the degree of Diploma in Mechanical Engineering at the University of Thessaly

Volos, 2020

UNIVERSITY OF THESSALY
SCHOOL OF ENGINEERING
DEPARTMENT OF MECHANICAL ENGINEERING

SIMULATION AND ANALYSIS OF THREE SOLAR ASSISTED GROUND SOURCE HEAT PUMP SYSTEMS

by

GEORGIOS-FILIPPOS ASPETAKIS

Submitted in partial fulfillment of the requirements for the degree of Diploma in Mechanical Engineering at the University of Thessaly

Volos, 2020

Approved by the Committee on Final Examination:

Advisor	Dr. Nikolaos Andritsos, Professor, Department of Mechanical Engineering, University of Thessaly
Member	Dr. Vasilis Bontozoglou, Professor, Department of Mechanical Engineering, University of Thessaly
Member	Dr. Georgios Charalampous, Assistant Professor, Department of Mechanical Engineering, University of Thessaly

Date Approved:

Acknowledgements

I would like to thank Nikolaos Andritsos for his guidance, Sokratis Markos for providing information about the buildings investigated and Alexandra Elbakyan for assisting me with research.

SIMULATION AND ANALYSIS OF THREE SOLAR ASSISTED GROUND SOURCE HEAT PUMP SYSTEMS

GEORGIOS-FILIPPOS ASPETAKIS

Department of Mechanical Engineering, University of Thessaly

Supervisor: Dr. Nikolaos Andritsos

Professor

Abstract

The sector of buildings is one of the largest energy consumers in Europe and has great potential for energy savings. Studies have shown that saving energy and integrating renewable energy sources to the heating and cooling of buildings is the most cost-effective method for reducing greenhouse gas emissions. In Greece, solar energy fits that role perfectly, given the high solar radiation potential of the region. Combining solar power with other renewable energy sources such as geothermal energy, further improves savings. In this study, three Solar Assisted Ground Source Heat Pump configurations comprised of Flat-Plate, Photovoltaic and hybrid Photovoltaic/Thermal collectors are designed as upgrades to the existing GSHP system installed in a university building complex in Volos, Greece. These systems were simulated with the dynamic system simulation tool TRNSYS and afterwards analyzed energetically as well as economically, to find the most suitable alternative that is cost- and environment- friendly. Results of the analysis showed that the PV system is the optimal solution due to its substantial energy savings and low cost compared to the PV/T system. The FPC configuration did not reduce energy consumption sufficiently.

Key words: Solar Assisted Ground Source Heat Pump (SAGSHP), energy saving, TRNSYS simulation, greenhouse gas emissions reduction, Flat-Plate Collector, Photovoltaics, Photovoltaic/Thermal Collector

ΠΡΟΣΟΜΟΙΩΣΗ ΚΑΙ ΑΝΑΛΥΣΗ ΤΡΙΩΝ ΣΥΣΤΗΜΑΤΩΝ ΓΕΩΘΕΡΜΙΚΩΝ ΑΝΤΛΙΩΝ ΜΕ ΗΛΙΑΚΗ ΥΠΟΒΟΗΘΗΣΗ

ΓΕΩΡΓΙΟΣ-ΦΙΛΙΠΠΟΣ ΑΣΠΕΤΑΚΗΣ

Τμήμα Μηχανολόγων Μηχανικών, Πανεπιστήμιο Θεσσαλίας, 2020

Επιβλέπων Καθηγητής: Δρ. Νικόλαος Ανδρίτσος,

Καθηγητής

Περίληψη

Ο κτιριακός τομέας αποτελεί έναν από τους μεγαλύτερους καταναλωτές ενέργειας στην Ευρώπη και διαθέτει μεγάλες δυνατότητες εξοικονόμησης ενέργειας. Έρευνες έχουν δείξει ότι η εξοικονόμηση ενέργειας και η ενσωμάτωση ανανεώσιμων πηγών ενέργειας στα συστήματα θέρμανσης και ψύξης των κτιρίων αποτελούν την πιο αποδοτική μέθοδο για τη μείωση των εκπομπών του θερμοκηπίου. Στην Ελλάδα η ηλιακή ενέργεια αποτελεί την ιδανική λύση για αυτό, λόγω του υψηλού ηλιακού δυναμικού της χώρας. Ο συνδυασμός της ηλιακής ενέργειας με άλλες Α.Π.Ε, όπως η γεωθερμία, ενισχύει ακόμα περισσότερο την εξοικονόμηση ενέργειας. Σε αυτήν την μελέτη, σχεδιάζονται τρία διαφορετικά συστήματα γεωθερμικών αντλιών με ηλιακή υποβοήθηση αποτελούμενα από ηλιακούς θερμικούς συλλέκτες, φωτοβολταϊκά και υβριδικούς συλλέκτες ως αναβαθμίσεις του εξοπλισμού θέρμανσης/ψύξης κτιριακών εγκαταστάσεων του Πανεπιστημίου στο Βόλο. Τα συστήματα προσομοιώθηκαν στο περιβάλλον δυναμικής προσομοίωσης TRNSYS και έπειτα αναλύθηκαν ως προς την ενεργειακή και οικονομική τους απόδοση, για να βρεθεί η πιο προσιτή και φιλική προς το περιβάλλον εναλλακτική. Τα αποτελέσματα έδειξαν ότι το σύστημα με φωτοβολταϊκά αποτελεί τη βέλτιστη λύση διότι εξοικονομεί σημαντικά ποσά ενέργειας με χαμηλό κόστος συγκριτικά με το σύστημα των υβριδικών συλλεκτών. Οι θερμικοί συλλέκτες δεν κατάφεραν να μειώσουν την κατανάλωση ενέργειας του συστήματος επαρκώς.

Λέξεις-κλειδιά: γεωθερμική αντλία θερμότητας με ηλιακή υποβοήθηση, εξοικονόμηση ενέργειας, προσομοίωση TRNSYS, μείωση εκπομπών θερμοκηπίου, θερμικοί ηλιακοί συλλέκτες, φωτοβολταϊκά, υβριδικός φωτοβολταϊκός-θερμικός συλλέκτης

Contents

LIST OF FIGURES

1. INTRODUCTION

1.1 Motivation

The impending climate crisis, environmental pollution and energy shortage globally have motivated researchers to explore alternative technologies and the implementation of renewable energies to convert energy efficiently. The concept of heating and cooling buildings with renewable energy has increasingly gained ground the past years. With a consumption of 458 Mtoe (Million Tonnes of Oil Equivalent) in 2016, buildings account for 41% of the final energy consumption, 60% of the electricity consumption, in the European Union. Two thirds of this consumption are for residential buildings [1]. Buildings are therefore one of the largest energy consumers in Europe and by extension have the most cost-effective potential for energy savings. Studies have shown that saving energy is the most cost-effective method for reducing greenhouse gas (GHG) emissions [2].

The Energy Performance of Buildings Directive (EPBD), of the European Union, requires that all new buildings will have nearly zero-energy demand by the end of 2020, indicating that renewable energy sources (RES) would provide the majority of the energy that these buildings require. By the end of 2018 RES in buildings for heating and cooling was limited to 19.7% [3]. Due to this, there is a need of promoting energy efficiency in buildings and green technologies with the goal of reducing energy consumption and minimizing CO_2 emissions.

Heat pump systems (HPs) is a well-established technology that provides heating and cooling to buildings. Ground source heat pump systems (GSHPs) are a type of HPs that employ geothermal energy as their energy source. GSHPs possess a high coefficient of performance (COP) and low costs of operation, utilizing a renewable energy source with high heating and cooling efficiency. GSHPs have lower CO_2 emissions and lower electricity consumption than conventional systems. Besides that, they do not produce environmental air pollutants like nitrogen or sulfur oxides. Integrating solar energy with GSHPs is known as solar assisted ground source heat pump system (SAGSHPs). SAGSHP combines two renewable energy sources, solar and geothermal energy, in order to reduce the consumption of primary energy and CO_2 emissions which leads to a reduction of fossil fuel usage. Solar energy either increases the mixture temperature when entering the evaporator, causing the decrease of the

temperature leap performed by the heat pump or generates power that is directly provided to the GSHP [4].

1.2 Climate crisis

Climate crisis is perhaps one of the greatest challenges that humans need to address collectively. It has already negatively affected the planet, ranging from higher temperatures to sea level rise due to the melting of polar ice and more frequent storms and floodings, of greater magnitude. These changes will in turn bring about grave consequences to the integrity of ecosystems, water resources, public health, food distribution, industry, farming, transport and infrastructure. Its most severe impacts may still be avoided if efforts are made to transform current energy systems [5].

Greenhouse gases cause the greenhouse effect, where the surface temperature of a planet is increased by radiation that cannot be emitted back to deep space. Naturally occurring GHGs include water vapour, carbon dioxide (CO_2), methane (CH_4), nitrous oxide (N_2O) and ozone (O_3). In the last years, hydrofluorocarbons (HFC), perfluorocarbons (PFC), sulphur hexafluoride (SF_6), nitrogen fluoride (NF_3) concentrations have risen steeply. These gases are man-made and mostly used in industry. Other naturally occurring gases, which do not contribute directly to the greenhouse effect, but are either toxic or harmful to the environment, are carbon monoxide (CO), oxides of nitrogen (NOx), sulphur dioxide (SO_2) and non-methane volatile organic compounds [6]. GHG emissions associated with the production of energy are a major cause of climate change. The IPCC Fourth Assessment Report came to the conclusion that "Most of the observed increase in global average temperature since the mid-20th century is *very likely* due to the observed increase in anthropogenic greenhouse gas concentrations." The impact of all human activities on the climate is severe and requires the involvement of the entire international community in order to address the issue [7].

For the development of nations to be sustainable, energy production needs to have low to no environmental impacts. To be environmentally friendly, energy must be provided with minimal environmental damage and low emissions. Fossil fuel combustion accounts for 85% of the primary energy currently produced globally and 56.6% of all GHG emissions. In order to attain an equilibrium temperature increase of only up to 2.4°C, GHG concentrations would need to be stabilized around 490 ppm CO_2 in the atmosphere [7]. Lowering GHG emissions from the energy system is possible through various methods, while still providing desired energy supply. RES are very promising in displacing GHG emissions from the consumption of fossil fuels and thereby to tackle climate change. The full range of energy demands worldwide can be covered by renewable energy sources. RES are able to generate heat, electricity and mechanical energy, as well as fuels that can cover diverse energy requirements. Renewable energy is any form of energy that is replenished by naturally at a rate that equals or exceeds its rate of use. CO_2 emissions produced from RE are negligible or even zero.

To combat climate change, the existing model of development must change towards a sustainable, green economy of low or zero emissions with the help of technology. To lessen the effects of climate change, responses from governments, economic sectors and society in general in unison is required. The cost of limiting emissions and adapting to climate change might seem daunting, but is really low in comparison to the later cost caused by inactivity.

The European Council of March 2007, noted that, to achieve the goal of, stabilizing the emissions of GHG in the atmosphere to levels that prevent dangerous interference to the climate system, the total yearly median rise of temperature on the surface of the planet must not exceed 2 °C compared to the preindustrial levels. To achieve that, it is necessary to reduce the global GHG emissions until 2050 to a percentage of 50 % of the 1990 levels. The GHG emissions need to continue to fall even after 2020 as part of the European Community effort to participate in the global struggle of reducing emissions

The European Council has set up a thorough approach for the climate and energy policy, tackling climate change and increasing the energy security of the EU and converting into energy efficient low carbon emission economy.

The demands adopted by the state members are:

- Reduction of GHG emissions by at least 20% of the 1990 levels
- 20% of the consumption of the EU must come from RES
- Reduction by 20% in the consumption of primary energy by increasing energy efficiency.

These demands are known as 20-20-20 targets.

As of April 2020, despite reports of localized improvements in air quality and the reduction of primary energy consumption that the coronavirus lockdown caused, global CO_2 levels have increased alarmingly. The National Oceanic and Atmospheric Association (NOAA) released data showing that carbon dioxide levels have risen sharply. The monthly average concentrations, recorded at the Mauna Loa Observatory in Hawaii, were 416 parts per million (ppm) this year compared to 413.33ppm in April 2019. It's the highest concentration since records began in 1958 [8].

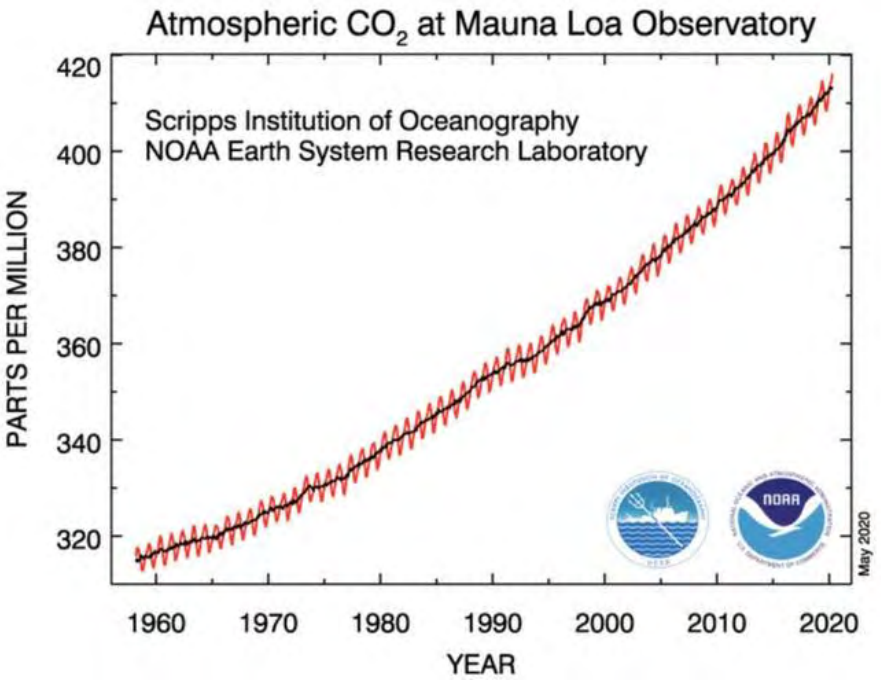

Fig. 1.1: Concentration of CO_2 in atmosphere (ppm) [8]

1.3 Energy mix of the European Union

Renewable energy is defined as the form of energy that does not get depleted due to its natural ability to renew itself. All RES originate, mostly from the suns radiation or from the heat generated in the core and mantle of the planet. RES consist of solar, geothermal, wind, hydro, wave, biomass, and even thermal waste. Renewable energy displaces fossil fuels in four different sectors: production of electricity, heating/cooling, engine fuels, and off-grid energy demand. Geographically, renewable energy sources can be found globally, whereas fossil fuels, which are clustered in limited locations. Utilization of RES and the promotion of energy saving overall is results in countering effectively the climate crisis and ensuring energy security in the region. Additionally environmental pollution such as air pollution is reduced and thereby improves the health of the general population, by reducing premature deaths caused by pollution and lowering related health impacts [9, 10].

In 2018, the available sources that covered the EUs energy demands, included of mostly the following: Petroleum products (crude oil) (36 %), natural gas (21 %), solid fossil fuels (15 %), renewable energy (15 %) and nuclear energy (13 %) [3].

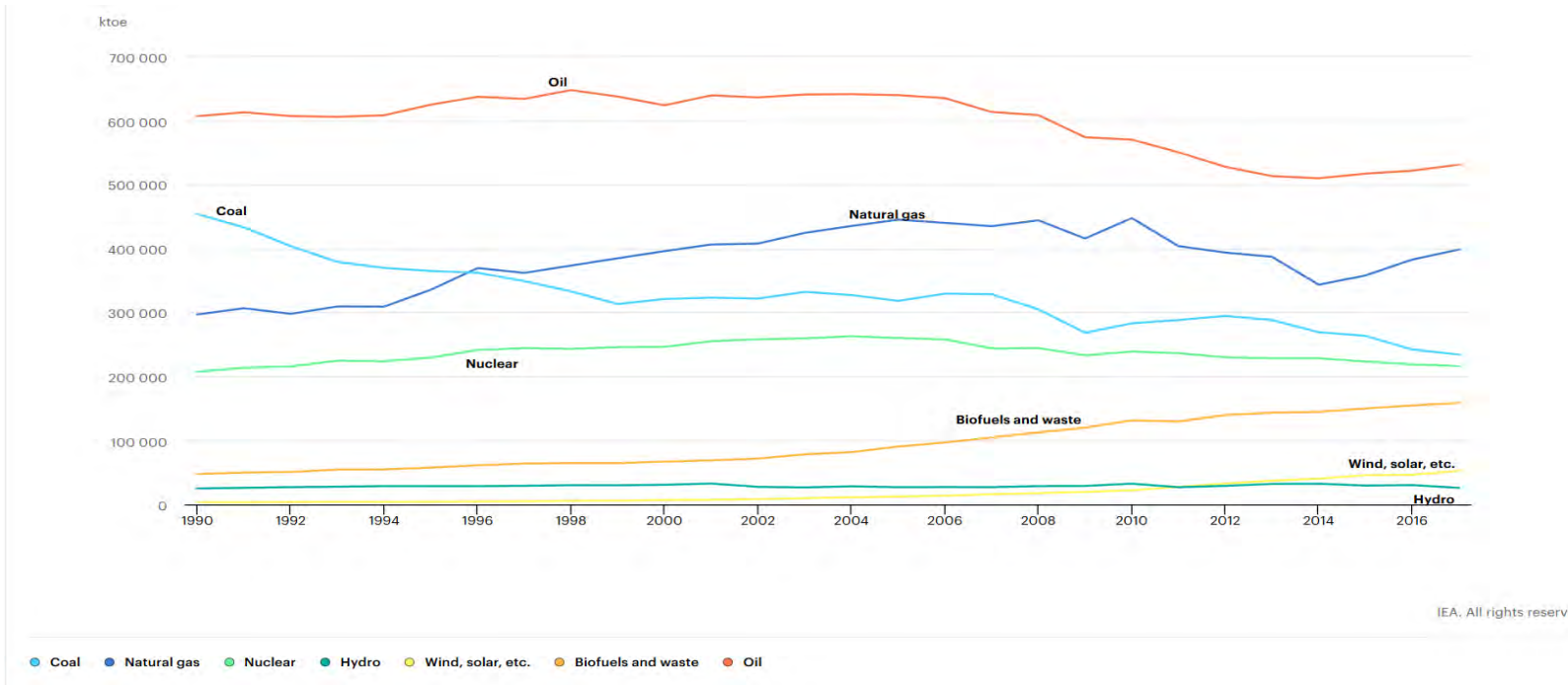

Fig. 1.2: Total primary energy supply by sector, for the EU [11]

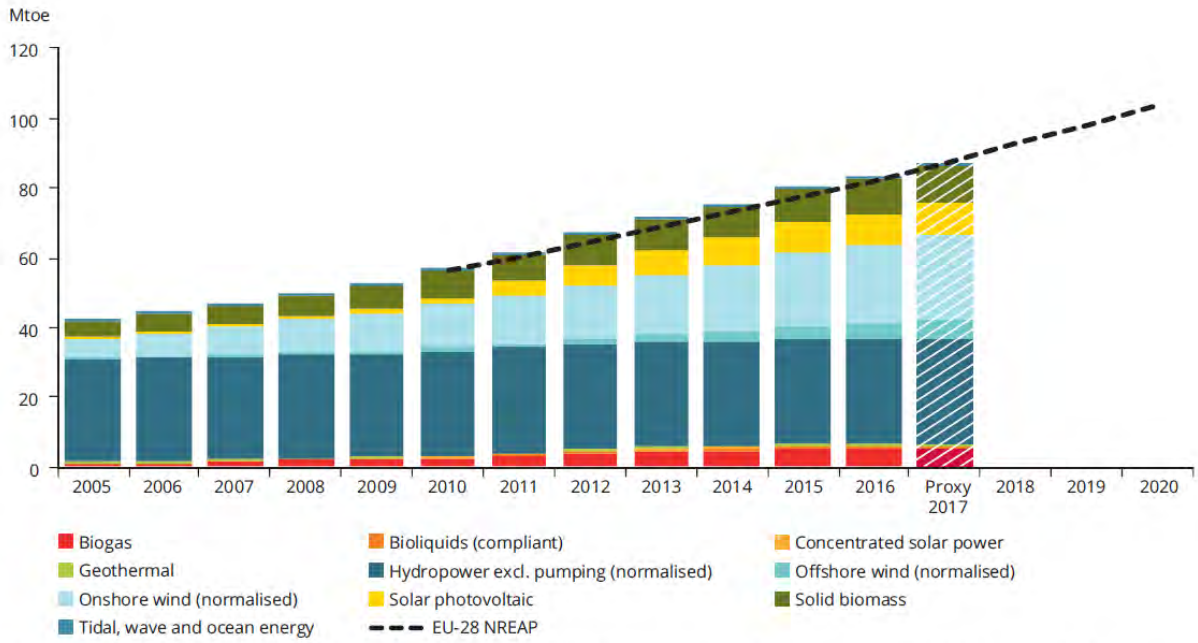

Notes: This figure shows the actual final RES-E consumption for 2005-2016, approximated estimates for 2017 and the expected realisations in the energy efficiency scenario of the NREAPs for 2018-2020. Wind power and hydropower are normalised. The consumption of RES accounts for only biofuels complying with the RED sustainability criteria.

Sources: EEA; Eurostat, 2018d; NREAP reports.

Fig. 1.3: Detailed shares of RES, EU, 2005-2017, in Mtoe [12]

According to the European environment agency (EEA), hydropower supplied the most electricity generated by RES (RES-E) in the EU in 2017, covering 35 % of total RES-E production (1 % less than the previous year). The coverage of hydropower dropped significantly from 70 % in 2005, because solar and wind energy utilization has progressed immensely over this period. Onshore wind covered 28 % of RES-E, more than double the coverage of 13 % in 2005. Solid biofuels remained stable in relative terms with 12 % in 2017 and 11 % in 2005. Solar energy made a huge leap from 0.3 % in 2005 to 11 % of RES-E. The remaining renewable sources rose from 4 % to 14 % of RES-E [12]. As for heating and cooling oriented renewable energy sources (RES-HC), the final energy consumption of solid biomass represented 83 % of total RES-HC. Heat pumps providing heating and cooling utilizing renewable energy provided 10 % of that amount. Renewable heat production from all other sources (geothermal, solar thermal, biogas) sum up for the remaining 7 %.

1.4 Energy mix of Greece

The energy mix of Greece varies from the rest of Europe, given its much higher consumption of solid and liquid fossil fuels, while natural gas has lower usage while nuclear energy production is absent. The share of RES has been increasing steadily over the last decade. The values of energy imports and energy consumption indicators, after 2009, are lower in comparison to previous years, displaying the effects of the economic collapse on the sector of energy in general. Final consumption of energy in Greece during 2018 was 16.6 Mtoe. The primary production of renewable energy for 2018 was 3 Mtoe. The leading RES for electricity generation was wind energy, accounting for 10% of total electricity production in 2018. Hydropower (9%) is next, solar power (6%) and the rest (geothermal, biofuels, waste, tidal energy) accounted for 1%.

Based on the 2018 data, RES-E was 1.33 Mtoe, 26% of the total electricity consumption in Greece (European median was 32%). The relative increase of RES-E from 2004 to 2018 is close to 220%. This is attributed largely to the rapid development of wind and solar power. RES-HC in Greece accounted for 30.2% in 2018, with the European average covering 19.7%. For RES in transport fuel (RES-T) consumption in Greece the percentage was 3.8% in 2018, with the EU-28 average being 8% [3, 9]. Energy consumption of buildings increased by 0.7% annually up to 2008, but then started declining by -0.6% annually until 2016. Following the economic collapse, the national total energy consumption decreased by 0.3% annually since 2010.

The average annual consumption per square meter for all types of buildings is around 200 kWh/m^2 in the European Union. Buildings that offer services consume on average 60%

more energy than their residential counterpart (300 kWh/m^2 as opposed to 170 kWh/m^2) [1]. To promote RES utilization in buildings, through a common framework, the European Parliament and Commission approved the Renewable Energy Directive 2009/28/EC. All existing buildings undergoing renovation in the EU must be transformed into a nearly zero-energy building (nZEB). This directive serves as a great prospect for the promotion of utilization of heat pumps for heating/cooling of new and existing buildings. Heat pumps use heat from the environment to attain the desired temperature level in the designated area. Ground-source heat pumps and air-to-water heat pumps can be installed to attain nZEB requirements and defossilization targets [13].

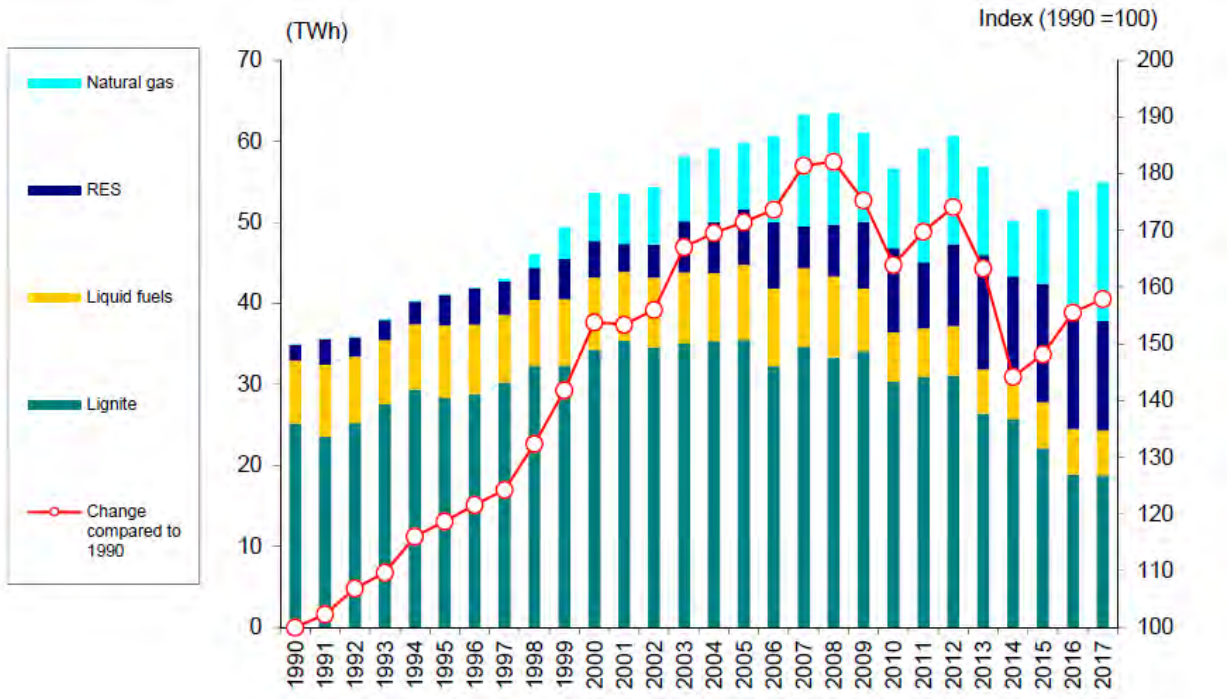

Fig. 1.4: Electricity production by energy type for Greece, 1990-2017,in TWh [6].

2. THEORETICAL BACKGROUND

2.1 Heat pumps

2.1.1 General

A heat pump (HP) is a thermal device that is based on a reverse Carnot thermodynamic cycle, which produces a thermal effect by consuming drive energy. The HP moves (pumps) heat from a source with low temperature to a another destination with a high temperature, consuming power, just like a water pump would transfer water from a low level to higher one against gravity, consuming energy. This operation can be utilized for various ends like water heating, cooling (and in turn space heating/cooling). In most HPs, the drive energy is electricity consumed by the compressor. This can be performed for either heating or cooling by reversing the flow of the working fluid.

Just like a refrigeration installation, the basic components of a heat pump are (Fig. 3.1):

- The compressor, which provides the energy needed for cooling or heating,
- The condenser that releases heat from the working fluid
- The evaporator that absorbs heat
- Pressure-lowering devices (expansion valves)
- A 4-way valve, that switches the HP mode from cooling to heating and reversely.

The process for cooling by a Heat pump is as follows:

Cooling mode

1. The working fluid enters the evaporator through an expansion valve. The valve lowers the pressure of the working fluid, which being in ambient temperature and atmospheric pressure, evaporates, absorbing heat from the area that has cooling demands.
2. Exiting the evaporator the working fluid has become a low temperature and pressure gas. It then enters the compressor. With compression pressure and temperature rise significantly.
3. The compressed hot working fluid reaches the condenser where, by transferring heat to the surrounding environment, it cools. At this stage the compressed gas gets liquefied.

4. In the end the working fluid reaches the expansion valve which restores the pressure back to atmospheric level, so that it gets evaporated again in the next stage.

After that the cycle is repeated continuously.

Heating mode

The same stages are followed in heating mode by the working fluid, but in this case the evaporator acts as a condenser transferring heat to the designated area, while the condenser acts like an evaporator that absorbs heat from the heat source. The switch is possible thanks to a 4-way valve that reverses the flow of the working fluid.

The process is described below:

1. The working fluid exits the compressor in high temperature, pressure and flows through the condenser, where it gets cool by releasing heat to the heating location.
2. Coming from the condenser the working fluid, in dual phase and high pressure, enters the expansion valve to reduce its pressure.
3. Now as low pressure and temperature liquid it flows through the evaporator, where heat from the heat source is absorbed
4. Finally it exits in low pressure gas form and heads to the compressor to repeat the cycle again.

In thermodynamic terms the process is described below and shown in Fig. 2.3:
1_2: isentropic compression in the compressor, which leads to increased pressure and temperature
2_2': isobar cooling in the condenser
2'_3: isotherm-isobar condensation in the condenser
3_3': isobar subcooling in the subcooler
3'_4: isenthalpic lamination in expansion valve
4_1: isothermisobar evaporation in the evaporator

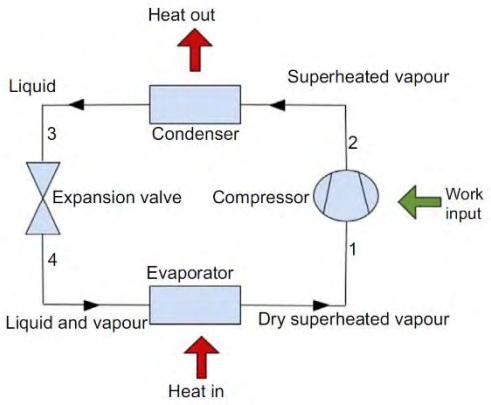

Fig. 2.1: Components of HPs [14]

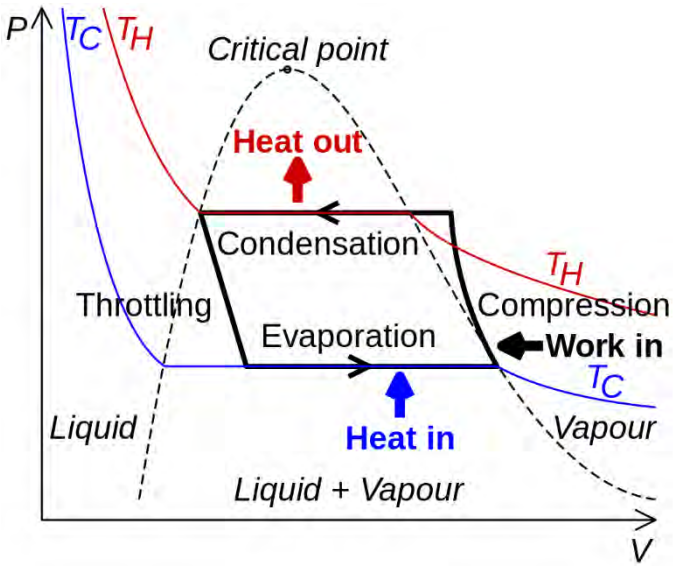

Fig. 2.2: P-V diagram of a HP[14]

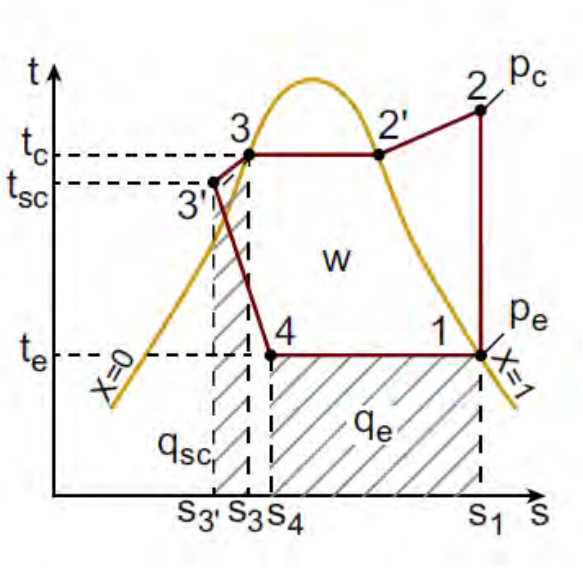

Fig. 2.3: T-s diagram of a HP [10]

2.1.2 Categorization of Heat Pumps

HPs are based on what heat exchanger they operate. These are:

1. Air-to-Air heat pumps. Both ends of the heat exchangers of the working fluid face air. In heating mode, the heat source is the air of the environment and heat is transferred to the air inside the building. In cooling mode the opposite takes place. They can be installed either as big central units that provide heating/cooling to a whole building or small for individual rooms (split type). The heat demand increases and the capacity of the HP declines as the external air temperature drops, caused by the reduction of the device efficiency. To counter this, electrical resistances can be additionally installed, acting as an auxiliary heat source. Consumption is unfortunately considerably increased, when those are in operation.

2. Air-to-water heat pumps. In these devices the medium through which heat is transferred from/to building to/from the working fluid is water. The most common installation of this type is a pipe network containing hot/chilled water that is connected to fan coil units in every room. Through the elimination of air ducts, it is significantly quieter. The other side is still connected to the air of the environment. It is mostly installed on the exterior of the building.

3. Water-to-Air heat pumps. The heat source/sink in this case is a body of water like groundwater, surface water (from rivers, lakes or seas) or discharged hot water (domestic, heat waste, cooling tower water).

4. Water-to-Water heat pumps, a combination of the above where both exterior sides of the heat exchangers face water. One side is the heat/cool source and the other is the water piping connected to terminal units throughout the building. These HPs report higher COP than others in general. A number of water-to-water HPs can be combined together to create a central unit to serve several smaller air-handling outlets. This results in a more flexible system that offers better control and requires less maintenance.

5. Ground-to-Air (or water) heat pumps, called geothermal or ground source (GSHP), where the rejection/absorption of heat takes place in the ground through a ground heat exchanger (GHX). The GHX can have various shapes and sizes, using different refrigerants based on the circumstances. Antifreeze-to-water HPs are used in closed loop ground source installations.

In Greece, widespread use of Air-to-Air and Air-to-Water heat pumps, is attributed to their lower installation and maintenance cost as well as the lack of groundwater reservoirs in urban areas [15].

Heat pumps can also be categorized to:
• Compact or Monobloc, where all components are housed in the same compartment
• Split where the condenser or evaporator are located elsewhere of the rest of the system.
• Heat pumps with electrically driven compressors.
• Heat pumps with thermally driven compressors In this case exhaust gases can pass through heat exchangers, rejecting heat into the building and therefore increasing the efficiency of the system.
• High temperature HPs (60 to 80 ℃).
• Low temperature HPs (40 to 60 ℃).

High temperature HPs are compatible with classic heat systems, while low temperature HPs are mostly used with fan coil and/or radiant floor systems. Inverter HPs, with variable compressor speed in contrast to on-off HPs that have only one available. The inverter types change speed based on the load, resulting in higher efficiency and lower consumption.

2.1.3 Performance and Emissions of a HP

The most important characteristic of a Heat Pump is called the *coefficient of performance* (COP) and is defined as the fraction of useful thermal energy Q_H produced to the electrical energy consumed W_{in} (shown in Fig. 2.5):

$$COP = \frac{Q_H}{W_{in}}$$

COP values for GHPs are in the range of 3 and 5, meaning that the heat delivered to the load space is 3 to 5 times the amount of the energy consumed by the heat pump. The latest technology gas burners, on the other hand, convert up to 95% of the chemical energy that is available in the gas to useable heat and therefore have an equivalent COP of about 0.95. Seasonal coefficient of performance (SCOP) or average COP over a heating (cooling) season, often indicated as the SPF or annual efficiency, is obtained if the above equation is used in summation of both usable energy and consumed energy during a season (year). In the heating mode, the COP of HP is defined as follows:

$$COP_{hp} = \frac{Q_{hp}}{P_{el}}$$

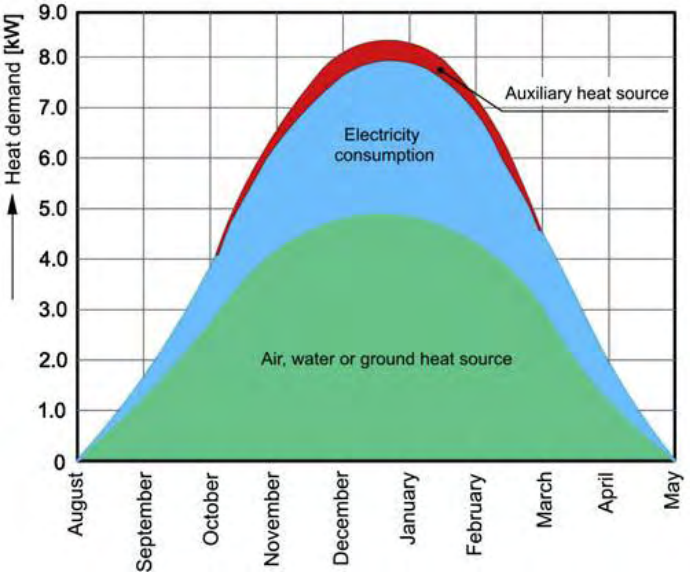

Fig. 2.4: Example of HP energy sources for the heating season [10]

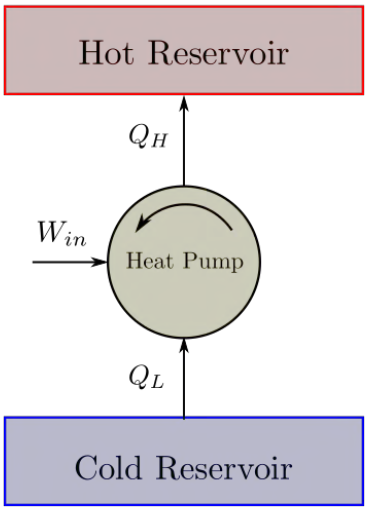

Fig. 2.5: Simplified view of a HP [16]

where Q_{hp} is the thermal power of heat pump, in W and P_{el} is the electrical energy consumed by the heat pumps compressor, in W. The COP is never stable, but relies on the working temperatures of the source and the area to be heated. Manufacturers provide documentation with detailed information for various temperatures and a standardized value (Eurovent standard) where the temperatures are specifically, 20°C for internal and 7°C for external air. In cooling mode, a HP functions like a central Air Conditioning unit. The

energy efficiency ratio (EER) is comparable to the COP but is designated only for cooling performance. The EER_{HP}, in $\frac{BTU}{Wh}$, is defined as:

$$EER_{hp} = \frac{Q_e}{P_{el}}$$

where $Q_e$is the cooling power of HP, in British Thermal Unit per hour $\frac{BTU}{h}$ and P_{el} is the compressor power, in W. The E.E.R. coefficient is also measured in Eurovent standard, with internal air temperature being 27℃ and external 35℃. The seasonal energy efficiency ratio S.E.E.R. is defined as the fraction of the energy transferred in cooling period to the energy spent by the compressor during the same period. The COP of an HP in cooling mode when the EER is known is described as follows:

$$COP_{hp} = \frac{EER_{HP}}{3.412}$$

where value 3.412 is the transformation factor from Watt in Btu/h.
The sizing factor (SF) of the HP is defined as the ratio of the HP capacity Q_{hp} to the maximum heating demand Q_{max} as

$$SF = \frac{Q_{hp}}{Q_{max}}$$

The SF can be optimized depending on the energy demands, source temperature and the schedule followed. With HP electricity consumption being the most important source for GHG emissions [17], other potential contributors like the total life cycle of the device,drilling, refrigerant are neglected. Applying an emission factor g, in kg CO_2/kWh, the annual greenhouse gas emissions, in kg CO_2, for a heat pump can be obtained as:

$$C_{HP} = gE_{el}$$

The emission factor differs from region to region. Although carbon dioxide (CO_2) is considered the key GHG, several other composites contribute in different intensities to the greenhouse effect. Their total effect is usually normalized to the specific effect of CO_2, and all emissions are expressed in CO_2 equivalents.

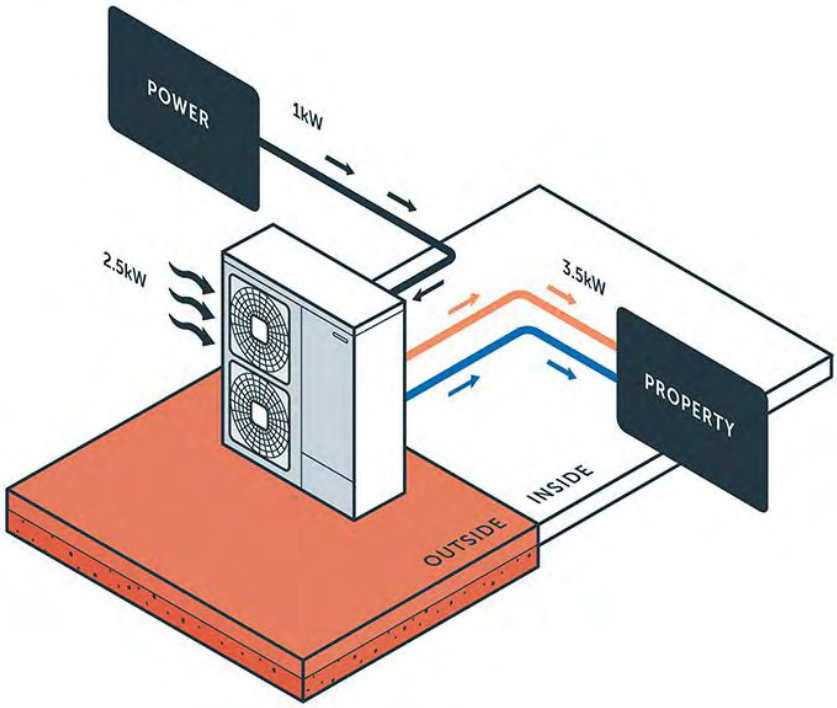

Fig. 2.6:

Example of an Air Source HP. 1 kW of electricity is consumed to transfer 2.5 kW of heat from the external air, producing a total heating effect of 3.5 kW [18].

2.2 Geothermal energy

2.2.1 General

Geothermal energy is defined as the thermal energy stored below the surface of the solid Earth. The vast energy contained originates mainly from planetary and geological processes. After the creation of our planet, it has been slowly cooling and by conduction and convection this primordial heat is transferred to the subsurface. Geological processes, particularly the decay of radioactive isotopes with vast half-life spans enclosed in mineral rock, increase the existing heat flow. The amount of heat released at the Earth's surface varies from one location to another, due to differences in geology. On average, the Earth's heat flow measures 57 $\frac{mW}{m^2}$ in the continental crust and 99 $\frac{mW}{m^2}$ in the oceanic crust [19]. A drop of the temperature of the ground outwards can be observed, caused by the continuous cooling from the interior of the planet towards the surface. The geothermal gradient, meaning the rate of change of temperature with depth, depends on the thermal characteristics of the rock formations. Maximum values, of 40–80 °C per km, can be measured in areas with volcanic activity or areas with particularly thin crust, where magma is quite close to the surface like in mid-oceanic ridges [20]. The section of the ground that is closest to the surface, is affected by the outside air temperature. Shallow ground is influenced by seasonal variations of the outside temperature. Below that, the ground temperature is essentially stable and the same as the average air temperature, which is the effect used in cellars for storing food and wine. Further below, the planetary geothermal gradient takes over.

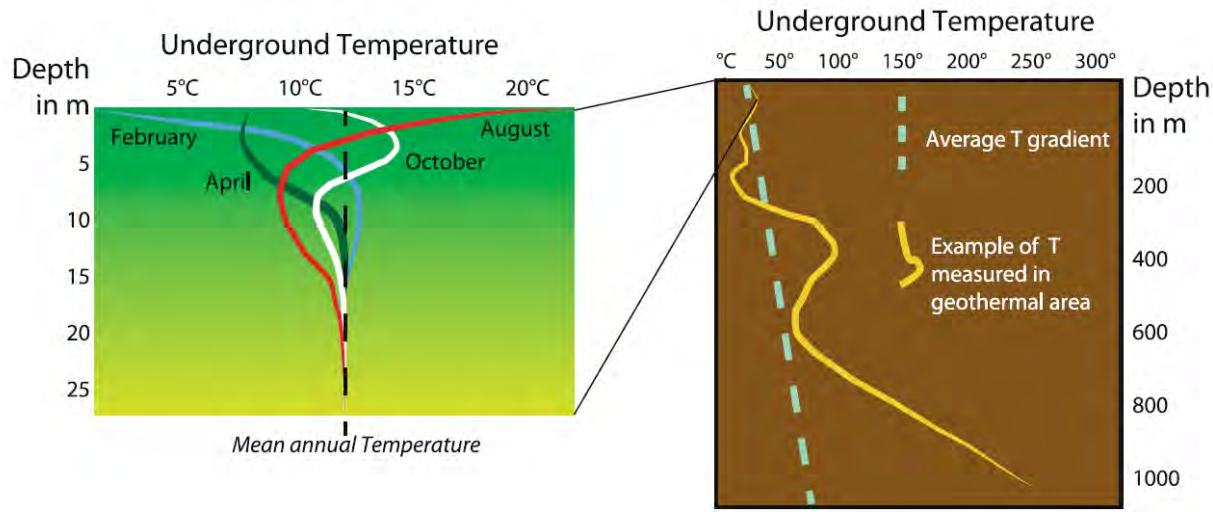

Fig. 2.7: Mean underground temperature profiles for 4 different months and illustration of geothermal gradient [9].

For centuries, geothermal springs have been used for bathing, heating and cooking. But only in the early 20th Century did people start to consider the heat from inside the Earth as a practical source of energy. Today, depending on the temperature of the fluid, geothermal waters are used for many different applications, including electricity generation, although this is not always necessary as geothermal energy can be employed directly as heat without further conversion into other types of energy. The main types of geothermal heat production technologies are used for space heating and cooling (including heat pumps), bathing and swimming, agricultural, industrial processes, and aquaculture.

The applications of geothermal energy in agriculture, comprise of a plant-growing temperature control in open fields and greenhouses. Soil can be heated by burying thin pipelines where warm fluids are circulated. Heating of greenhouses is achieved by the forced circulation of air in heat exchangers, hot-water circulating pipes or ducts located in or on the floor, finned units located along the walls and under benches, or a combination of these methods. In aquaculture, heat controls the breeding of aquatic forms of life. The installation capacity relies on the temperature of the geothermal source, the temperature required for the breeding of fish, and the heat lost from these pools. In industry, the processes that can exploit geothermal heat are usually heating, evaporation, drying, distillation and sterilization of products, de-icing of roads in regions with heavy snowfall, and the extraction of salt by evaporating water. Minor utilizations of geothermal springs range from the bottling of water and carbonated drinks, production of paper, food processing and milk pasteurization to uses in the pulp and paper processing and leather industry.

Particularly in countries with cold climate conditions, a substantial portion of the final energy consumption accounts for space heating. This energy load could be met by geothermally heated fluids at the required temperature. Directly after extraction from the ground, fluids can either be circulated in the heating system or more conventionally, exchange heat through a heat exchanger. Devices and equipment that exploit the constant thermal profile of the shallow underground for heating/cooling belong to shallow geothermal technologies. Technologies developed to retrieve and use temperatures above the annual mean air temperature that are located in the deep underground are referred to as deep geothermal [9].

2.2.2 Deep Geothermal Energy

In deep geothermal energy technologies, water is mainly utilized as a heating medium to extract energy from underground. As the crust is permeable to fluids, surface water, essentially rainwater, penetrates the ground and exchanges heat with the rocks. Wells are then used to extract the warm or hot water circulating in the underground rocks to make use

of their heat. For viable economic use of deep geothermal resources, aquifers with high temperatures have to be tapped. In areas with moderate heat flow, drilling to depths of at least 2 km is vital to reach a temperature of $80\ °C$, which is regarded as the lower limit for district heating in Europe. Deep wells in South Germany have recently reached a borehole length of up to 6 km to tap thermal waters with temperature of more than $140\ °C$ [21].

Geothermal fluids are generally re-injected into the underground in a doublet or triplet system, where one well is used as a heat producer and one as a re-injector. It is essential to reinject the fluids back to the underground after their heat extraction in order to preserve the natural conditions in the aquifer. Geothermal plants that did not reinject their wastewater encountered terrible pressure drops and caused of adjacent wells to lose productivity. An electrical submersible pump (ESP) draws the geothermal fluid to the surface. ESP's face numerous problems when temperatures surpass 120 °C, requiring long downtimes for repairs or fully replacing it. Precipitation of carbonate and sulphide minerals are observed when the temperature is over 100 °C that can cause damage to the whole installation. Heat exchangers are utilized to transfer heat from the geothermal fluid to the fluid of the grid, preventing thus their mixing and subsequently the corruption of the grid water. The circulation of the working fluid to the district heating grid is performed by powerful pumps.

Geothermal energy employs great load capacity. A large number of annual full load hours is achieved this way. To cover peak demands oil or gas burners can be installed.

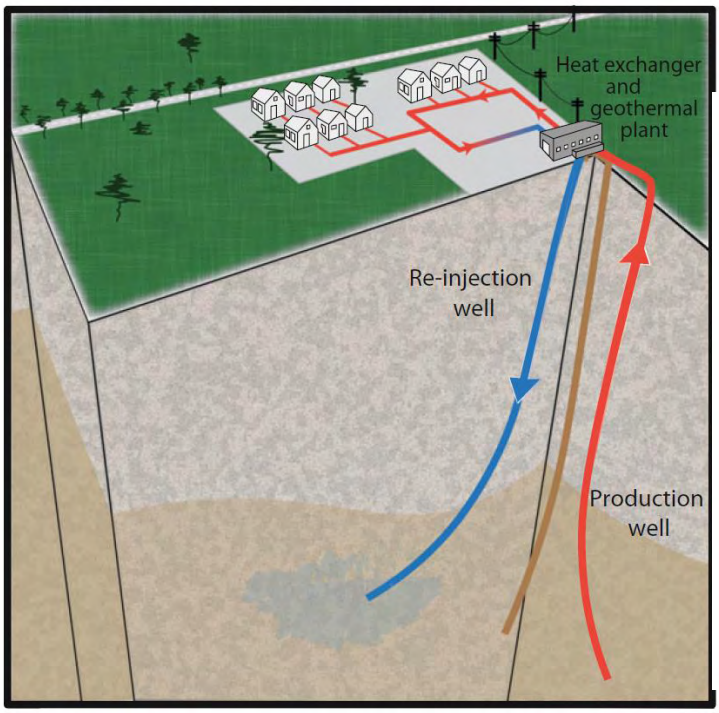

Fig. 2.8: Doublet system for heating network [9].

Fig. 2.9: Carbonate precipitation in pipe [21].

2.2.3 Shallow Geothermal Energy

Shallow geothermal systems, that utilize water with a temperature below 25 °C, work quite similarly to deep systems. To cover the required heat/cool loads, *ground source heat pumps* (GSHP) are used. GSHPs are consisted of a wide variety of systems that can utilize ground-water, ground, or surface water as heat sinks/sources. These systems have been categorized into three subgroups by ASHRAE [22]:

1. ground-water heat pump (GWHP) systems,
2. surface water heat pump (SWHP) systems,
3. ground-coupled heat pump (GCHP) systems.

Many similar expressions exist like earth energy system (EES) or geothermal heat pump (GHP).

In addition systems are categorized based on what kind of loop they utilize. These are:

Closed loop geothermal systems utilize a mix of water and antifreeze which cycles through pipes buried in the ground instead of pumping fresh groundwater to transfer heat. Closed loop geothermal systems can be further subdivided into different categories.

- Horizontal - Horizontal closed loop geothermal systems are systems in which pipes are buried horizontally in the ground. These systems require significant area as the whole length of the loops must be covered.
- Slinky – The slinky is a variation of the aforementioned system. In a slinky loop system, the piping is laid horizontally, but looks like a flattened and spread out slinky because multiple semi-loops are laid close to each other. This reduces the total length required because the heat transfer area per square meter is increased.
- Vertical - Pipes are installed vertically deep in several wells instead of placing the pipes horizontally. The pipes encase the other coaxially or are linked together at the bottom by a U-bend. Grout is used to fill the boreholes in order to achieve favorable thermal conductivity.

The loop dimensions depend on the moisture concentration, the type of soil, the average ground temperature and the thermal behavior of the conditioned building.

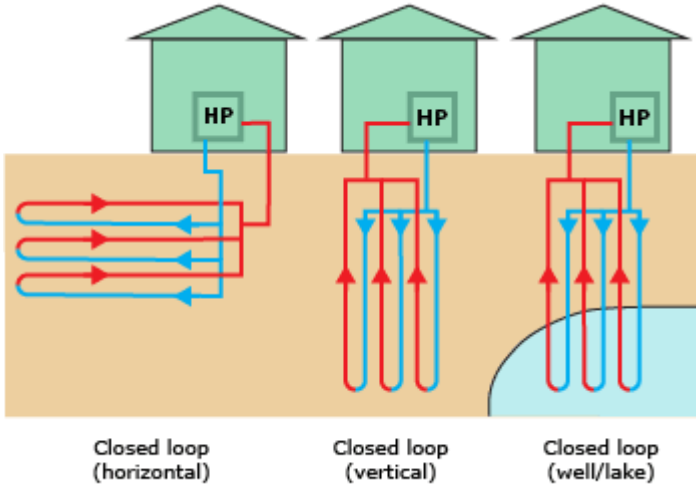

Fig. 2.10: Types of closed loop systems [23].

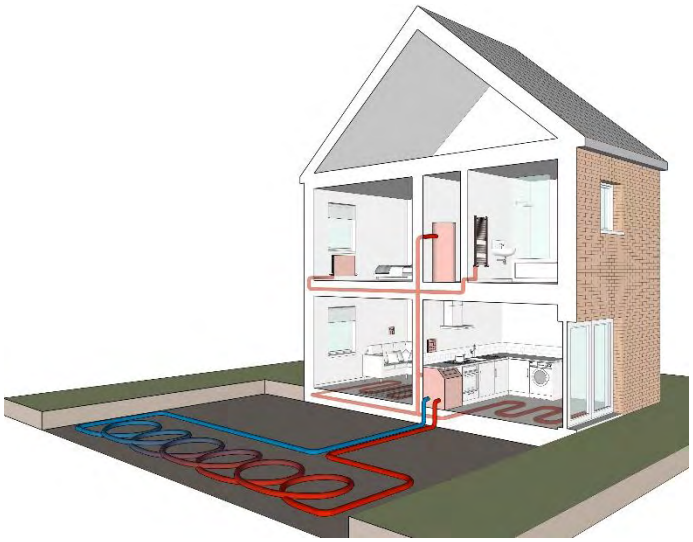

Fig. 2.11: Slinky system [24].

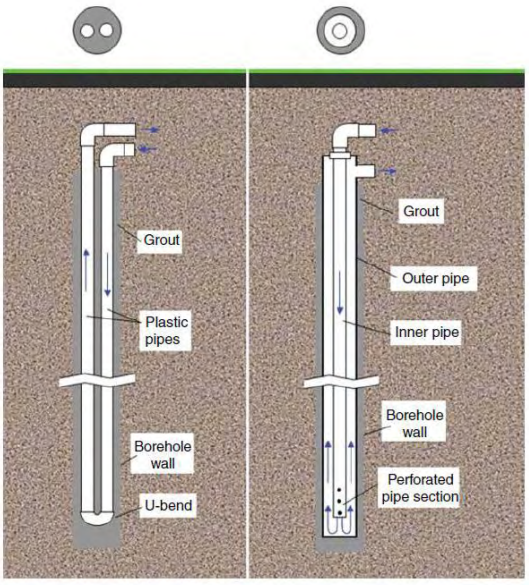

Fig. 2.12: U-bend and coaxial types [25]

Open loop geothermal systems utilize ground- or surfacewater as a transfer fluid to exploit geothermal energy. Due to the fact that water has exceptional thermodynamic properties and that groundwater has a similar temperature to the ground nearby, by being naturally insulated, open loop geothermal systems are considered as the most efficient selection for HPs. Water wells, ponds and lakes can be utilized as both sinks and sources of heat. Every installation has unique variables that need to be considered and numerous factors that define the space, cost required and the overall efficiency of the system. Horizontal collectors which are installed up to a depth of not more than 2 m are a variation of solar thermal utilization because they utilize mostly solar radiation. The effectiveness of the system relies on the concentration of moisture in the ground, its coverage and the shading of the collector field. The heat exchanger can either be installed in a trench or directly in the ground

installed horizontally. Generally, the area required for the loops should be twice as big as the surface designated for heating. Drilling is necessary and therefore are mostly installed simultaneously with the construction of new private houses.

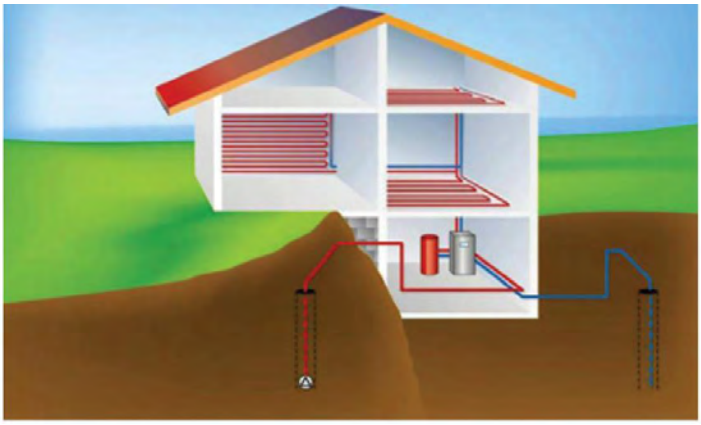

Fig. 2.13: Illustration of an open loop system [15].

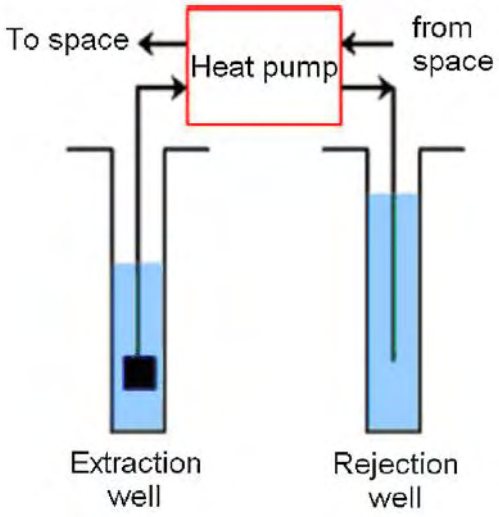

Fig. 2.14: Ground-water heat pump [26].

2.2.4 Ground Source Heat Pumps

The process of the heat pump was described previously. Common air conditioning systems use the external air as a heat source/sink. Geothermal or ground source heat pump (GSHP) systems typically utilize loops in shallow ground or groundwater. The heat pump system can be deployed for heating and cooling If a 4-way valve, that reverses the cycle, is installed. Shallow GSHP systems for heating/cooling exploit the stable temperature found during the whole year at those depths. In heating season ground-source

HPs are more efficient that conventional, air-to-air heat pumps because the temperature of the ground is higher than that of the air.

Utilizing groundwater for heat/cool applications is the most efficient form of shallow geothermal energy. An aquifer with sufficient permeability can be accessed with two wells serving as a production and a reinjection well respectively. Prospecting the porosity, permeability, hydrogeological properties and groundwater flow velocity, is required to determine the correct displacement between the reinjection and production wells, the correct piping flow rate and the suitable heat exchanger [27].

The most significant advantages/limitations of GSHP systems are listed below:

Ground coupled HPs

Horizontal	Vertical
Advantages	*Advantages*
- Low installation cost	- Less space is required
	- More efficient
Limitations	*Limitations*
- Significant space needed	- Drilling is required

Ground-water HPs

Advantages	*Limitations*
-Low installation cost, especially for large systems	-Dependence on water quality (sediments, corrosion, bacteria etc.)
-Drilling for groundwater technology is widely established	-Reinjection needs to comply with regulations
-Groundwater has stable temperature throughout the whole year	-Sufficient water
	-Maintenance

GSHPs are a promising solution to achieve low-energy consumption buildings. To attain high efficiency in the overall system, system parameters, design and operation need to be optimized in order to maximize COP and SPF. To accomplish that a heat pump either with an inverter in compressor or with compressors in series can be used, so as to adjust the heat pump operation according to the user's energy profile. GSHPs for heating, cooling and domestic hot water production are employed mostly in moderate climates, particularly in Mediterranean countries, where during the winter season heating is necessary but cooling as well during the summer, given the fairly high temperatures that rise annually. For such circumstances, a 4-way valve is required for the refrigeration cycle to be reversible.

2.2.5 Global share of geothermal energy

The report of the 2015 World Geothermal Congress, showed that the total geothermal capacity for thermal uses reached 70.3 GW, by the 83 countries taking part [28]. The global shares of this capacity were 55% for geothermal heat pump systems, 20% for pools and spas and 15% for space heating (mostly for district heating). All other applications accounted for 9% (industry mostly) .

2.2.6 Current state of geothermal energy in Greece

Geothermal energy is exploited in Greece solely through direct use, in thermal spas, greenhouses, soil heating, aquaculture, agriculture, drying and GSHPs. Increased interest is found in seawater space cooling, mainly for seaside hotels, operating only during the summer. Most geothermal applications, are found in northern Greece. By 2016, the total installed capacity of geothermal applications was 232 MWth, with GSHPs accounting for 64%, thermal spas for 18% and greenhouse heating for 14.5%. The increase of GSHP system installations lately, has brought significant growth to the Greek geothermal market [29]. This particular increase is attributed to several causes. The public attitude has shifted positively towards this novel technology while the air-conditioning sector has seen steady growth lately. Additionally, the Association of Greek Geothermists launched a campaign promoting the utilization of GSHPs. Other than that, the licensing process for the drilling of wells or for groundwater usage in open systems, has become easier. Most importantly though, the high oil prices in 2008 in combination to the relative stability of electricity prices in the country, led to a wider adoption of GSHPs [30]. This is not enough though. To achieve the goals set by the EU for heating/cooling by RES, 50 ktoe capacity must be contributed to GSHPs until the end of 2020. That is equivalent to 265 MWth installed, of which 45% is closed-loop systems, 40% open-loop systems and 15% horizontal systems [15].

Geothermal energy exploitation is severely underdeveloped in Greece, given its great geothermal potential. A substantial amount of geothermal fields have been identified through research the last 40 years. The islands of Milos and Nisyros have a total proven geothermal electricity generation of 25 MWe, with estimates indicating that even 250 MWe can be reached. Probable areas with fluids up to $120\ ^{\circ}C$, suitable for electricity generation, have been identified in the islands of Lesvos, Chios and Samothraki and in the geothermal fields of Aristino, Eratino and Akropotamos. Specifically in Eratino, water had a temperature of $125\ ^{\circ}C$ at 1350 meters. In promising areas, water temperatures typically reach up to $100\ ^{\circ}C$ at depths less than 1000 m. A conservative estimate of the national total low-enthalpy geothermal potential is 1000 MWt.; [30]. Yet, its utilization is limited. The total lack of power production through geothermal energy, is attributed mostly to the local societies' opposition created by the bad experience of the Milos Island pilot power plant (1970–80s). Environmental

pollution caused by deficiencies and errors during construction and operation, brought forth strong pushback against this kind of power generation. This in turn has made local communities and authorities view the large scale exploitation of high temperature deep geothermal resources (for resources with temperatures above 90 °C) negatively, until this day in several locations. In contrast, low temperature deep geothermal (resources with temperatures between 25 and 90 °C) utilization is perceived much more positively [31].

Mainly, along the volcanic arc of the southern Aegean (Milos, Nisiros, Santorini),there is great potential for thermal desalination of seawater, as there is dire need for drinking water in these dry coastal areas. This would be a far cheaper and environment friendly alternative to the current method, supplying the islands by freshwater cargo ships.

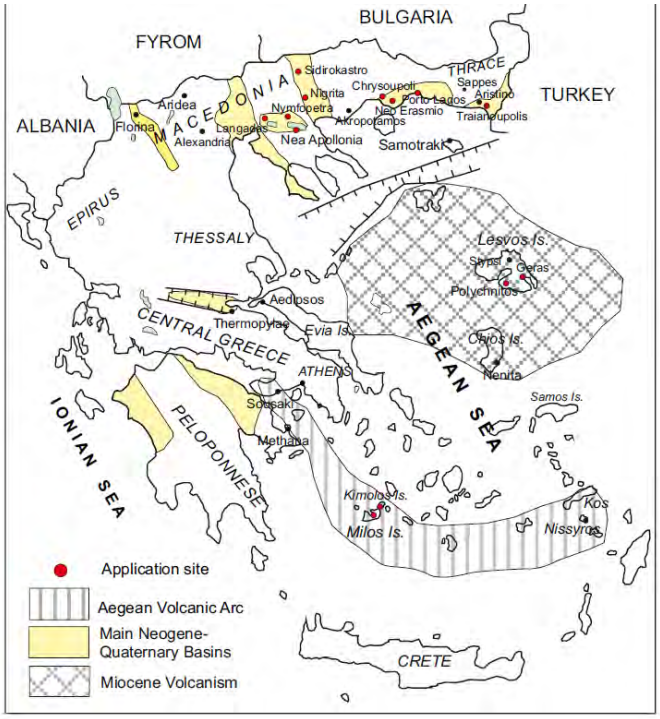

Fig. 2.15: Map of high potential geothermal areas in Greece [30].

2.2.7 Environmental Impact

The utilization of the energy stored in the ground might affect the environment negatively. Usually the scale of the environmental impacts is directly linked to the size and

depth of the installation. Shallow geothermal systems effortlessly avoid catastrophes by taking necessary precautions. The most serious hazard is thermal pollution, when the drill holes locations are incorrectly dug or the flow of the fluid extracted is higher than advised. in Doublet system plants have a very restricted footprint on the environment due to the fact that the extracted underground fluid is directly reinjected right after passing through the heat exchanger at the surface. Any modification to the environment must be calculated carefully in advance, in agreement with regulations, because even a slight alterations can set off a chain of events. A minor increase in the temperature of a body of water by discharge waste-water could destroy its ecosystem. Using deep geothermal sources with high temperatures, especially in regions around active volcanos, might actively harm the environment. Gases such as carbon dioxide, ammonia, methane and traces of other compounds can be released into the atmosphere. Air pollution sources like arsenic, sodium chloride, mercury and boron might also be discharged into the environment. Thermal pollution caused by wastewater from geothermal plants are also possible. There are counter measures for this fortunately. Dangerous compounds can be removed from the geothermal fluids through special treatment. Gas emissions can be reduced through various technologies already established in the industry. CO_2 might be released by the fluids of the geothermal plants, though minimal amounts compared to the combustion of fossil-fuels.

The share of renewable energy is improved by the utilization of geothermal heat i and air pollution emissions are reduced. Seasonal or weather changes have no significant impact on geothermal installations and can consequently generate energy almost constantly unlike other RES whose capacity changes over time. Geothermal energy performs quite well in the aspect of lifecycle and emissions when compared to other RES. The greenhouse gas emissions discharged by geothermal plants, as stated by the IPCC [7], place among the lowest of all energy sources. The overall emissions are particularly low because no combustion is required for electricity and heat generation from geothermal energy. Only geothermal fluids which have a high concentration of gases are excluded from this. As for GSHPs, they consume up to 44% less energy compared to air-to-air heat pumps and up to 72% less than standard A/C with electric resistance heating. [9].

2.3 Solar Energy

Solar energy is the result of electromagnetic radiation released from the sun by the thermonuclear reactions occurring inside its core. All of the energy resources on earth originate from the sun (directly or indirectly), except for nuclear, tidal, and geothermal energy. Essentially all types of energy in the world originate from the sun. Photosynthesis followed by complex chemical reactions created all known fuels such as coal, oil, wood and natural gas. Wind and tide energy are also creations of the sun, because they are produced by temperature changes in diverse locations of the planet.

Solar energy can be converted to chemical, electrical, and thermal energy. The most important process is photosynthesis, where plants collects solar energy and transforms it to chemical type. Normally, photosynthesis creates glucose from the combination of solar radiation, CO_2 and H_2O, with O_2 as a side product. It is perhaps the most important known biochemical process and almost the entirety of life on the planet depends on it. Conventionally, there are two categories of solar energy capturing devices based on how it is converted: either electricity or heat, with Photovoltaic modules or thermal collectors respectively. Only a miniscule fraction of the total incident solar radiation that reaches the planet is harvested today.

2.3.1 Solar thermal collectors

Solar thermal collectors are a variation of heat exchangers that convert solar radiation into thermal energy through a transport medium or a Heating Transfer Fluid (HTF). Its various applications range from domestic hot water (DHW) heating, space cooling/heating to industrial process heating and power generation. Two forms of thermal collectors are described below, Flat-Plate Collectors and Evacuated Tube Collectors

Flat plate collectors (FPC) are the simplest and most widely used collector type. It is used to absorb solar energy, convert it into heat, and then to transfer that heat to stream of liquid or gases. Solar radiation travels through the transparent cover and reaches the flat plate located below. A spectral selective coating might be painted on the surface to augment the absorption of the solar energy. Copper tubes containing the HTF are located under the surface. Energy is transferred to the HTF that flows inside the tubes. The FPC is the cornerstone of any solar energy collection system designed for the generation of hot water with low temperature (less than 60 °C), or with medium temperature, meaning less than 100 °C.
FPCs are typically permanently installed in a location and does not track the course of the Sun. The collectors should be oriented directly towards the equator, facing south in the northern

hemisphere and north in the southern. The best tilt angle of the collector is typically the value of the locations latitude with deviations depending on the application. Both direct and diffuse solar radiation are captured by the device, and little maintenance is needed. They are far less complicated than concentrating collectors. The collectors are mostly used in DHW heating, air conditioning of buildings and various industrial process that require thermal energy. An FPC generally consists of the following components:

- Multiple sheets of glass make up the glazing through which radiation is transmitted.
- Piping in which the HTF flows.
- Flat plate that absorbs radiation to which the piping is attached.
- Intake and exit manifold of the HTF.
- Insulation to limit heat transfer to the environment from the rear and sides of the collector.
- Cover to shield the interior from dirt and humidity.

The goal of a FPC is to accumulate as much solar energy as possible at the lowest possible price. An extended life cycle of the FPC should be guaranteed, even with the constant negative impact of the Sun's ultraviolet radiation. Acidity induced erosion or blockage must be avoided. Glass is the most established glazing for flat plate collectors since it is able of transmitting up to 90% of the *incoming shortwave* solar radiation while blocking the bulk of *outgoing longwave* radiation emitted from the absorbing surface. Low-iron glass can achieve a transmittance factor of 0.90 at normal incidence. Plates made of plastic possess a high transmittance factor for shortwave radiation as well, however their transmittance factor for longwave radiation might reach 0.40. Selective coating that limits the reflection of radiation as well as the texture of the plate can increase the total transmission considerably. So in essence, the goal is to absorb as much of the radiation as possible through the glazing, while minimal heat is lost from the glass to the atmosphere and through the insulated rear of the cover. The heat absorbed by the surface is transferred to the HTF. The rate at which the plate absorbs shortwave solar radiation relies on the color and texture of the coating and on the incidence angle. Through various chemical and electrolytic processes, selective surfaces can be created that have high absorptance α values and low emittance ε values. These surfaces are most suitable when ambient air temperature is low, thereby balancing the heat lost due to the temperature difference with an increased solar gain. The most widely used metals for absorbing surfaces are copper, stainless steel and aluminium. Corrosion of these metals must be taken into account. The most common insulators are glass and mineral wool and glass foam. Polyurethane is utilized for applications with lower temperatures [10].

Solar air collectors operate principles similarly to FPCs.
Instead of liquid flowing through the collector, air is circulated by an electric fan. The main components are:

- absorbing surface

- glazing
- casing
- insulation
- electric fan

This form of solar collector has not penetrated the market of Europe successfully yet (no more than 2% of the liquid FPC market). Lack of the required know-how and experience of the end users and simultaneously the fact that this collector form cannot generate DHW, might be the reason.

A fraction the total solar radiation incident on the glazing, determined by transmittance, reaches the absorbing surface where it is converted into thermal energy. The glazing stops radiation from escaping the collector.

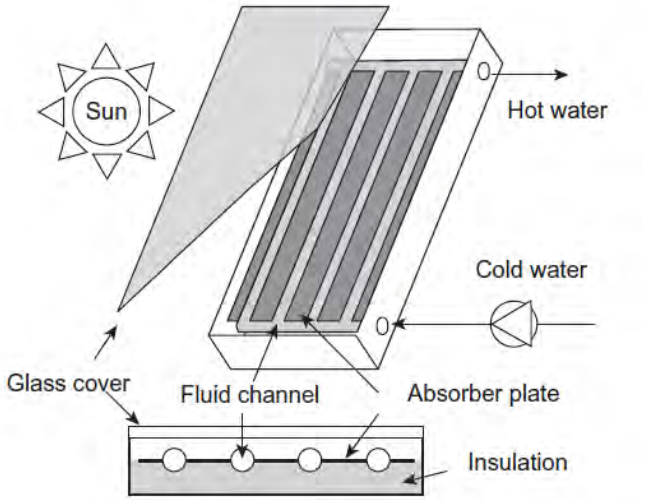

Fig. 2.16: Schematic diagram of a FPC [10].

Evacuated-tube collectors are typically a set of parallel rows of transparent glass tubes, where the absorber surfaces are located, linked to a header pipe. By pumping out all the air in the tubes, therefore creating a vacuum, eliminates convection heat losses. This way high temperatures are achievable, which allows the collectors to generate more thermal energy for demanding processes like in industrial heating and solar cooling. Evacuated-tube collectors combine the insulation caused by the vacuum and a highly selective surface coating to achieve a greater thermal result compared to flat-plate collectors in the temperature range above 80 °C. Lately, ET collectors have become a major part of solar thermal exploitation, particularly in residential applications that require higher temperatures like domestic hot water production or heating. Two types of ETCs exist: Direct flow U-tube collectors and Heat-pipe collectors.

Direct flow evacuated tube collectors, or U-tube collectors, 2 copper pipes are located inside an evacuated tube. The first is for the input flow and the other is the return. The pipes are joined at the bottom with a U-bend. The flow and the return pipes are separated by the absorption fin. U-tube collectors do not have the same flexibility as the heat pipe equivalent, since a whole system draining is necessary if a tube cracks open.

Heat pipe-evacuated collectors consist of a heat pipe, meaning a highly efficient thermal conductor, located in an evacuated tube. This collector is made up from the same parts as the U-tube, their only difference being the lack of a U-turn which has been replaced with a thermal tube compactly full with a substance that is vaporized by solar radiation. The resulting vapors rise to the top of the tube and condensate which transfers the condensation latent heat of to the heating transfer fluid and after that the cycle starts again. This way, the fluid is heated by flowing through the collector pipes.

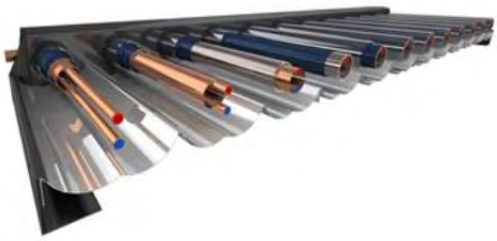

Fig. 2.17: Direct flow collectors [32]

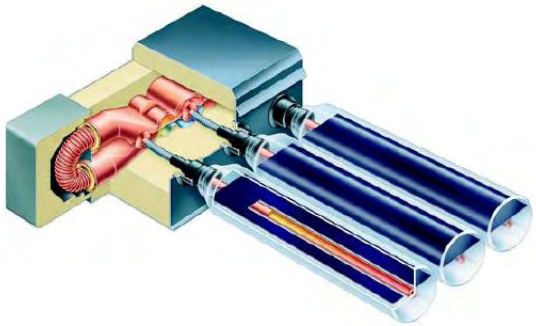

Fig. 2.18: Heat pipe collectors [32]

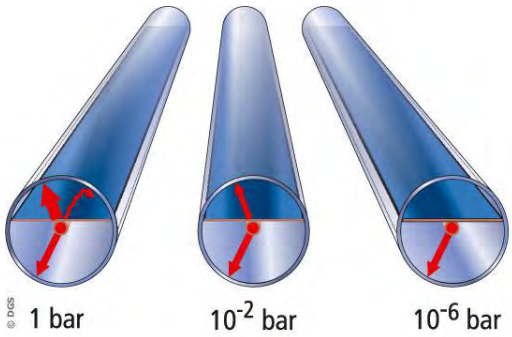

Fig. 2.19: Losses from ETC. Convection and advection losses are minimized at low pressure (vacuum). [33]

The most widespread heating transfer fluid is regular water, a mixture of glycol and water or simply air. 2 forms of solar thermal systems exist, the thermosiphon and the forced-circulation. The way the heating transfer fluid is circulated in the collector and the storage tank is what distinguishes them. Thermosiphonic systems, utilize the “thermosiphonic phenomenon “and generally produce DHW. Thermosiphon systems circulate the heating transfer fluid between the storage tank and collector using gravity. The fluids temperature is increased by flowing through the collector and consequently its density decreases allowing it therefore to rise to the upper part of the storage tank and later when its temperature drops, flows back to the lower end of the collector. With the thermosiphonic phenomenon, the use of a pump can be entirely avoided. This collector form is well established in European countries with high solar coverage [21].

2.3.2 Solar Photovoltaic Collectors

Photovoltaic (PV) solar technologies generate electricity by exploiting the photovoltaic effect, in which solar energy is directly converted to electricity. The device that is used for this purpose is called a solar cell. These cells are clustered into one uniform device called a PV module (panel). A PV array consists of several modules connected in series and/or parallel to generate the desired power. Solar cells produce electricity directly from electromagnetic radiation, especially light, without any moving parts. The PV effect was discovered by Becquerel in 1839 but not fully developed as a power source until 1954 by Chapin, Fuller, and Pearson using doped semiconductor silicon.

Solar rays consist of photons which are discrete energy amounts. An atom of silicon in a crystal lattice absorbs a photon of the incident solar radiation, and if the energy of the photon is high enough, an electron from the outer shell of the atom is freed. This results in the formation of a hole where there is a lack of an electron and one electron is exiting the crystal structure. These typically vanish spontaneously as electrons recombine with holes. The recombination process can be halted by a potential barrier, a thin layer or junction across which a static charge, that we can construct. The barrier can be constructed by doping the silicon of one side with tiny amounts of boron to create positively charged silicon (p-silicon), which has a deficiency of electrons in its outer shell, and that on the other side with phosphorus to form negatively charged silicon (n-silicon), which has an excess of electrons in its outer shell. By restricting the free movement of electrons, the electrons accumulate in the negative silicon side and there is a partial lack of electrons in the positive silicon. Should these layers be joined by external circuitry, a flow of electrons will pass through that circuit. Therefore by absorbing photons, free electrons are created in excess in the n-silicon and flow through the circuit towards the p-silicon. Metal bases on the lower part of the photovoltaic cell create the electrical contacts with metal meshes or grids on the above layer.

The efficiency of a solar cell is defined as the ratio of output power from the solar cell to the incident solar irradiance. The maximum potential efficiency of a solar cell depends on the absorber material properties and device design. With the multijunction technique, diverse

specially selected absorber materials are stacked, so that they can collect more of the solar spectrum since each different material can collect solar photons of different wavelengths. This results in increased solar cell efficiency. PV cells consist of organic or inorganic matter. Inorganic cells are based on silicon or non-silicon resources that can be divided as wafer-based cells or thin-fine cells. Silicon on wafers can be categorized into 2 forms: monocrystalline (one continuous crystal lattice) and multicrystalline (called also polycrystalline, consisting of many small crystals). A third, less used type is called amorphous, due to its lack of crystalline form.

Photovoltaic applications can be categorized into 2 key forms: those that are connected to the national power grid and those that are not connected (off-grid). Additionally, PV consumer products is growing market. Off-grid PV systems can significantly improve the living standards of regions with no electricity grid in developing countries. Grid-connected centralized PV systems are similar to central power plants. The energy generated is not linked to any specific energy consumer, and the system is specifically designed to supply power to the electricity network. Normally, such systems are installed permanently on the ground. Building integrated PVs (BIPV) have lately been introduced, that can be installed on walls and windows to allow daylight and passive solar gain [10, 34].

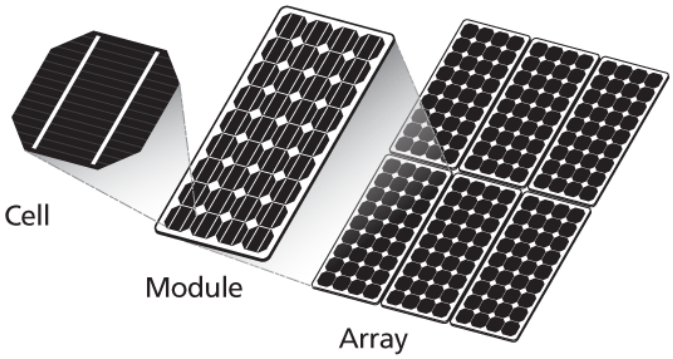

Fig. 2.20: Illustration of a PV cell, module and array [35].

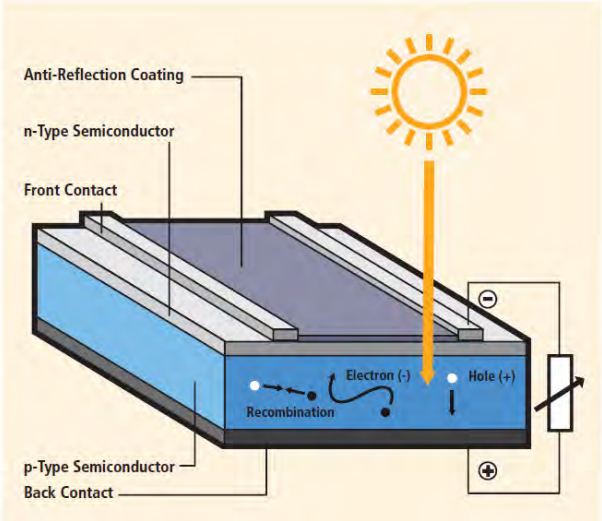

Fig. 2.21: Operation of a PV cell [7].

2.3.3 Hybrid PV/T systems

A device that converts solar energy into heat *and* electricity simultaneously is called a hybrid photovoltaic/thermal (PV/T) collector. A PV/T collector is a photovoltaic module which generates electricity but has a thermal component as well that absorbs the waste heat produced. This configuration can cover both thermal and electrical demands partially for numerous uses in the sector of buildings. PV/T collectors can at the same time generate thermal and electrical power, resulting in an increased total conversion efficiency of the captured solar energy. Only part of the solar radiation incident on the photovoltaic cells is converted successfully to electricity and the rest is converted into waste heat that consequently increases the temperature of the PV module. Depending on the type of the PV cell its peak efficiency can be in the range of 5–20%. The higher the temperature of the cells during operation is, the lower the conversion efficiency gets. For monocrystalline and multicrystalline silicon wafers, the efficiency drops by about 0.45%/°C for rising temperatures. Regarding the amorphous type, the loss rate is less, with a decrease of about 0.2%/°C in rising temperatures, subject to the design of the cell. The negative impact of high temperature can be reduced by removing the excess heat through the circulation fluid. Photovoltaic cells whose waste heat is correctly and timely extracted with lower temperature air or water, display better performance. The priority of hybrid collectors is to generate electricity. It is therefore essential to operate the cells at low temperature in order to sustain a favorable efficiency level. Natural convection already takes place in standard module but is unfortunately less effective if the surrounding air temperature is high. Forced circulation of air can be utilized as well. To achieve greater efficiency, heat can be removed by the circulation of water through a heat exchanger attached to the back of the collector. The heat extracted can be utilized for various applications. Thus, more energy is captured in total with the same collector area of a plain photovoltaic module. Other than increasing the efficiency of the PV cells and stabilize their I-V curve, which in turn affects their maximum power point.
The promising aspects of hybrid collectors are the following [36]:

- Twofold-generation: the same collector can generate electrical and thermal power simultaneously.
- Efficiency in terms of energy and area: high efficiency is guaranteed when the collectors are sufficiently cooled. When roof-panel spacing is limited, hybrid panels are a great solution.
- Extensive utilization: the thermal output is useful mostly for DHW but is suitable for cooling/heating as well and even certain industrial uses
- Inexpensive and flexible: easy installation in buildings with no significant alteration and reduced payback period.

Various forms of hybrid collectors area available, depending on the heat extraction fluid or the way solar radiation is captured, like water cooled and air cooled PV/Ts or PV/T-concentrating collectors. Solar photovoltaic and thermal collectors are will dominate the energy generation market in the near future.

Typically, the water-cooled collectors contain metallic sheet mounted with pipes to circulate the fluid and to avoid its direct contact with the back of the cells. A heat exchanger is located there and thermally insulation is placed on the back and the panel edges to minimize heat loss. The heat exchanger referenced above is similar to the one utilized FPCs, so the resources and technical design are already widespread in the solar market.

Water cooled collectors have higher efficiency than air cooled ones [37] because water has more favorable thermodynamic properties in relation to air. However, the low construction cost (minimal use of material) and operating cost among others, make PV/T-air systems a viable alternative for certain applications. Some general PV/T applications can be solar cooling, water desalination, greenhouse heating, solar HPs and A/C units, and building integrated collectors

.

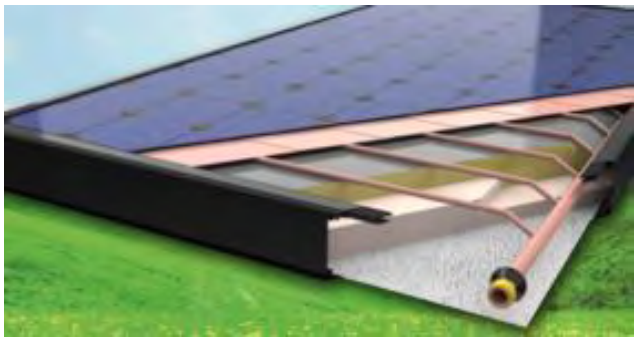

Fig. 2.22: Cross section of a PV/T [38].

2.3.4 Solar power in the EU and Greece

Solar power has become one of the cheapest technologies for energy generation worldwide. The sector has been growing rapidly, the world-wide installed capacity increased from around 40 GW in 2010 to more than 600 GW in 2019, with about 130 GW installed in the EU. Between 2009 and 2018, production costs decreased by 75% while steady market grow was seen. In Europe, about 5% of the EU's final electricity demand is covered by PV currently. In 2018, the EU market grew by 8GW, and by an estimated 15-17GW in 2019. The solar market is expected to continue to grow from 2020 onwards, making solar power a cornerstone of the EU's transition to clean energy. The coming decade is expected to see continued growth, mostly driven by increased self-consumption and more rooftop PVs installation. This will result in economic growth and creation of jobs: in 2018, the solar PV industry accounted for 117.000 full-time jobs and it is expected to sustain nearly 175,000 full-time jobs in 2021, with estimates of between 200,000-300,000 jobs in 2030 [39].

Greece has among the highest potential for solar energy utilization in the EU, due to its geographical location and weather conditions. Total installed solar thermal power capacity

in Greece as of the end of 2018 was 3.3 GWth. That translates into a 2.3 million tons of CO2 emissions reduction every year. The Greek market grew by 4% in 2018, having already increased by 16.2% between 2016 and 2017 (from 272 000 to 316 000 m2) [40].

In 2019, the PV market rose by 3.1% in comparison to the previous year, still being low given the great solar power potential. By the end of 2019, PVs covered around 7% of the electricity demand, bringing Greece to *fourth place globally* (after the Honduras, Italy and Germany) in PV coverage of the total electricity consumption. In 2019, 160 MWe were installed, raising the total PV production to 2.828 MWe [41].

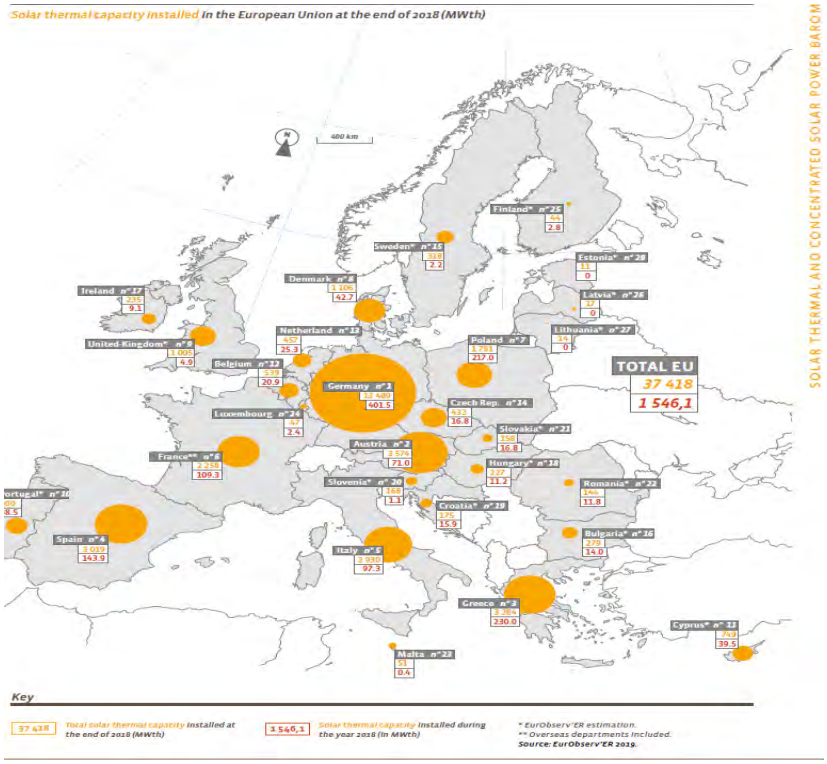

Fig. 2.23: Solar thermal capacity in the EU [40]

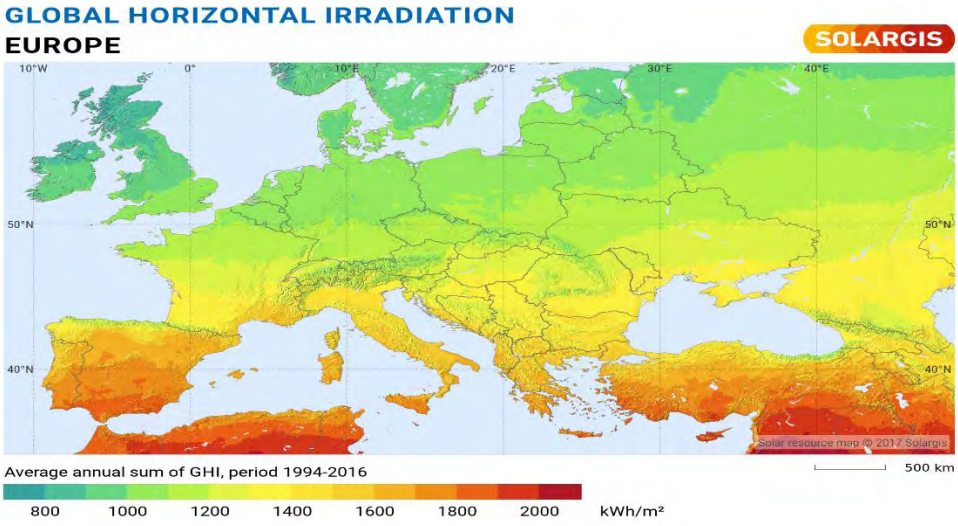

Fig. 2.24: Global horizontal radiation map of the EU [42].

2.4 Solar Assisted Ground Source Heat Pumps

Buildings represent the biggest and most cost effective potential for energy savings. Studies have shown that saving energy is the most cost effective method to reduce GHG emissions. At present heat use is responsible for almost 66% of the energy demand in houses and utility buildings for space heating and hotwater generation in the EU, whereas the energy demand for cooling is growing year after year [1, 43]. Integrating RES to buildings, specifically their heating and cooling, is the ideal way to limit electricity and by extent fossil fuel consumption. Solar energy, not only being vastly accessible, but also able to be harvested by conventional and affordable devices, seems the most promising alternative for the defossilization of building consumption. FPCs and PV modules are already established technologies and their market has been growing fast. As mentioned before, for areas with high solar energy potential, like Mediterranean countries, the exploitation of solar energy is of great significance, should they achieve the energy goals set by the EU. Greece with an average solar prospective gain of about 1600 kW h/m^2 per year [44] is among the absolute top in solar energy utilization, yet there is still room for improvement. Solar energy currently covers mostly electricity generation and DHW production, so to fully integrate RES into the national energy profile, energy systems for other applications such as space heating and cooling need to be developed.

The hybrid PV/T collector, producing electricity and useful heat simultaneously, is the next big innovation in the building sector. Heat pump technology gains increasingly more attention the last years because of its low electricity consumption. Especially in Greece, heat pumps have begun replacing conventional boiler heating systems because of the high fossil fuel cost.

The next step is to combine solar energy utilization with heat pumps, creating environmentally and financially sustainable systems.

The combination of solar energy and geothermal energy, through the use of a heat pump, is called ***Solar Assisted Ground Source Heat Pump*** (SAGSHP). Combining a HP with FPC, the liquid/vapor mixture going through the evaporator in the heat pump unit, is preheated by the hot stream coming from the solar collector, resulting in increased temperature and pressure in comparison to a unit depending solely on the ground source heat. This could significantly improve the COP of the heat pump compared to a conventional one. With PVs instead of consuming electricity from the grid, solar energy is powering the GSHP. PV/Ts combine these features, resulting in substantial energy savings.

2.5 Literature Review

The potential of SAGSHPs has not been overlooked by the scientific community and various studies ranging from energetic evaluation to designing efficient control systems, have been published globally. Some notable are described in the next segment:

Pärisch et al. [45] investigated the behavior of a GSHP under nonstandard conditions combined with FPCs. Numerous variable were considered when the system was studied. Results demonstrated that higher source temperatures lead to the rise of the value of COP of the HP with source temperatures below 20 °C.

Fang et al. [46] studied the performance of a HP and A/C system connected to a PV/T. Parameters like evaporation and condensation pressure, the inherent COP of the HP, the temperature of the water source, the efficiency and temperature of the photovoltaics have been examined. Results indicated that the average efficiency of the complete system reaches from 10.4% and up to 23.8% compared to that of a conventional modules. Furthermore, the heated water can reach 42°C while the systems average COP is 2.88. As such the HP/AC unit coupled with PV/Ts is a feasible solution for diverse purposes.

Li et al. [47] investigated a solar assisted air-to-water HP for DHW production and space heating of a 2200 m^2 building with total collector area up to 160 m^2. The system turned out to be viable due to substantial energy savings.

To cover the heating, cooling and electricity needs of a hotel in Italy, a triple generation system was designed and studied. The results revealed that the seasonal COP had a value of 4 for cooling/heating and a very attractive payback period of 6 years. The most important parameter of the system was the total collector area. Locations with low solar coverage like Freiburg, Berlin and Paris had reduced system efficiency [48].

The operation of a SAGSHP system with a U-shaped ground heat exchanger was studied by Ozgener and Hepbasli [49, 50]. Exergy efficiencies of 71.8% and 67.7% were calculated for the HP and the overall system respectively. The studies indicated that the SAGSHP system is not able to cover the thermal needs of a greenhouse in regions with lower ambient air temperatures, thus making it feasible only in regions with Mediterranean climate or warmer.

The heating performance of a ground source HP system coupled to photovoltaic panels was examined. A NZEB approach was taken for the building. The energy generated by the PV panels was more than enough to cover the heat pumps demands and even sent some to the grid. The efficiency of the panels reached 16% and the HP COP was around 4.0 [51].

The effect of PCMs on SAGSHP systems was investigated by Plytaria et al [52]. 3 systems were simulated: flat plate, photovoltaic/thermal and a combination of FPC and PV collectors. PCMs were examined in order to improve the storage capacity and the HPs operation during peak electricity demand periods. Utilization of PCMs resulted in a 40%

reduction of heating loads with the hybrid collector system having the lowest consumption of grid-supplied electricity.

Banjac [53] explored the concept of a SAGSHP connected to a underground thermal storage tank for the heating of a residential house in Serbia. To calculate its performance, the SAGSHP was modeled by a numerical simulation. The integration of solar and geothermal energy resulted in significant energy savings. The volume of the underground tank constituted the most important system parameter.

In a NZEB residential house in Sweden Thygesen and Karlsson [54] simulated 3 SAHP systems. The systems investigated were: a HP system coupled to PVs or solar thermal collectors and a system with PVs and thermal collectors. Results showed that the PV-HP configuration was the optimal solution.

A financial examination of a SAGSHP system for space cooling/heating was conducted by Yang et al. [55]. Despite the high initial capital needed for the SAGSP system due to the GHE and solar collectors, the annual operation costs dropped considerably. This was caused by high rates of energy saving and a high overall efficiency of the system.

The heating system of the Green Energy Lab in China was simulated with TRNSYS by Andersen and Li [56]. The SAGSHP model reported a 26% reduction in electricity consumption.

Bellos et al. [57] simulated 3 systems with PV, FPC and PVT combined with a water source heat pump and compared them to an air source heat pump-PV configuration, the electricity cost being the major parameter for the feasibility of systems. PVT is the most promising and environment friendly alternative, as it leads to exceptionally low grid consumption and the air source-PV is most sustainable for current electricity prices.

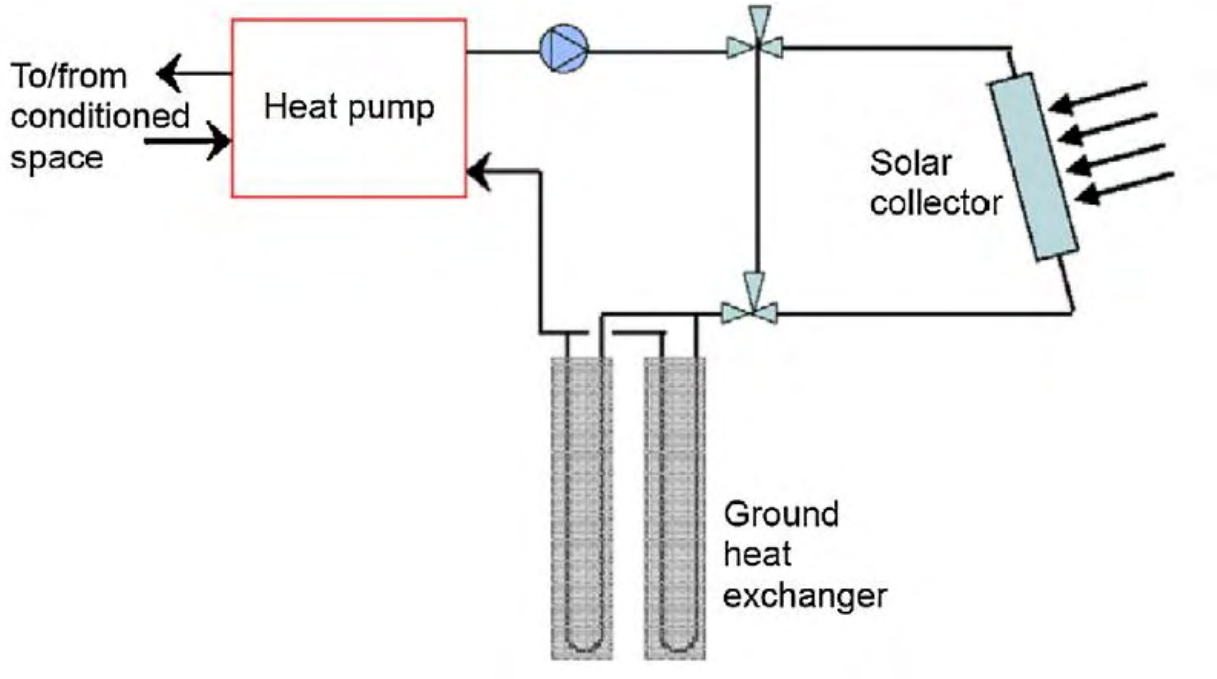

Fig. 2.25: Diagram of a combination of GCHP and solar collectors [26]

3. SIMULATION STUDY

To fully assess the potential of SAGSHPs, a university complex has been chosen for simulation and three alternative SAGSHP concepts are investigated and in the end compared energetically and economically.

The examined buildings are located in Volos, Greece and were built to house the Department of Electrical and Computer Engineering which belongs to the School of Engineering of the University of Thessaly. There are 2 separate buildings, of 4 levels each, with a total area of 2644 m^2. The larger of the two, accommodates the student facilities like classrooms, labs, amphitheater etc. The other is used for offices, administration and conference rooms.

The building is located at sea level and according to KENAK in a type B climate zone [58] (based on the annual heating degree-days, with B being the second warmest). In type B climate zone, temperatures are more moderate during both winter and summer. Two Ground-water HPs have been installed, one in each building, with capacities of 159/130 kW and 121/97.2 kW heat/cool respectively. The HPs draw brackish water located a few tens of meters below the surface. The groundwater has an average temperature of 17.1 °C throughout the year. A natural gas boiler and central A/C have also been installed but are used exclusively when heat/cool demands exceed the peak design load, which is rare and as such will not be included in the simulations, considering the focus of the study is the operation of SAGSHPs.

3.1 The SAGSHP systems simulated

The 3 Solar Assisted Ground Source Heat Pumps systems simulated are the following:

1. FPCs are installed for preheating the water coming from the ground and then entering the Groundwater HP.

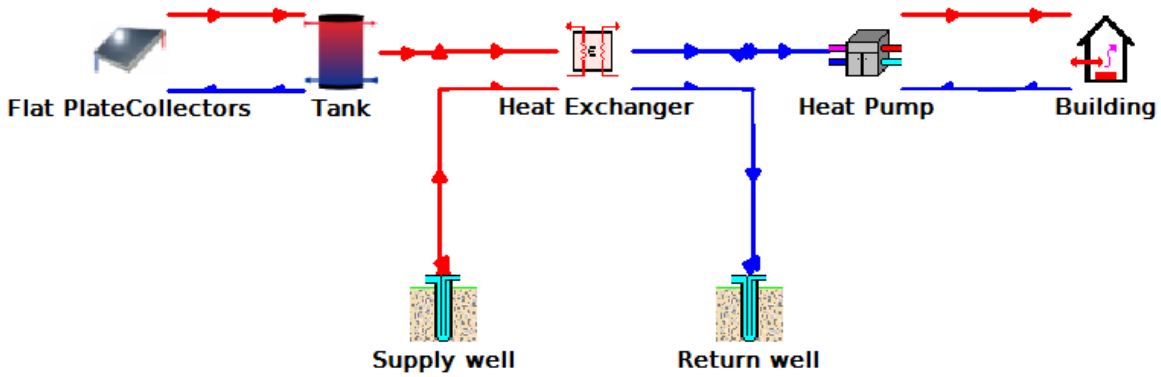

2. PV panels are installed, that provide a percentage of the required electrical power when there is demand, otherwise feeding it to the grid, through a net metering strategy.

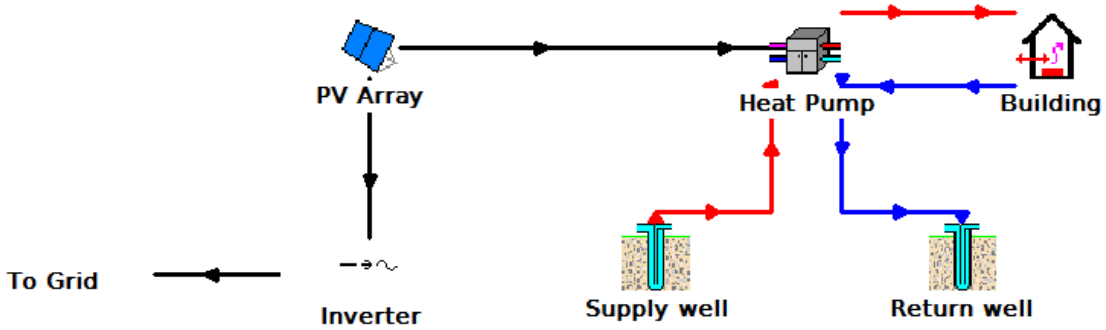

3. PV/Ts are installed, combining the aforementioned processes.

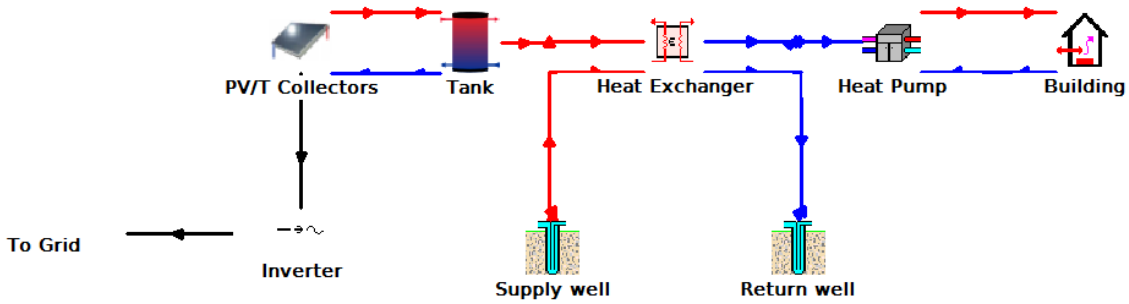

The previous diagrams present a simplified view of the installations. Although the simulation software can model the thermal behavior of buildings (even with multiple zones), only the heating/cooling systems are simulated. That is because the heating/cooling performance has already been investigated, before the completion of construction. The technical service of the university, which is responsible for construction planning and designing of the two buildings, reports that the GWHPs capacities were chosen to deliver even the peak heating/cooling loads.

The FPC, PV, PV/T panels can be installed on the southern building's roof of 400 m^2 which is more than adequate for these systems. The buildings orientation is at 20° to the North-South axis, providing excellent capability of installing any panels facing south (azimuth=0). Being the tallest building in the area, no physical objects can shade the panel array.

Fig. 3.1: Rooftop area of 400 m^2, suitable for solar panel installation (photo and measurements taken from the national land registry of Greece) [59].

3.2 TRNSYS Simulation Tool

The existing GSHPs found in the university buildings are modelled and simulated with TRNSYS tool. TRNSYS is a modular simulation environment for the simulation of transient systems, including multi-zone buildings. It is used by engineers and researchers globally to model novel energy concepts, from simple DHW systems to the design and simulation of buildings and their equipment, including control strategies, occupant behavior and *alternative energy systems* (wind, solar, photovoltaic, hydrogen systems). TRNSYS was chosen for this study because of its vast library of components, including the advanced RES devices that are the focus of this analysis, and its ability to simulate large dynamic systems with numerous inputs and outputs.

The University of Wisconsin-Madison Solar Energy Lab and Colorado State University Solar Energy Applications Lab began joint research of new solar technologies in the 1970s, funded by the ERDA (currently DOE). PhD candidate, S. Klein from the University of Wisconsin-Madison developed a software package in FORTRAN language to model the energy profile of buildings. This program was later named TRNSYS and has been commercially available since 1975. For 45 years, it has been highly successful, mainly due to its open, modular structure. The source code of the kernel as well as the component models is delivered to the end users. This simplifies extending existing models to make them fit the user's specific needs. Additionally, it allows users and third-party developers to easily add custom component models, using all common programming languages (C, C++, PASCAL, FORTRAN, etc.). Moreover, TRNSYS can be easily connected to many other applications, for pre- or postprocessing or through interactive calls during the simulation (e.g. Microsoft Excel, Matlab, etc.).

TRNSYS simulations are constructed by connecting individual component models (known as Types) together into a complete model. These individual components represent a piece of equipment that can be represented by a system of equations to calculate its performance, such as pumps, pipes, chillers, solar collectors, etc. These are then connected together in the TRNSYS environment similarly to how they would be connected in real life. After initiating the simulation, at each of its timestep, the kernel calls the Type routines once in the order that the Types appear in the input file. It then checks the inputs to the Types and re-calls each Type that inputs have changed from the previous call. It continues this process until the inputs to all of the Types are no longer changing. Then it moves to the next timestep and repeats the process. When a simulation is complete, TRNSYS displays the online plotter, writes an error log file and any output files that have been set-up for the simulation.

Types in TRNSYS are basically black boxes. The TRNSYS kernel feeds inputs to the black box and in turn, the black box produces outputs. The kernel takes care of solving the system of black boxes. Time dependent inputs are referred to as *Inputs* while time independent inputs are referred to as *Parameters*. At each iteration and at each time step, a component turns the current values of the *Inputs* and *Parameters* into *Outputs*.

Fig. 3.2:TRNSYS logo [60]

For all simulations, after testing several values, a timestep of 3 minutes was utilized, as it captures all the necessary details while being time efficient as well. The simulations run for 8760 hours, from the 1st of January 00:00 to December 31st 23:00, a whole year. The types used in TRNSYS are described next, listing all of the necessary Inputs and Parameters as well as the mathematical models that the kernel runs while executing their subroutines.

For better comprehension, details of Types found in all simulation scenarios are presented first. Afterwards Types utilized in specific models are described.

3.3 General simulation components

3.3.1 Weather Data Processor, Type 15

The component reads hourly meteorological data from an external weather data file, interpolating the data (including solar radiation for tilted surfaces) at timesteps of less than one hour, and transfers it to other TRNSYS components. The model also calculates numerous variables like mains water temperature, the effective sky temperature, and the heating and cooling season forcing functions.

Parameters	
File Type	Related to input file
Logical unit	Related to input file
Tilted Surface Radiation Mode	-3
Ground reflectance - no snow	0.2
Ground reflectance - snow cover	0.7
Number of surfaces	1
Tracking mode	1
Slope of surface	45
Azimuth of surface	0 (South)

The parameters above are needed for the calculation of the incident radiation on the panels. These are the same for all: Azimuth = 0 (facing South) and their slope of 45°. The Outputs on the right are the result of reading values the input file and various calculations. This type can read numerous weather file formats such as Typical Meteorological Year Version 3 (TMY3) files, Energy+ format (.EPW), International Weather for Energy Calculations (IWEC) format, Canadian Weather for Energy Calculations (CWEC) format, Meteonorm formats (.TM2), German TRY formats and more.

In this case Energy+ format (.EPW) is used, the reason being described next.

The weather file concerning the examined buildings in Volos, was taken from the PVGIS database and resource map [61]. PVGIS is a web application that provides solar radiation data to users, in order to estimate the energy generation of potential solar plants as well as a TMY generator for most regions of the world. It is free to use, with no restrictions on and with no registration necessary.

PVGIS has been developed at the European Commission Joint Research Centre, at their respective lab in Ispra, Italy since 2001. The focus of PVGIS is research in solar resource assessment, photovoltaic performance studies, and the dissemination of knowledge and data about solar radiation and PV performance. Its most known work is the online PVGIS web application, but there is a large amount of research done to achieve results as accurate as possible. The current version is PVGIS 5. Each new version of PVGIS extends the available regions and adds new calculation tools.

Outputs
Dry bulb temperature
Dew point temperature
Wet bulb temperature
Effective sky temperature
Mains water temperature
Humidity ratio
Percent relative humidity
Wind velocity
Wind direction
Atmospheric pressure
Total sky cover
Opaque sky cover
Extraterrestrial solar radiation
Global horizontal radiation (not interpolated)
Direct normal radiation (not interpolated)
Solar zenith angle
Solar azimuth angle
Total horizontal radiation
Horizontal beam radiation
Sky diffuse radiation on the horizontal
Ground diffuse radiation on the horizontal
Total diffuse radiation on the horizontal
Angle of incidence for horizontal
Total tilted surface radiation for surface
Beam radiation for surface
Sky diffuse radiation for surface
Ground reflected diffuse radiation for surface
Total diffuse radiation for surface
Angle of incidence for surface
Slope of surface
Azimuth of surface
Latitude
Longitude
Shift in solar time hour angle
Site elevation
Heating season indicator
Cooling season indicator
Monthly average temperature
Monthly minimum temperature
Monthly maximum temperature
Annual average temperature
Annual minimum temperature
Annual maximum temperature
Global horizontal illuminance
Direct normal illuminance
Diffuse illuminance on horizontal
Zenith luminance
Horizontal visibility
Ceiling height
Precipitable water
Aerosol optical depth
Snow depth
Days since last snowfall
Month
Hour of the month
Hour of the day
Day of the year
Day of the month
Ground reflectance

At the moment the calculations that can be made with PVGIS are:

- Performance of grid-connected PV
- Performance of tracking PV systems
- Performance of off-grid PV systems
- Monthly radiation
- Daily radiation
- Hourly radiation
- But most importantly for this study, a TMY tool to generate Typical Meteorological Year (TMY) data of solar radiation, temperature and other meteorological data, used in many fields, for instance in the calculation of the energy performance of buildings.

A *typical meteorological year* (TMY) is a collection of meteorological data for a specific location, listing hourly values of solar radiation and various meteorological resources for a period of 1 year. The values are generated from a database of a much longer duration, no less than twelve years. The values are particularly selected in order to represent the whole range of weather phenomena for the designated locality, while still providing yearly averages that are consistent with the long-term averages of that location. TMY files are often used in building simulations, to properly evaluate the potential heating and cooling loads when designing the building. The files are utilized in the modelling of solar energy systems including solar heating or DHW systems. Because they display mostly typical instead of extreme weather, designers should not utilize these databases worst-case scenarios are modeled at a location.

The TMY tool of PVGIS can be used to interactively visualise all the data or to download as a text file. The output can be of EPW, JSON or CSV format.

Among other things, a TMY file can contain hourly values of:

- Dry Bulb Temperature
- Relative Humidity
- Global Horizontal Irradiance
- Direct Normal Irradiance
- Diffuse Horizontal Irradiance
- Infrared Radiation
- Wind Speed
- Wind Direction
- Air Pressure

Some data visualization is given next:

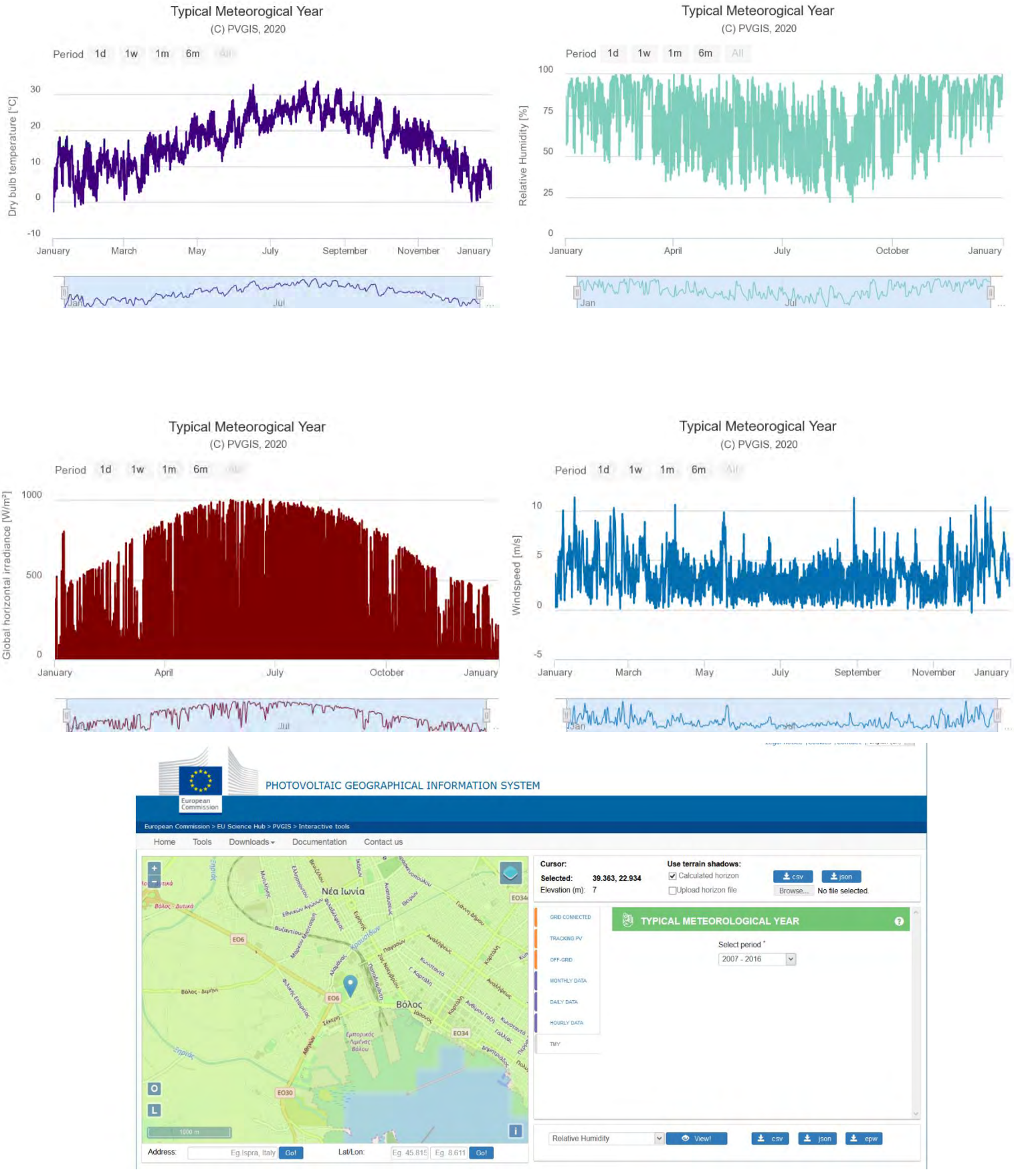

Fig. 3.3: Screenshot of the TMY tool in PVGIS [61].

The output of the weather component can be connected to various other Types, like the Psychometrics calculation, FPC panel, PV panel, PV/T panel, control components and generally any Types that require basic inputs like ambient temperature. The panels Types are useless without the radiation values calculated by the weather component.

3.3.1.1 Calculation of Radiation

The total radiation on a tilted surface (in this case the FPCs, PVs and PV/Ts), was calculated by the model developed by Perez et al [62]. This model accounts for circumsolar, horizon brightening, and isotropic diffuse radiation by empirically derived "reduced brightness coefficients". The reduced brightness coefficients, F'1, F'2, are functions of sky clearness, e, and sky brightness, Δ, parameters.

$$\varepsilon = \frac{\frac{I_d + I_{dn}}{I_d} + 1.041\ \theta_z^3}{1 + 1.041\ \theta_z^3}$$

Where θ_z is:

$$\Delta = \frac{I_d}{I_{on}} = \frac{I_d}{I_o}$$

And

$$\mathrm{F1} = \mathrm{F11}(\varepsilon) + \mathrm{F12}(\varepsilon)\ \Delta + \mathrm{F13}(\varepsilon)\ \theta\ \mathrm{Z}$$
$$\mathrm{F2} = \mathrm{F21}(\varepsilon) + \mathrm{F22}(\varepsilon)\ \Delta + \mathrm{F23}(\varepsilon)\ \theta\ \mathrm{Z}$$

The Perez coefficients (F_{11} etc.) can be found in corresponding tables. The angular location of the circumsolar region is determined by the ratio a/c.

$$\frac{a}{c} = \frac{\max[0, cos\theta]}{\max[cos\ 85, cos\theta z]}$$

The tilted surface diffuse radiation can be estimated by the following

$$I_{dT} = Id\ [0.5\ (1 - F'1)\ (1 + cos\ \beta) + F'1(a/c) + F'2\ sin\ \beta]$$

Thus the total radiation incident on a tilted flat surface for all tilted surface radiation modes is

$$I_T = I_{bT} + I_{dT} + I_{gT}$$

where I_{bT} is Beam radiation on tilted surface and I_{gT} is Ground reflected radiation on a tilted surface, which are contained in the TMY file.

3.3.2 Water-to-Water Heat Pump, Type 668

Obviously the groundwater heat pump is present in all scenarios. The component simulates a single-stage HP. The HP heats or cools one liquid flow by rejecting energy to or absorbing energy from a second. The component follows the same temperature level control of an actual HP. When the incoming control signal is ON in either heating or cooling mode, it is activated and runs at the capacity read from data files until the control signal turns to OFF. This component is part of the TESS library.

The component relies on data found in manufacturer catalogs for HPs. The core of the model is based on 2 data files: a file containing cooling performance data, and a file containing heating performance data. From these sources *power draw and capacity* of the HP (in cooling/heating) as functions of evaporator fluid temperature and condenser fluid temperature.

The Type668 heat pump is equipped with two control signals, one for heating and one for cooling. If the heat pump is determined to be ON in heating mode, Type668 calls the TRNSYS Data subroutine with the entering source and load fluid. The Data routine accesses the heating performance data file and returns the machine's heating capacity and power draw. The same procedure is followed for cooling. So when the control signal is ON. $Q_{abs} = Q_{tr} - P_{HP}$ is absorbed from the source liquid stream and transferred to the load liquid stream.

The Parameters of this component are solely for the heating and cooling performance files and shall not be presented.

Inputs
Inlet source temperature
Source flow rate
Inlet load temperature
Load flow rate
Cooling control signal
Heating control signal

Outputs
Outlet source temperature
Source flow rate
Outlet load temperature
Load flow rate
Heat transfer to load
Heat transfer from source
Heat pump power
Coefficient of Performance (C.O.P)

The inlet source temperature is the temperature of the groundwater, 17.1 °C, after passing through a heat exchanger of efficiency η=1. The cooling and heating control signal inputs are linked to differential controllers, accepting values of 1 and 0 when there is demand or not. With heating and cooling control schemes, the temperature difference between Outlet load and Inlet load of the HP is always 5°C, described later in the control component section. Inlet load and source flow rates as well as Inlet load and source flow rates are provided by pumps depending on whether heating or cooling is needed. More details are presented in the pumps section. Heat transfer to load, heat transfer from source, heat pump power and COP values are then written into output files, to be processed later for data visualization and other necessary calculations.

3.3.2.1 Heat Pumps installed

The core of the simulations, the Groundwater HPs installed in the two buildings are the ***CWW/K/WP 302P and CWW/K/WP 393P models of CLINT*** with nominal heat/cool capacities of *121/97.2 kW and 159/130 kW respectively***.** Key pages, containing necessary data about the HPs, are presented in the appendix. The cooling and heating performance data files, read by the Type 668 components, have been constructed from the values found on pages 12 and 13 respectively, which are the HPs cooling and heating capacities and their corresponding electrical power input, relative to the condenser outlet and evaporator outlet temperature.

Fig. 3.4: CWW/K/WP reversible heat pump unit

		TEMPERATURA ACQUA USCITA CONDENSATORE °C / *CONDENSER LEAVING WATER TEMPERATURE °C* WASSERTEMPERATUR AM VERFLÜSSIGERAUSTRITT °C / *TEMPERATURE SORTIE EAU CONDENSEUR °C* (Δt in/out=5K)							
		30		**35**		40		45	
	To(°C)	**kWf**	**kWe**	**kWf**	**kWe**	**kWf**	**kWe**	**kWf**	**kWe**
302-P	5	96,5	19,7	90,2	21,8	83,6	24,2	76,8	27,1
	6	100	19,7	93,6	21,8	86,9	24,2	79,9	27,1
	7	104	19,7	**97,2**	**21,8**	90,3	24,2	83,1	27,1
	8	108	19,7	101	21,8	93,8	24,2	86,3	27,1
	9	112	19,7	105	21,8	97,3	24,2	89,7	27,1
	10	116	19,7	108	21,8	101	24,2	93,1	27,2
393-P	5	131	25,5	121	28,5	110	31,8	98,2	35,6
	6	136	25,6	126	28,5	114	31,8	102	35,6
	7	141	25,6	**130**	**28,5**	119	31,8	106	35,7
	8	146	25,6	135	28,5	123	31,9	110	35,7
	9	152	25,6	140	28,5	128	31,9	114	35,7
	10	157	25,6	145	28,5	133	31,9	119	35,7

kWf: Cooling capacity (kW)
kWe: Power input (kW)
To: Evaporator leaving water temperature (Δt in./out = 5 K)

		TEMPERATURA ACQUA INGRESSO/USCITA CONDENSATORE °C *CONDENSER INLET/OUTLET WATER TEMPERATURE °C* WASSERTEMPERATUR AM VERFLÜSSIGEREIN-AUSTRITT °C *TEMPERATURE DE L'EAU ENTRÉE/SORTIE AU CONDENSEUR °C*					
	To (°C)	30/35		35/40		**40/45**	
		kWt	kWe	kWt	kWe	kWt	kWe
302-P	8	131	23,2	122	25,8	112	28,8
	9	136	23,3	126	25,8	117	28,8
	10	141	23,3	131	25,8	**121**	**28,8**
	11	146	23,3	136	25,8	126	28,8
	12	151	23,3	141	25,8	130	28,8
	13	157	23,3	146	25,8	135	28,8
393-P	8	181	30,7	165	34,2	148	38,4
	9	188	30,7	171	34,3	153	38,4
	10	195	30,7	178	34,3	**159**	**38,4**
	11	202	30,7	184	34,3	165	38,4
	12	209	30,7	191	34,3	171	38,4
	13	216	30,8	198	34,4	178	38,5

To :Evaporator leaving water temperature (Δt in/out = 5 K)
kWt : Heating capacity (kW)
kWe : Power input (kW)

Fig. 3.5: Cooling and heating performance data tables, for the 302-P and 393-P models of the CWW/K/WP series

3.3.3 Synthetic Building Load Generator, Type 686

Hourly cooling and heating loads are generated for a synthetic building based on peak loads and provided harmonic functions used to justify seasonal, hourly and weekday/weekend deviations. Random noise can be generated as well on both an hourly basis and a daily basis to calculate a more realistic profile of building loads. This component is perfect for simulations

in which peak loads are already provided. It delivers realistic loads without the time-consuming process of modeling an entire real building.

Parameters	
Which Day of the Week is Sunday?	7
Peak Cooling Load Hour	12
Peak Heating Load Hour	9
Start of Cooling Season	3240
End of Cooling Season	6192
Start of Heating Season	7320
End of Heating Season	2520
Weekday Offset for Cooling	0.4
Weekday Multiplier for Cooling	0.5
Weekend Offset for Cooling	0
Weekend Multiplier for Cooling	0
Weekday Offset for Heating	0.2
Weekday Multiplier for Heating	0.5
Weekend Offset for Heating	0
Weekend Multiplier for Heating	0
Seasonal Offset for Cooling	0.0
Seasonal Multiplier for Cooling	1.0
Seasonal Offset for Heating	0.0
Seasonal Multiplier for Heating	1.0
Standard Deviation for Daily Noise	0.2
Standard Deviation for Hourly Noise	0.1
Peak Cooling Load	130/97.2 kW for 393P/302P
Peak Heating Load	159/121 kW for 393P/302P

Outputs
Cooling Load
Heating Load
Multiplier for Seasonal Cooling
Multiplier for Seasonal Heating
Multiplier for Daily Cooling Load
Multiplier for Daily Heating
Daily Noise Multiplier
Hourly Noise Multiplier

Peak cooling load was chosen at noon (12:00) as temperature and general heat gains are maximize around that time. For heating, 9:00 in the morning was decided upon, as that is the time when lectures start and heating has been turned off since the previous day. The cooling season for buildings in climate zones A, B starts May 15th (3240 hrs.) and ends September 15th (6192 hrs.). Likewise, the heating season starts November 1st (7320 hrs.) and ends 15th of April (2520 hrs.), according to KENAK [58]. Apart from the peak loads, the rest of the parameters are used for the periodical behavior of the loads and the introduction of randomness. Universities are closed on weekends and therefore their multipliers are set to 0. Hourly and daily noise can cause the peak condition to be exceeded as well as the choice of offset and multiplier parameters for the seasonal and daily variations of the load. They have been therefore set to values lower than the defaults. The peak loads have been set to values of the HPs capacities as it was designed that HPs capacities would cover the heating and cooling peaks, as was described earlier.

The hourly heating and cooling loads for a building are defined in this component as:

$$Load = DesignLoad * X_{day} * X_{hour} * X_{noise,hour} * X_{noise,day}$$

3.3.4 Holiday Calculator, Type 95 

The component performs numerous "calendar computations" based on the starting date of a TRNSYS simulation and the elapsed time. These results may be useful when dealing with time-dependent load patterns. The outputs of this component include the year, month, date, and day of week, hour of day and an indication as to whether the current time step falls on a holiday or on a non-holiday. Type 95 accounts for leap years and daylight savings time.

Parameters	
Mode	2
Year	2020
Initial simulation start time	0
Daylight savings time flag	2
Month of holiday	Each holiday month inserted here
Date of holiday	Each holiday date inserted here

Outputs
Hour of day
Hour of year
Day of year
Day of week
Month
Date
Year
Weekend Flag
Holiday flag

The heating and cooling loads from Type 686, after being generated, are then passed through this component that might increase the values depending on what day is simulated. For example, when it happens to be a holiday, loads are zero but on Mondays in heating season they are increased because the HPs have not operated for two consecutive days, thus the temperatures of the buildings have fallen.

As stated before, the heating season is between November 1st (7320 hrs.) and 15th of April and cooling is from May 15th (3240 hrs.) till September 15th (6192 hrs.). Universities in Greece operate for 10 months (closed for July and August), five days a week, 13 hours a day (8:00 to 21:00) according to KENAK [58]. Only during these hours and when it is not a holiday, is the heating/cooling load value let through to the component responsible for applying loads on a liquid stream (explained in the next segment). The holidays accounted for in this simulation are (taken for 2020):

Christmas 24/12-7/1
Clean Monday 2/3
Independence Day 25/3
Easter 13/4-24/4
May Day 1/5
Holy Spirit Day 1/6
National Anniversary 28/10
Anniversary of Polytechnic Sc. 17/11

3.3.5 Heating and Cooling Loads Imposed on a Flow Stream, Type 682

This model simply imposes a user-specified load on a flow stream and calculates the resultant outlet fluid conditions. Often in simulating an HVAC system, the heating and cooling loads on the building have already been determined, either by measurement or through the use of another simulation program and yet the simulation task at hand is to simulate the effect of these loads upon the system. This component allows for there to be an interaction between such pre-calculated loads and the HVAC system by imposing the load upon a liquid flowing through a device. Type682 can be thought of as an interaction point between a building load and the liquid working fluid in an HVAC system.

Mathematically, this model is very simple, the user provides the flow rate, specific heat, and temperature of liquid at a point in the system loop. The building loads are added to, or subtracted from that liquid, resulting in an outlet temperature just past the interaction point.

$$T_{out} = T_{in} + \frac{\dot{Q}}{\dot{m}C_p}$$

According to the sign convention, a positive load will result in an outlet temperature higher than the inlet temperature and vice versa; a negative load results in an outlet temperature lower than the inlet temperature.
The sole parameter of this Type, is the specific heat of the fluid and is set to 4.19 kJ/kg*K.

Inputs
Inlet temperature
Inlet flow rate
Load

Output
Outlet temperature
Outlet flow rate
Heat transfer

Inlet temperature and flow rate are supplied by the water-to-water HP (type 668) and the temperature increases or decreases depending on the load which is supplied by the load generator (686) after meeting the holiday/operational hours requirements.

3.3.6 Storage Tank, Uniform Losses, Type 60

Type60 models a stratified liquid storage tank. It allows multiple heat exchangers within the tank and unmatched numbers of inlet and outlet flows. Type60 models a vertically cylindrical tank with one inlet and one outlet flow. Users may define between 0 and 3 (inclusive) internal heat exchangers. It further includes calculation of losses from the tank to

the flue if desired and assumes that all stratification nodes of the tank are uniform in size and that the UAs between each node and the ambient are equal.

The thermal performance of a water-filled sensible energy storage tank, subject to thermal stratification, can be modeled by assuming that the tank consists of N (N ≤ 100) fully-mixed equal volume segments. The degree of stratification is determined by the value of N. If N is equal to 1, the storage tank is modeled as a fully-mixed tank and no stratification effects are possible. Options of fixed or variable inlets, unequal size nodes, temperature dead band on heater thermostats, incremental loss coefficients, internal submersed heat exchangers, non-circular tanks, horizontal tanks are all available.

The water in the piping network of the buildings, that is heated or cooled, is simulated by this component. The total volume has been set to 2 m^3. In essence, water flows from the tank (piping network) to the HP, is heated or cooled, then flows through type 682 and therefore loses or gains heat and in the end flows back to the tank, changing its average temperature. To simulate the control of the heat pump, in heating season its temperature has to be kept at 45°C +/- 1 and for cooling it is 7°C +/- 1. These are the nominal temperatures that the HPs produce and are therefore chosen for the desired temperature of the water in the piping network as well as its terminal fan coil units. More details are found in the differential control segment. Instances of this component are also used for the heat storages of the FPCs and PV/T systems. These are studied in detail in their corresponding sections.

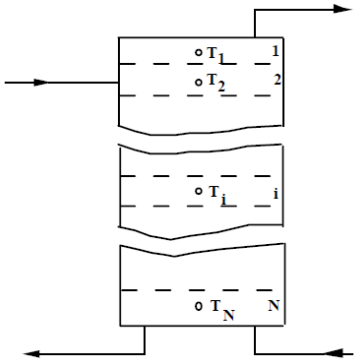

Fig. : 3.6

Illustration of the stratified storage tank

3.3.7 ON/OFF Differential Controller, Type 2

This controller generates a control function γ0 that can have values of 0 or 1. The value of γ0 is chosen as a function of the difference between upper and lower temperatures, TH and TL, compared with two dead band temperature differences, ΔTH and ΔTL. The new value of γ0 is dependent on whether γi = 0 or 1. The controller is normally used with γ0 connected to

γi giving a hysteresis effect. For safety considerations, a high limit cut-out is included with this controller. Regardless of the dead band conditions, the control function will be set to zero if the high limit condition is exceeded. This controller instance uses unit descriptions of °C so that it is readily usable as a thermostatic differential controller.
Mathematically, the control function is expressed as follows:
If the controller was previously on:

$$\text{If } \gamma\text{i} = 1 \text{ and } \Delta\text{TL} \leq (\text{TH} - \text{TL}), \gamma\text{o} = 1$$
$$\text{If } \gamma i = 1 \text{ and } \Delta\text{TL} > (\text{TH} - \text{TL}), \gamma\text{o} = 0$$

If the controller was previously off:

$$\text{If } \gamma\text{i} = 0 \text{ and } \Delta\text{TH} \leq (\text{TH} - \text{TL}), \gamma\text{o} = 1$$
$$\text{If } \gamma\text{i} = 0 \text{ and } \Delta\text{TH} > (\text{TH} - \text{TL}), \gamma\text{o} = 0$$

However, the control function is set to zero, regardless of the upper and lower dead band conditions, if Tin > Tmax. This situation is often encountered in domestic hot water systems where the pump is not allowed to run if the tank temperature is above some prescribed limit.

Parameters	
No. of oscillations	7
High limit cut-out	100 for heating, 0 for cooling

Inputs
Upper input temperature Th
Lower input temperature Tl
Monitoring temperature Tin
Input control function
Upper dead band dT
Lower dead band dT

For heating, the Upper input temperature Th is set to 45 and the Lower input temperature Tl is the average temperature of the tank resembling the piping network. For cooling, Th is the average tank temperature and Tl is set to 7. Dead bands are set to 1°C. More instances of the diff. controller are used, like in changing the flow rate that the hydronic pumps provide or the control of the FPC and PV/T systems. Details are given in respective sections.

3.3.8 Variable Speed Pump, Type 110 

Type 110 models a variable speed pump that is able to maintain any outlet mass flow rate between zero and a rated value. The mass flow rate of the pump varies linearly with

control signal setting. Pump power draw, however, is modeled using a polynomial. Pump starting and stopping characteristics are not modeled, nor are pressure drop effects. Type110 takes mass flow rate as an input but ignores the value except in order to perform mass balance checks.

Type 110 sets the downstream flow rate based on its rated flow rate parameter and the current value of its control signal input. For the two pumps of the main loop, there are three levels of flow rate. One for zero flow (signal = 0) and one for each season. That is because the evaporator and condenser have different operating flow rates and when the heating season changes to cooling and vice versa, they switch loops e.g. in heating season the evaporator is connected to the groundwater-HP loop and in cooling changes to the HP-building loop.

The operational flow rates of the condenser and evaporator for the 302P and 393P models according to the technical manual are:

302-P	*MODEL*	393-P	
	Evaporator:		
4,64	*Water flow (1)*	6,23	l/s
	Condenser:		
5,69	*Water flow (1)*	7,59	l/s

3.3.9 Heat Exchanger with Constant Effectiveness, Type 91

A zero capacitance sensible heat exchanger is modelled as a constant effectiveness device which is independent of the system configuration. For the constant effectiveness mode, the maximum possible heat transfer is calculated based on the minimum capacity rate fluid and the cold side and hot side fluid inlet temperatures. In this mode the effectiveness is input as a parameter and the concept of an overall heat transfer coefficient for the heat exchanger is not used.

In all instances of this component, the efficiency has been set to 1.

Parameters	
Heat exchanger effectiveness	1
Specific heat of hot side fluid	4.19
Specific heat of cold side fluid	4.19

Inputs	Outputs
Hot side inlet temperature	Hot-side outlet temperature
Hot side flow rate	Hot-side flow rate
Cold side inlet temperature	Cold-side outlet temperature
Cold side flow rate	Cold-side flow rate

Online graphical plotter (Type 65), Printer - to output file (Type 25) and Integrator (Type 24) have been extensively used for graphs, creating data files integrating various hourly rates (e.g. electricity consumption of the HP). Details of these components are trivial and not presented here.

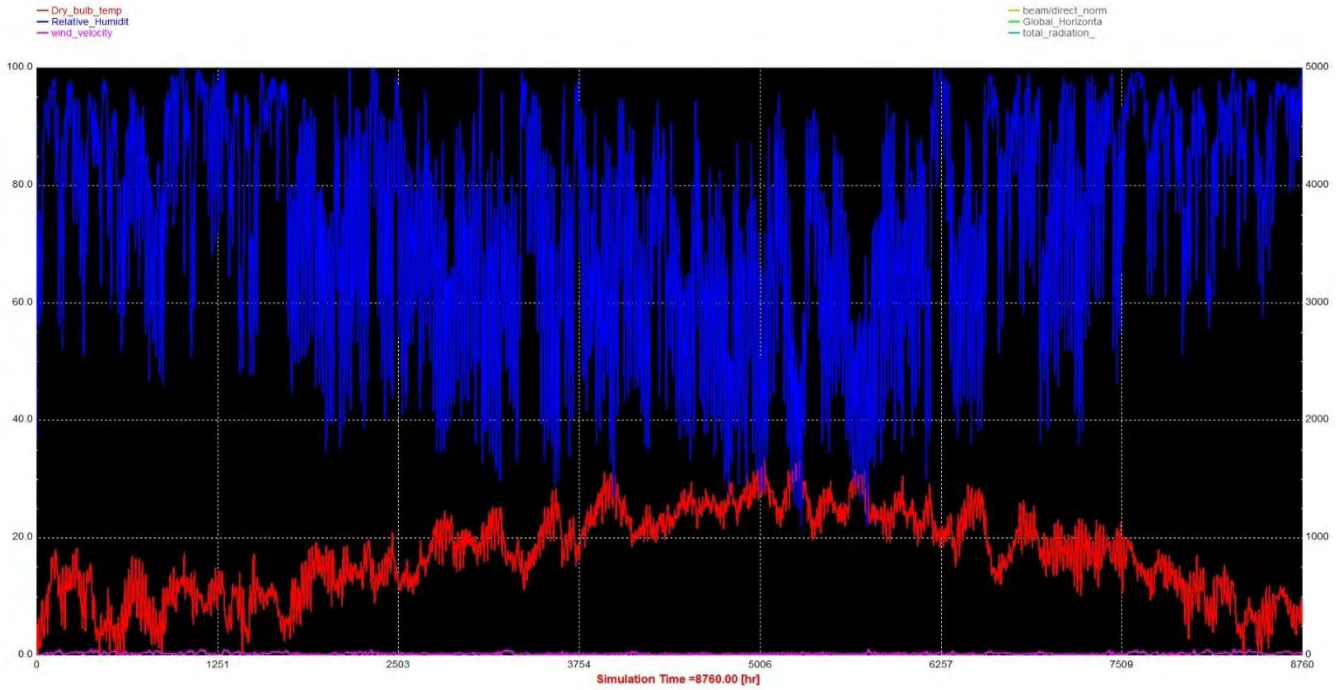

Fig. 3.6: Snapshot from the online plotter

In the next segment details and components for specific systems are presented.

3.4 Flat Plate Collector (FPC) system

In this system, water is heated by an array of FPCs and stored in an insulated hot water tank. When there is sufficient hot water, a secondary pump turns on, circulating water from the tank to a heat exchanger and back. In the heat exchanger, heat flows from this loop to another water flow with groundwater temperature. This results in a rise in temperature (e.g from 17 to 20°C) of the source flow and sequentially *in higher COP and therefore energy savings*.

The position of the sun can be calculated by its altitude β above the horizon and its azimuth ϕ in horizontal plane. To determine the *angle of incidence* θ between a direct solar beam and the normal to the surface, the surface azimuth ψ and the surface-solar azimuth γ must be known. γ is the angular difference between the solar azimuth ϕ and the surface azimuth ψ.

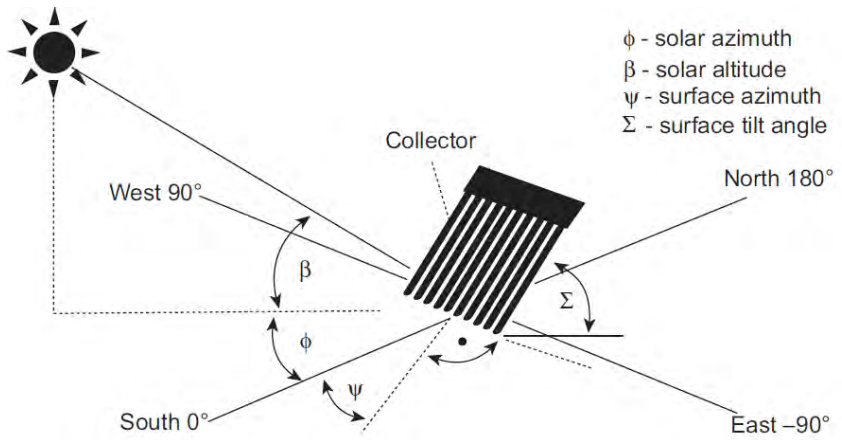

Fig. 3.7: Collector angles [10].

The angles δ, β, and ϕ are always positive. For a surface with tilt angle Σ (measured from the horizontal), the angle of incidence q is given by [10]

$$\cos\theta = \cos\beta \cos\gamma \sin\Sigma + \sin\beta \cos\Sigma$$

For vertical surfaces, Σ = 90 degrees, while for horizontal Σ=0. Hour angle ω is the angular displacement of the sun east or west of the local meridian due to rotation of the earth on its axis at 15 degrees per hour. When a beam of thermal radiation is incident on the surface of a body, part of it is reflected away from the surface, part is absorbed by the body, and part is transmitted through the body. The various properties associated with this phenomenon are the fraction of radiation reflected, called reflectivity (r); the fraction of radiation absorbed, called absorptivity (a); and the fraction of radiation transmitted, called transmissivity (s). The three quantities are related by the following equation:

$$\rho + \alpha + \tau = 1$$

Solar radiation that is captured consists of a) direct (beam) solar radiation, b) diffuse solar radiation, and c) ground reflected radiation. The total radiation received from the sun, of a horizontal surface at the level of the ground for a clear day, is the sum of the direct, diffuse

and reflected radiations. Direct radiation depends on the orientation of receiving surface while diffuse and reflected radiation are dependent on surface orientation.

$$I_T = I_B + I_D + I_G$$

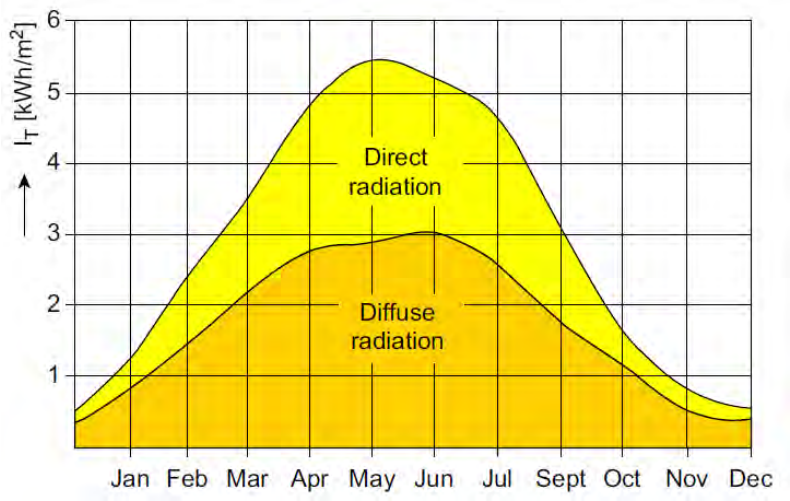

Fig. 3.8: Direct and Diffuse radiation [10].

The instantaneous efficiency η of a collector operating under steady conditions is defined mathematically as

$$\eta = \frac{Q}{A_c I_T} = \frac{mc_p(t_i - t_o)}{A_c I_T}$$

where Q is the usable energy of collector, Ac is the collector surface area and Iτ is the solar radiation intensity. The Hottel-Whillier-Bliss form gives [22]:

$$Q = A_c[I_T(\alpha\tau) - U_L(t_p - t_a)]$$

U_L is the overall heat loss coefficient, tp is the absorber plate temperature and ta is the ambient air temperature. Thus,

$$\eta = (\alpha\tau) - \frac{U_L(t_p - t_a)}{I_T}$$

After some modifications a general form can be written as

$$\eta = \eta_0 - \alpha_1 \frac{(t_m - t_a)}{I_T} - \alpha_2 \frac{(t_m - t_a)^2}{I_T}$$

where η0, a1, and a2 are constants relative to the considered solar collector, $t_m = \frac{t_i - t_o}{2}$ is the average of the fluid inlet and outlet temperatures.

3.4.1 Solar Collector component, Type 1

This component is obviously the core of this system. It models the thermal performance of a flat plate solar collector. The solar collector array may consist of collectors connected in series and in parallel. The thermal performance of the collector array is determined by the number of modules in series and the characteristics of each module. The user must provide results from standard tests of collector efficiency versus a ratio of fluid temperature minus ambient temperature to solar radiation. The fluid temperature may be the inlet temperature, the average temperature, or the outlet temperature. In Type1, there are 5 possibilities for considering the effects of off-normal solar incidence. In the instance of Type1 used here, the incidence angle modifiers are read from an external data file as a function of the transversal and longitudinal incidence angles.

The *Incidence Angle Modifier (IAM)* is a parameter that affects significantly the collector efficiency. Collector tests are generally performed on clear days at normal incidence so that the transmittance - absorptance product (τα) is nearly the normal incidence value for beam radiation, $(\tau\alpha)_n$. The intercept efficiency, FR $(\tau\alpha)_n$, is corrected for non-normal solar incidence by the factor $(\tau\alpha)/(\tau\alpha)_n$. By definition, (τα) is the ratio of the total absorbed radiation to the incident radiation. In this instance of Type1, the incidence angle modifiers are read from an external data file as a function of the incidence angle.

Parameters	
Number in series	Numerous values were tested
Collector area	Numerous values were tested
Fluid specific heat	4.190 kJ/kgK
Efficiency mode	2
Tested flow rate	140.4 kg/hr.m^2
Intercept efficiency	0.67
Efficiency slope	3.61 kJ/hr.m^2.K
Efficiency curvature	0.017 kJ/hr.m^2.K^2
Optical mode 3	3
Logical unit	64
No. of IAM's in file	5

Inputs	**Outputs**
Inlet temperature	Outlet temperature
Inlet flow rate	Outlet flow rate
Ambient temperature	Useful energy gain

Incident radiation Total horizontal radiation Horizontal diffuse radiation Ground reflectance Incidence angle Collector slope

The Flat Plate Collector chosen for this simulation is the **PHAETHON collector of SOL E.P.E. (SONNE AKTION) [Coll. Code 1186]**, manufactured in Greece. Data for the collector performance was taken from the test report of solar & other energy systems laboratory "Demokritos" National Center for Scientific Research. The report complied to the EN 12975-2 / ISO 9806-1 standards. Pages with essential information about the collector can be found in the appendix. A summary of used data is shown next.

Gross area: 1.99 m2

Aperture area: 1.8 m2

Number of covers: 1

Cover materials: ..... Tempered glass

Heat Transfer Medium.....Water

Material: .....copper tubes – one piece aluminium sheet 0.5 mm thickness

Surface treatment: ..... Selective coating

Insulation..... 30 mm (back)/ 20 mm (side) of Rockwool

The laboratory tested the collector in numerous conditions in order to acquire its general performance data. A second order fit to the test results gives an instantaneous efficiency shown below:

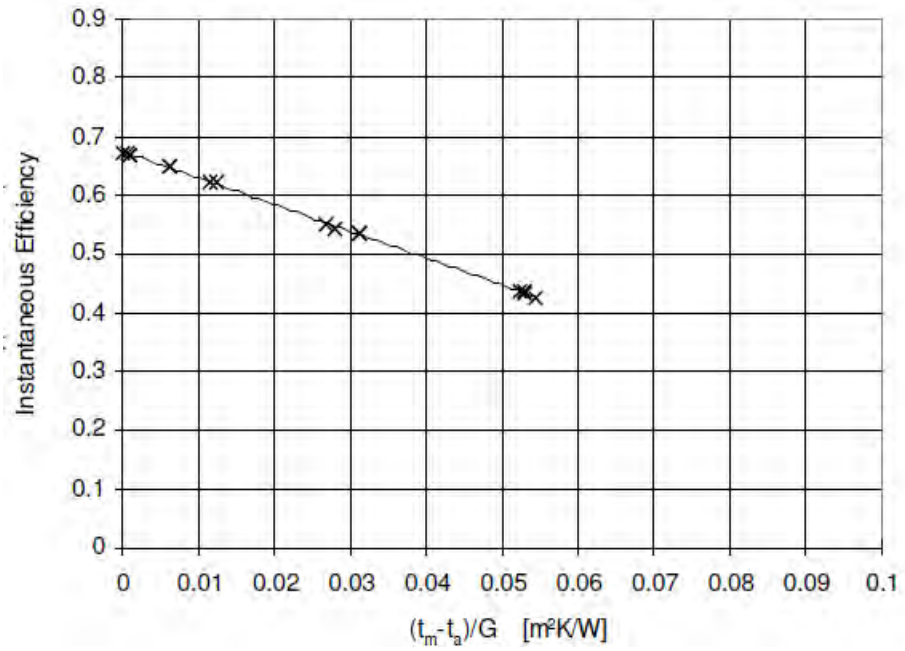

With coefficients:

$$\eta_0 = 0.67$$

$$\alpha_1 = 4.52 \frac{W}{m^2 K}$$

$$\alpha_2 = 0.0002 \frac{W}{m^2 K^2}$$

The tests for the Incidence Angle Modifier give:

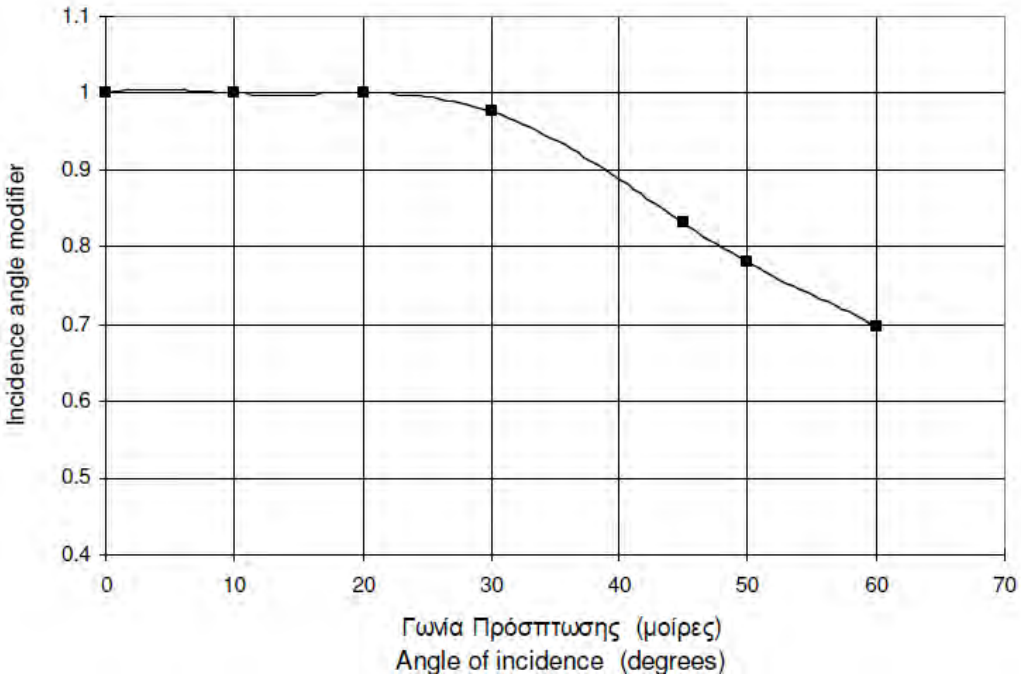

Γωνία *Angle*	0^0	30^0	45^0	50^0	60^0
K_θ	1.00	0.98	0.83	0.78	0.70

The coefficients of the report were supplied to the FPC Parameters (dissimilar values are observed, that is because they have different units) and the IAM test results were written into the IAM file that the component reads.

The incident, horizontal diffuse and total horizontal radiation as well as the ground reflectance and ambient temperature were supplied to the collector by the weather component. A series of collector slopes were tested and the optimal value was found to be 45°, with azimuth = 0 obviously. The collector feeds, through a pump, a thermal storage tank. Similarly, multiple values for the tank volume were tested and no discernable differences were observed above 1 m^3. The collector pump functions only when there is sufficient radiation, of more than 80 W/m^2. A second pump, connecting the tank with a heat exchanger, whose

opposite side faces the HP source loop, turns ON when the average tank temperature reaches 25°C. By doing this, water that has been heated to 17.1°C by the groundwater heat exchanger, gets heated again by the FPC loop, before entering the HP. This is configured to only work during the heating season though. In summer, DHW can be provided by this system.

Fig. 3.9: Photo of the FPC used in the simulation [63].

3.5 Photovoltaic (PV) system

This system utilizes an array of PVs installed on the roof, to provide electrical power to the GSHPs. By covering part of or the whole electricity demand of the GSHPs, less energy is consumed from the grid. This directly translates to less or no GHG emissions produced for the heating and cooling of the examined buildings. As there is a mismatch between energy generation and consumption in this system and a net metering scheme is employed. An arrangement of batteries can be utilized as well but that option was avoided, because as of 2020, they are still prohibitively expensive for systems of this capacity. Not only that, the batteries would also degrade over time and eventually need replacement.

Net-metering allows energy producers to cover a significant part of their electricity consumption, while utilizing the national power grid as an indirect energy storage for the green energy produced. The process is the following: Electrical energy is generated by the PVs during the day. When the GSHP turns on, all electrical output is fed to it, plus supplementary power in case that is not enough. When the GSHP is off, the electrical output is transferred to the grid through the inverter. When there is no solar generated electrical output, power is drawn from the grid. In the end of the month (or day) a net from the total values of generated and consumed power is created and the according bill is calculated.

Concerning net metering, legislation in Greece states that for private or public legal entities seeking to install PVs that benefit the public, the power installed can reach up to 100% of the total consumption (otherwise only up to 50% is allowed)[Law cited: ΥΑΑΠΕΗΛ/Α/Φ1/οικ.24461 (ΦΕΚ Β’ 3583/31.12.2014)] [64]. Maximum legal power generation in net metering is 500 kW.

3.5.1 Photovoltaic Array, Type 94

This component models the electrical performance of a photovoltaic array. Type 94 may be used in simulations involving electrical storage batteries, direct load coupling, and utility grid connections. It employs equations for an empirical equivalent circuit model to predict the current and voltage characteristics of a single module. This circuit consists of a DC current source, diode, and either one or two resistors. The strength of the current source is dependent on solar radiation and the IV characteristics of the diode are temperature-dependent. The results for a single module equivalent circuit are extrapolated to predict the performance of a multi-module array. For crystalline modules (either single crystal or polycrystalline technology), Type 94 employs a “four-parameter” equivalent circuit. The values of these parameters cannot be obtained directly from manufacturers’ catalogs. However, Type 94 will automatically calculate them from available data. Type 94 also includes an optional incidence angle modifier correlation to calculate how the reflectance of the PV module surface varies with the angle of incidence of solar radiation.

In electronics, the link between the direct current (DC) through an electronic device and the DC voltage is called a current–voltage characteristic of the device. These charts are used to determine basic parameters of a device and to model its behavior in an electrical circuit. These characteristics are also known as I–V curves, referring to the standard symbols for current and voltage.

The four parameter model assumes that the slope of the IV curve is zero at the short-circuit condition. The IV characteristics of a PV change with both insolation and temperature. The PV model employs these environmental conditions along with these four module constants: Module photocurrent at reference conditions ($I_{L,ref}$,), Diode reverse saturation current at reference conditions ($I_{o,ref}$,), Empirical PV curve-fitting parameter (γ), and Module series resistance (Rs) to generate an IV curve at each timestep. These are empirical values that cannot be determined directly through physical measurement.
Type 94 calculates these values from manufactures' catalog data.
Afterwards, PV current and voltage values are calculated.
The current-voltage equation is:

$$I = I_L - I_o \left[\exp\left(\frac{q}{\gamma k T_c} (V + I R_s) \right) - 1 \right]$$

Where: q is electron charge constant, k is the Boltzmann constant and Tc the module temperature. Rs and γ are constants. The photocurrent I_L depends linearly on incident radiation:

$$I_L = I_{L,ref} \frac{G_T}{G_{T,ref}}$$

The reference insolation G_{ref} can be given as a component parameter. It is nearly always defined as 1000 W/m^2. The diode reverse saturation current I_o is a temperature dependent quantity:

$$\frac{I_o}{I_{o,ref}} = \left(\frac{T_c}{T_{c,ref}} \right)^3$$

The equations, in respective order, give the current implicitly as a function of voltage. Once Io and IL are found and, Newton's method is employed to calculate the PV current. In addition, an iterative search routine finds the current (I_{mp}) and voltage (V_{mp}) at the point of maximum power along the IV curve.

Parameters	
Module short-circuit current at reference conditions	9.88 A
Module open-circuit voltage at reference conditions	40.3 V
Reference temperature	298 K
Reference insolation	1000 W/m^2
Module voltage at max power point and reference conditions	33.2 V
Module current at max power point and reference conditions	9.31 A
Temperature coeficient of Isc at (ref. cond)	0.00494
Temperature coeficient of Voc (ref. cond.)	-0.11687
Number of cells wired in series	60
Number of modules in series	Multiple values were tested
Number of modules in parallel	Multiple values were tested
Module temperature at NOCT	318 K
Ambient temperature at NOCT	293 K
Insolation at NOCT	1000 W/m^2
Module area	1.635 m^2
tau-alpha product for normal incidence	0.95
Semiconductor bandgap	1.12
Slope of IV curve at Isc	0
Module series resistance	-1

From these parameters the four module constants are calculated which are then used in turn to find the voltage and current and therefore the power output.

Inputs
Total incident radiation
Ambient temperature
Load voltage
Flag for convergence promotion
Array slope
Beam radiation
Diffuse radiation
Incidence angle of beam radiation

Outputs
Array voltage
Array current
Array power
Power at maximum power point
Fraction of maximum power used
Voltage at MPP
Current at MPP
Open circuit voltage
Short circuit current
Array fill factor
Array temperature

All of the inputs are supplied by the weather component. From the outputs the power at maximum power point is supplied to the inverter, whose operation is described later.
The parameters of the PV were supplied by the technical manual of the panels selected. Pages of the manual with photovoltaic and electrical data can be found in the appendix.

3.5.1.1 PV panels simulated

The panels ***DualSun Flash 310M*** were chosen to be simulated. This was mainly because DualSun provides the same panel as a PV or a PV/T, with exactly the same photovoltaic performance. With this approach the difference in the performance of the PV and PV/T systems can be observed clearly. These panels are made 94.7% by recycled panels.

PHOTOVOLTAIC DATA		
Number of cells per module	60	
Cell type	PERC Monocrystalline	
Nominal power (P_{mpp})	300 Wp	310 Wp
Module efficiency	18,3 %	19,1 %
Rated voltage (V_{mpp})	32,6 V	33,2 V
Rated current (I_{mpp})	9,19 A	9,31 A
Open circuit voltage (V_{oc})	39,9 V	40,3 V
Short circuit current (I_{sc})	9,77 A	9,88 A
Power output tolerance	0 / +5W	
Maximum system voltage	1000 V DC	
Reverse current load	20 A	
NOCT	45 ± 2°C	
Connectors	MC4 / MC4 compatible	
Application class	Classe II	
Voltage temperature coefficient (μV_{oc})	-0,29 %/°C	
Current temperature coefficient (μI_{sc})	0,05 %/°C	
Power temperature coefficient (μP_{mpp})	-0,39 %/°C	

Fig. 3.10: Photovoltaic data of the DualSun Flash 300-310M panel.

3.5.2 Regulator / Inverter, Type 48

In photovoltaic power systems, two power conditioning devices are needed. The first of these is a regulator, which distributes DC power from the solar cell array to and from a battery (in systems with energy storage) and to the second component, the inverter. If the battery is fully charged or needs only a taper charge, excess power is either dumped or not collected by turning off parts of the array. The inverter converts the DC power to AC and sends it to the load (in this case the GSHP) and/or feeds it to the grid. TYPE 48 models both the regulator and inverter.

Mode 0 operates without a storage battery. The power output by the array is simply multiplied by an efficiency factor and sent to the load, with any excess fed back to the grid. When the load exceeds the array output, the grid furnishes the difference.

Parameters	
Mode	0
Efficiency	0.85

Inputs
Input power
Load power

Outputs
Power in
Power out
Excess power

Efficiency of 0.85 is common for inverters. The power output of the PV array is coupled to this component and its outputs are linked to the electrical load of the GSHP. In the net metering scheme the power sent to the grid is measured for the calculation of the bill in the end of the month.

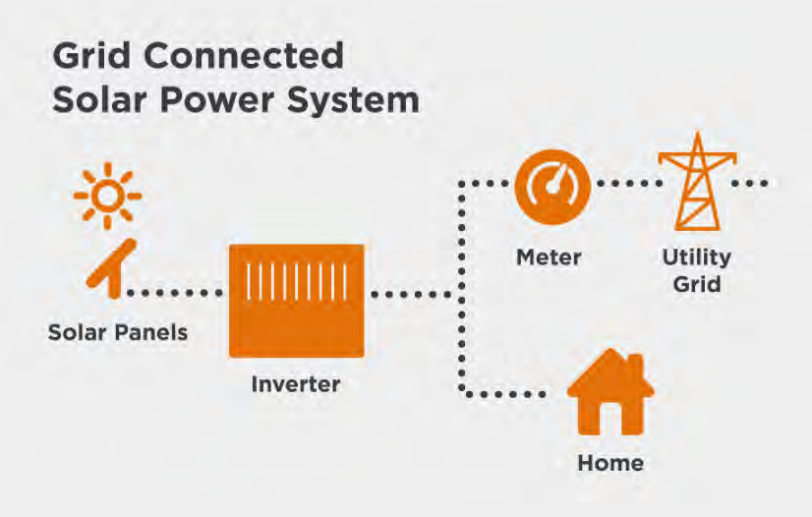

Fig. 3.11: Example of a net metering system connected to the grid [65].

3.6 Photovoltaic-Thermal PV/T system

In this system hybrid PV/T panels that generate electrical power and heat are installed. Its operation is the combination of the previously explored systems, by providing electrical energy to the GSHP and simultaneously preheating the source flow, but with a single device. Should FPC and PV systems be installed separately on the same roof, substantial area would be needed. Thus, space saving is considerable, when PV/Ts are utilized. The system reduces GHG emissions by reducing the amount of grid supplied energy and by increasing the COP of the GSHP. Net metering is implemented once more for the generated electrical power and a 1 m^3 hot water storage tank is used again.

3.6.1 PV/T Collector, Type 50

This component adds a PV module to the standard flat-plate collector. It simulates a combined collector and incorporates both the analysis and work of Florschuetz for flat plate collectors operated at peak power [66]. The analysis makes use of the I-V curves of the cells (or array) in solving for peak power or for current output at some imposed voltage.

The useful heat gain is given by:

$$Q = F_R A_c [I_T(\alpha\tau) - U_L(t_p - t_a)]$$

It is the same equation used in the flat plate collector component with the addition of an thermal efficiency factor F_R.

And the electrical output is:

$$Q_e = \frac{A_c I_T \eta_\alpha}{\alpha}\left\{1 - \frac{\eta_r \beta_r}{\eta_\alpha}\left[F_R(t_i - t_a) + \frac{I_T}{U_L}(1 - F_R)\right]\right\}$$

where η is the actual or reference efficiency of the photovoltaic modules and β is the power temperature coefficient.

In this component Mode 1 is employed: the thermal loss coefficient of the collector is constant and given as a parameter.

Parameters	
Mode	1
Collector Area	Multiple values were tested
Collector Fin Efficiency Factor	0.96
Fluid Thermal Capacitance	4.19 kJ/kg.K
Collector plate absorptance	0.6817
Collector loss coefficient	16.66 W/m^2K
Cover transmittance	0.9
Temperature coefficient of solar cell efficiency	0.0039
Reference temperature for cell efficiency	25 °C
Packing factor	1

Inputs
Inlet fluid temperature
Fluid mass flow rate
Ambient temperature
Incident radiation
Cell efficiency

Outputs
Outlet fluid temperature
Fluid flowrate
Rate of useful energy gain
Collector loss coefficient
Transmittance-absorptance product
Electrical power output
Average cell temperature
Apparent thermal loss coefficient

The parameters' values were obtained by the data found in the technical manual of the PV/T panels utilized, shown below. The PV/Ts are in a solar loop consisting of a primary pump connecting the panels with a storage tank which in turn is connected to a heat exchanger that preheats the source flow, through a secondary loop. Electrical power output is supplied to the inverter of the system. The component is supplied temperature and flow rate of the fluid by the primary pump when the radiation exceeds 80 W/m^2. Two modes have been configured, one for each season. In heating season, if the hot water storage tank average temperature exceeds 25 °C, the secondary pump is turned on, in order to heat the source flow. In cooling season, as there is no need for preheating the flow, when the tank temperature reaches 45 °C water is discharged (can be utilized as DHW) and replaced by water from the general supply, with a temperature of 23 °C, according to KENAK for the city of Volos in the summer [58]. This is performed due to the fact that the panels can be damaged at high temperatures but more importantly because of the correlation of the PV efficiency and operating temperature, as stated before. Cooling the photovoltaic cells improves electricity output by 5 to 15% depending on usage [67].

3.6.1.1 PV/Ts simulated

Like previously mentioned, the PV and PV/T panels chosen for the simulation are the same PV panel, only in the PV/T case a water heat exchanger is installed in the rear to capture the heat losses. The model is ***DualSun Spring 310M***. The photovoltaic performance of the panel has already been discussed in a previous segment. Thermal data is presented below.

THERMAL DATA			
Gross area	1,635 m^2		
Volume of heat transfer liquid	5 L		
Maximum operating pressure	1,5 bar		
Pressure loss per panel (Pa | *mmWS*)	Portrait	Landscape	
	59 | *6*	167 | *17*	at 32 L/h
	461 | *47*	961 | *98*	at 100 L/h
Hydraulic input/output	DualQuickfit® fittings		
	Non-Insulated	Insulated	
Maximum temperature	70 °C	75,6 °C	
Optical efficiency a_0	58,9 % *	58,2 % *	
Heat loss coefficient a_1	16,0 W/K/m^2 *	10,8 W/K/m^2 *	
Heat loss coefficient a_2	0 W/(m^2,K^2) *		

* The a_0, a_1 et a_2 coefficients are the measured values from testing during EN 9806:2017 certification at KIWA for unglazed collectors with a **windspeed $u = 1 m/s$: $a_0 = n_0 - c_6 * u'$; $a_1 = c_1 + c_3 * u'$; $u' = u - 3$.**

Fig. 3.12: Photo and cross section of the PV/T used in the simulation [67].

4. RESULTS

Multiple simulations ran for 8760 hours with 3 minute timestep for each of the SAGSHP systems for various collector area values.

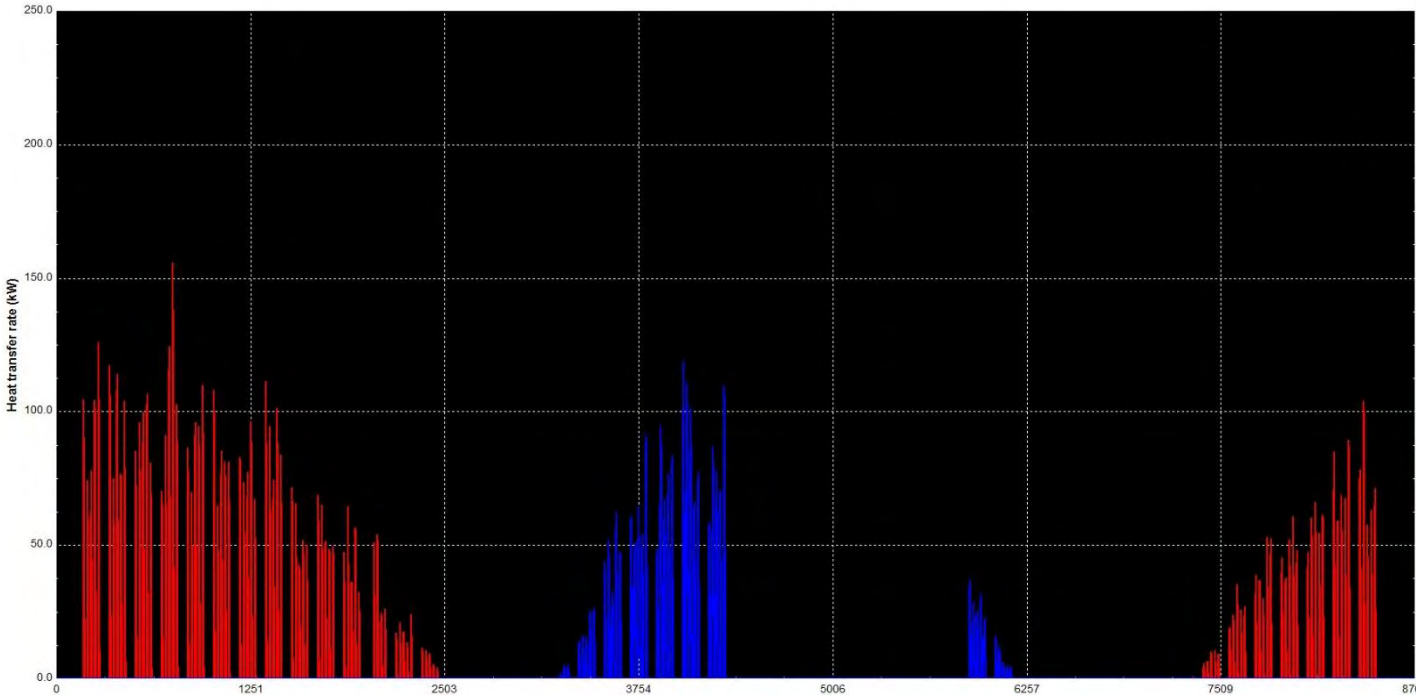

The snapshot above is from the online plotter component, showing the heating (red) and cooling (blue) loads over a period of one year, in kW. The large gap in the cooling season is due to the closing of the university in July and August. The other gaps represent either holidays, weekends or the periods when no heating/cooling is required. A chart with the heating COP of the two GSHPs based on the temperature of source flow is presented below.

Fig. 4.1: COP for different source temperatures

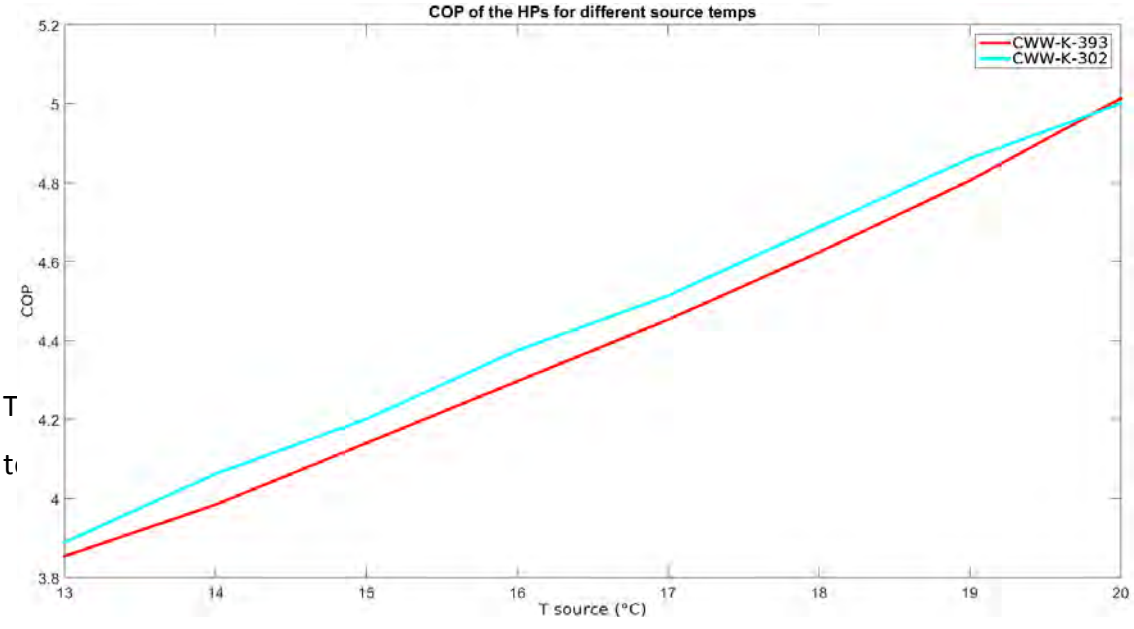

T same

t

4.1 FPC system

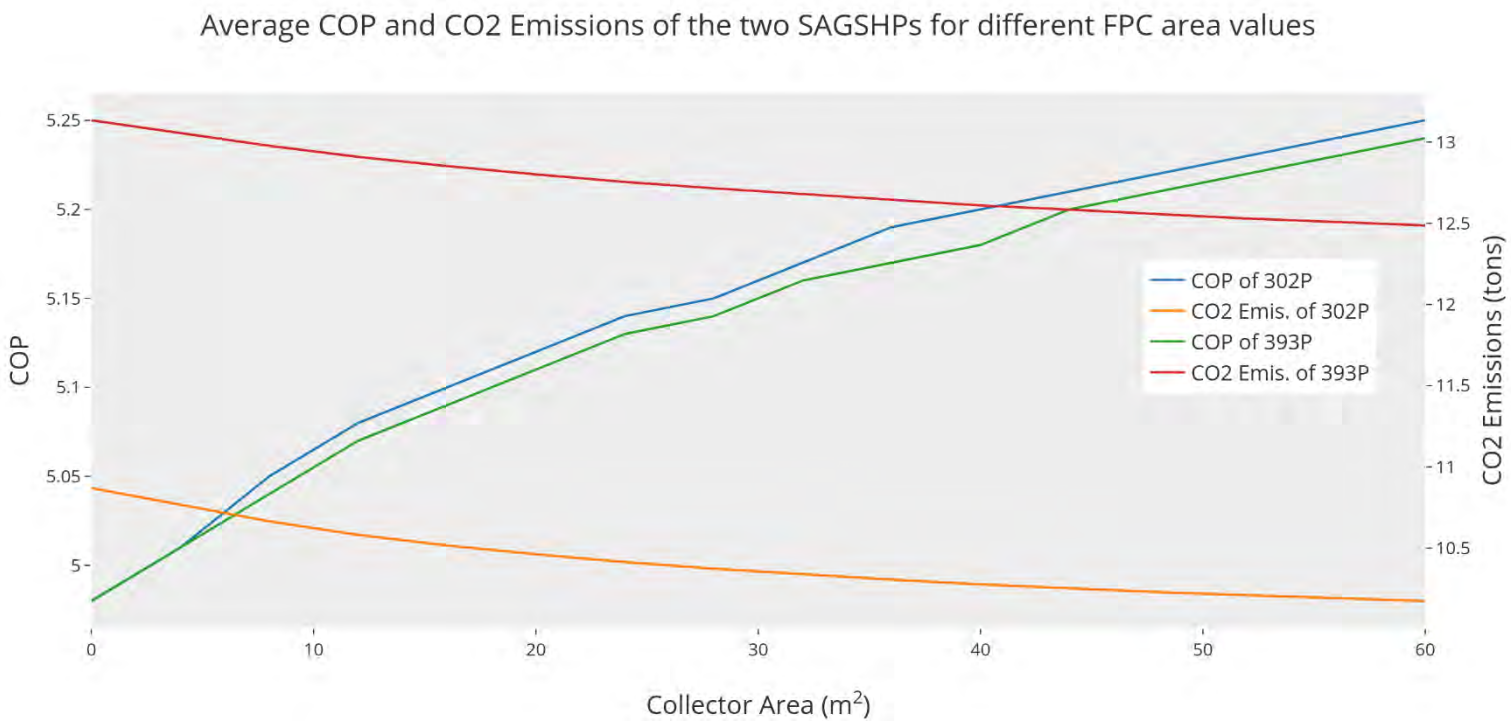

Fig. 4.2: Average COP and CO_2 emissions of the SAGSHPs for different FPC area values

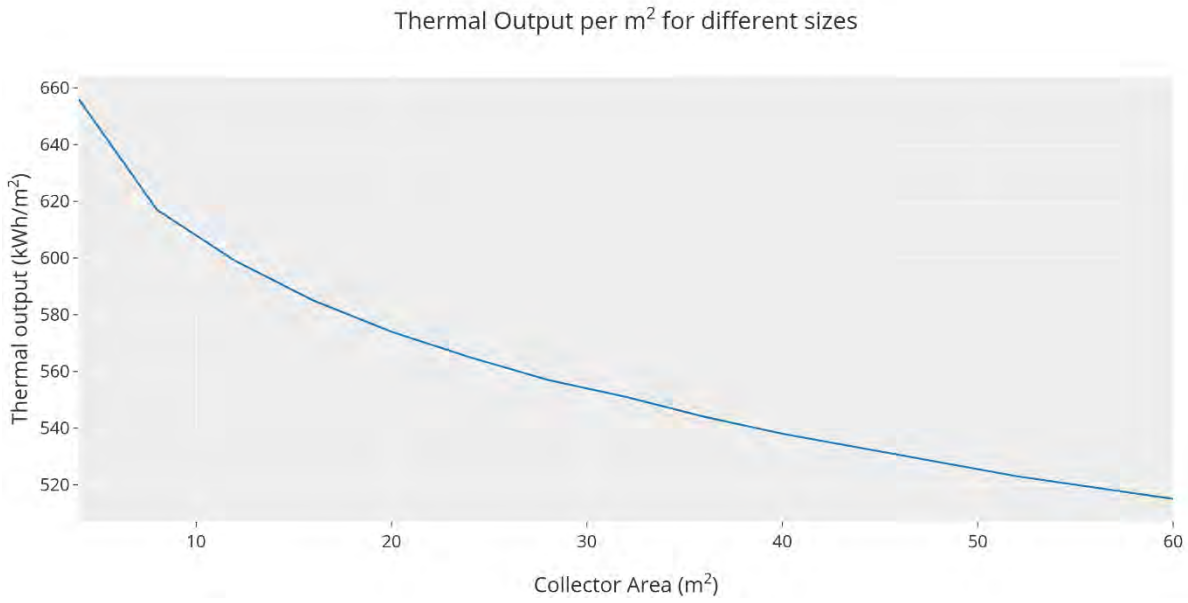

Fig. 4.3: Thermal output per m^2.

The efficiency and emissions of the SAGSHP system were investigated. In the first chart the average COP over a year and the CO_2 emitted from the FPC system are shown. Reduced CO_2 emissions are observed the higher the total collector area is. A 60 m^2 solar field can reduce

emissions by half a ton. This is the result of the higher average COP for a year achieved by increasing the total collector area. For the same temperature the 302P model has a marginally higher COP value. A 60 m^2 solar field increases the COP by up to 5%. Increasing the size of the solar field further than 60 m^2 does not increase the COP at the same rate (therefore not shown) and that can be explained by the next chart, where the thermal output per m^2 is displayed. The thermal efficiency drops the larger the solar field is. This is due to the higher fluid temperatures flowing through the collectors, thereby reducing the heat transfer rate between the FPC absorbing surface and the fluid.

4.2 PV system

Here the solar fraction f is the fraction of the total energy generated by the PV to the total energy consumption of the GSHP. As mentioned before, the emissions of all GHG have been combined into a single CO_2 emission value for easier visualization and comprehension. The emission reduction of the energy supplied to the GSHP *and* the energy supplied to the grid, have both been accounted for, since the latter, wherever it is utilized, remains a RES generated energy quantity. Negative values can therefore be observed, implying the SAGSHP system not only has a zero carbon footprint but essentially reducing emissions regionally, by supplying power to the grid for other consumers. The 302P system reaches f = 1 around 40 m^2 and the 393P around 50 m^2. That is also the maximum capacity that can be installed according to the legislation, as stated before in the net metering section.

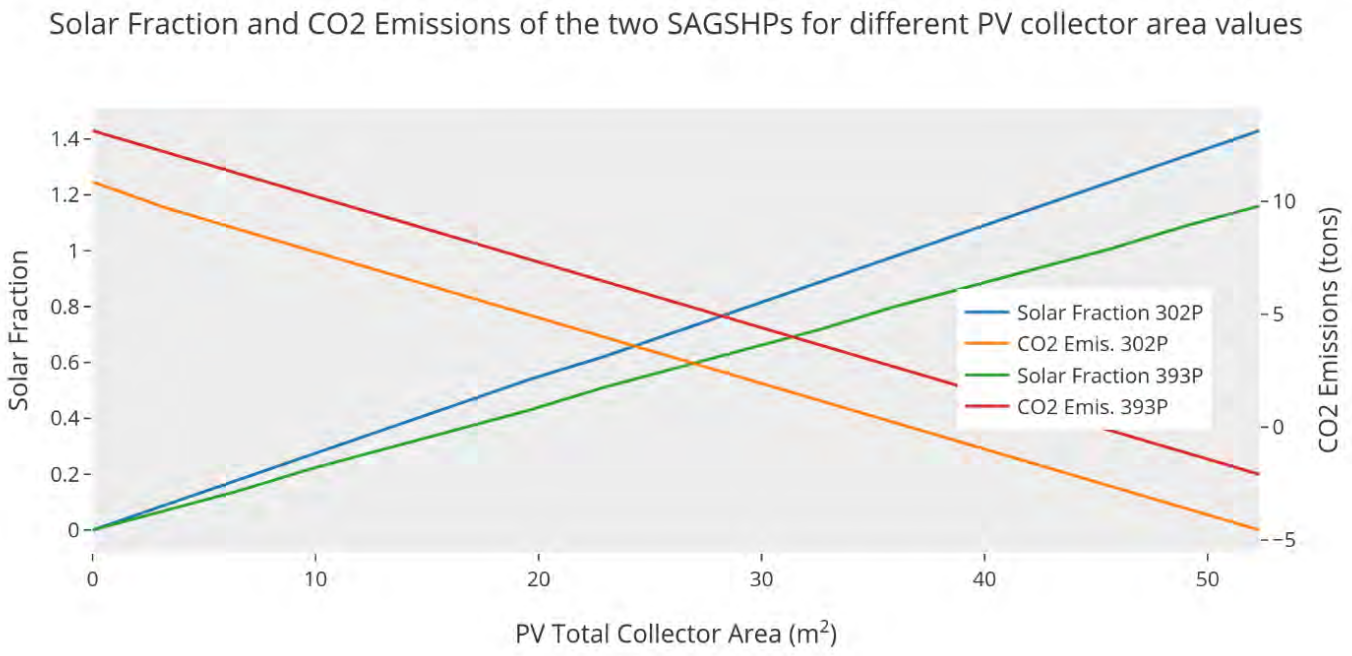

Fig. 4.4: Solar fraction and CO_2 emissions for PV collectors

4.3 PV/T system

The PV/T system generating simultaeously electrical and thermal power requires combining the previous analyses. The average COP and solar fraction of the two systems for different area values are presented below.

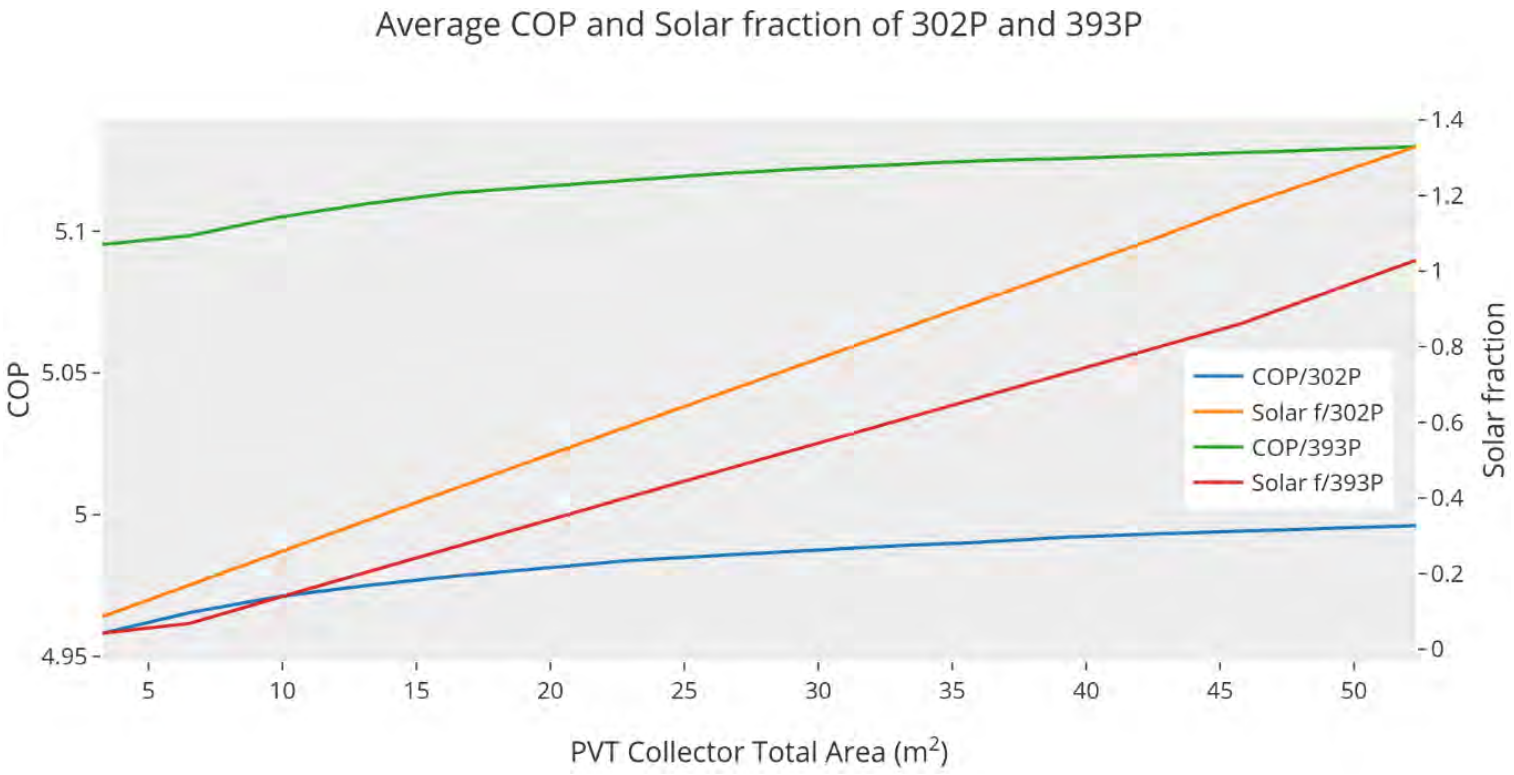

Fig. 4.5: Average COP and solar fraction for PV/T collectors

It is observed that the COP rises only minimally even for a large solar field. A 50 m^2 field barely improves the COP by 1%. This is quite lower than the COP rise achieved by the FPC system and is attributed to the lower absorptance-transmittance product of the PV/T panels compared to the FPC ones. The result is that less thermal energy is absorbed per panel and the temperature of the fluid is lower that the FPC equivalent, leading to lower source flow temperatures. Increasing the size of the solar field, decreases the thermal efficiency of each panel, as shown below. The electrical output and generally the solar fraction is close to the PV equivalent, generating slightly more power.

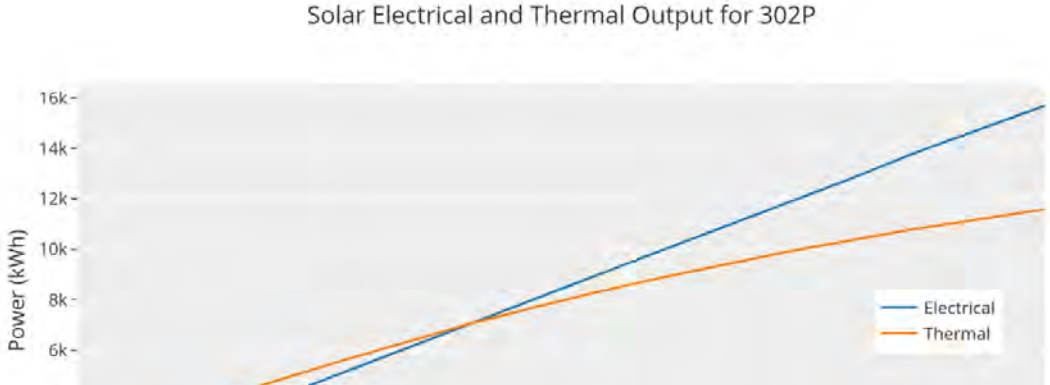

Fig. 4.6: Electrical and thermal output of the PV/T collectors

4.4 Energetic analysis and comparison of the three SAGSHP systems

The systems are compared to each other in terms of total consumption, power supplied from the grid and total emissions. Only the energy behavior of the 302P model is presented as their energy profiles are identical, the 393P requiring about 30% larger solar field for the same relative results. The total annual power consumption of the systems is shown first.

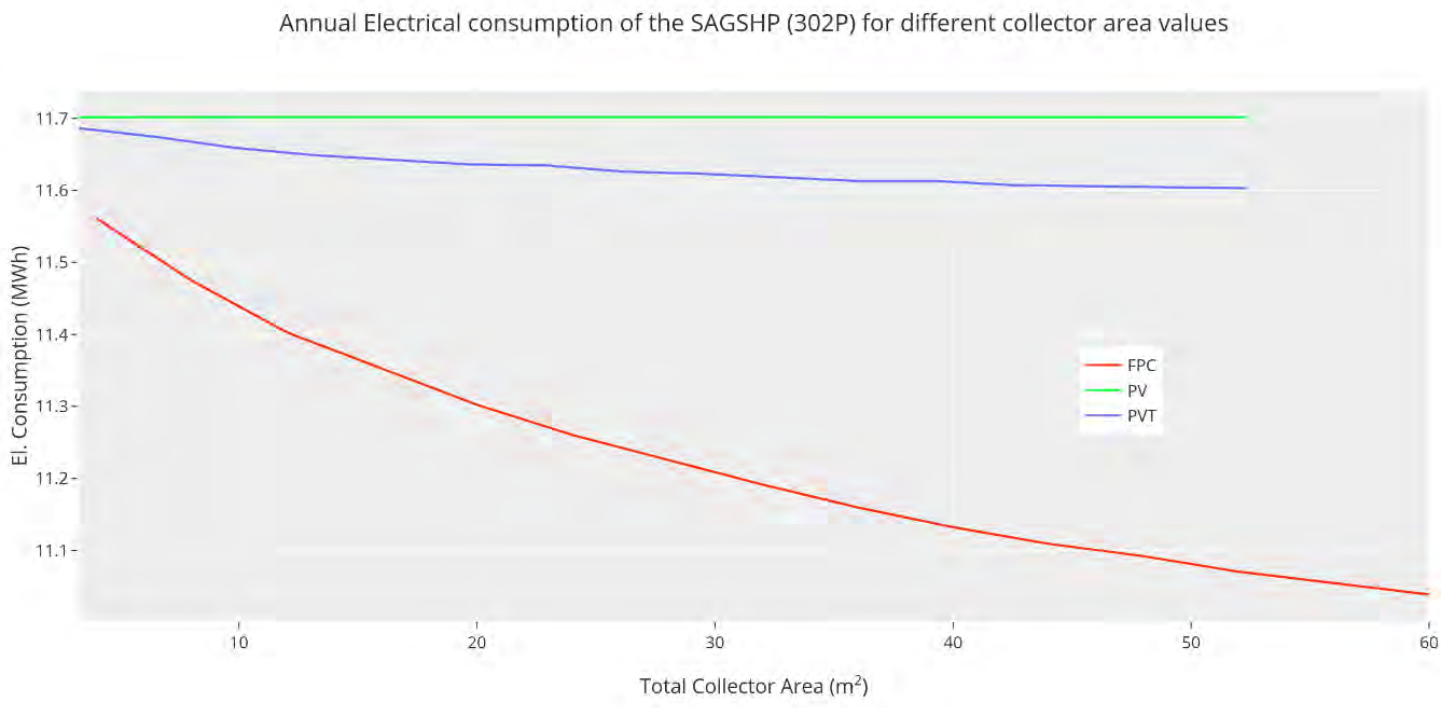

Fig. 4.7: Electrical power consumption of all collectors

The FPC system consumes less energy in total than the PV and PV/T systems, up to 0.8 MWh less for a large solar field. The PV has a stable consumption rate since the COP does not change and the PV/T has slightly less consumption, up to 0.1 MWh less. This could lead to the assumption that the FPC system is the most energy efficient but the next chart reveals the opposite. The power provided to the GSHP directly by the grid has been graphed against different collector values. This does not inlcude the power output of the PV and PV/T systems feeded to the grid, like when the university is closed or when there is no need for heating/cooling, which is significant.

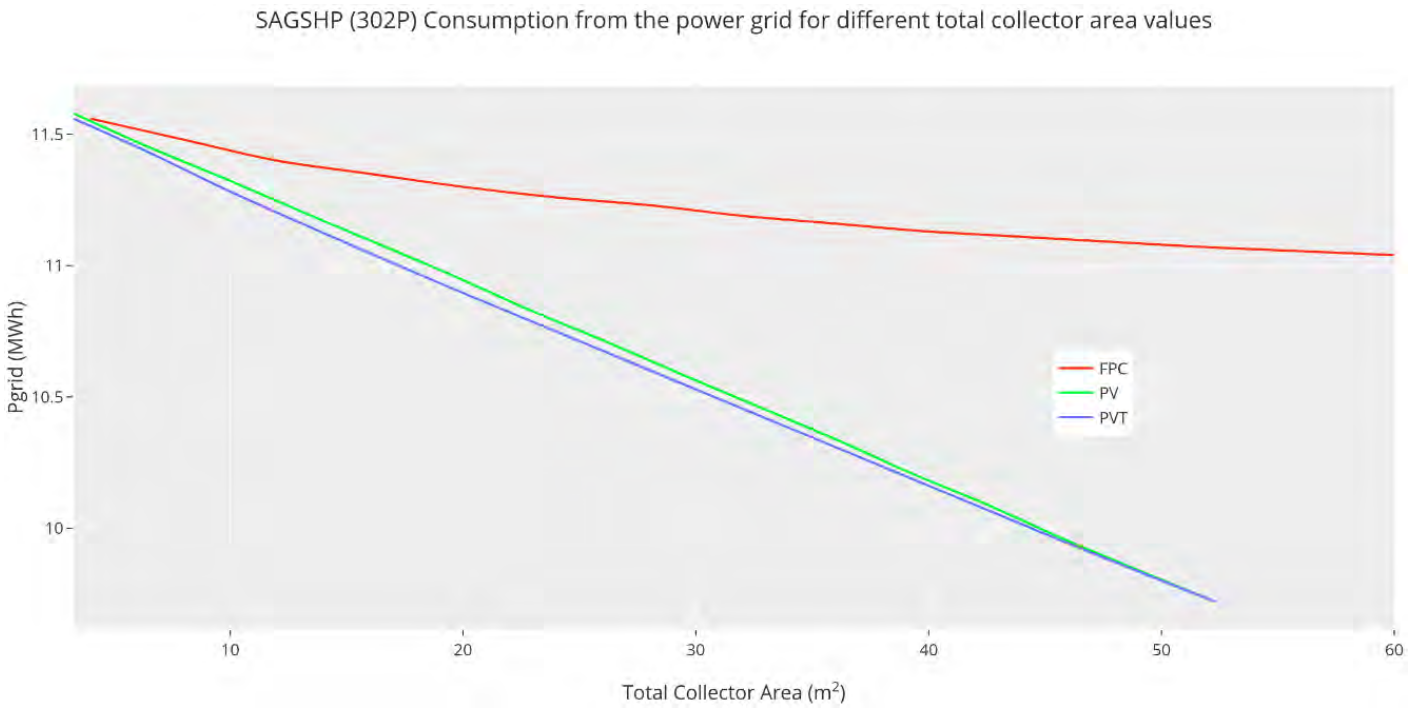

Fig. 4.8: Consumption of grid-supplied power

It is immediately evident that the FPC system consumes significantly more power from the grid that the other alternatives, despite consuming less energy in general. PV and PV/T have an almost identical performance, the latter consuming slightly less power due to its marginally higher COP values. These systems can save up to 1.5 MWh of grid-supplied power compared to a FPC configuration and 2 MWh to a non-solar system. To better comprehend the impact of the solar generated power on the performance of the systems, an example of a 36 m^2 solar field is presented below. Even though the FPC has the lowest consumption overall, the other configurations are superior (energy wise) because they generate power that directly reduces the amount of energy drawn from the grid. To investigate if this could be improved, more simulations for the FPC were conducted, up to 120 m^2, yet those configurations still could not beat the performance of the 36 m^2 PV and PV/T solar fields, regarding grid-supplied power.

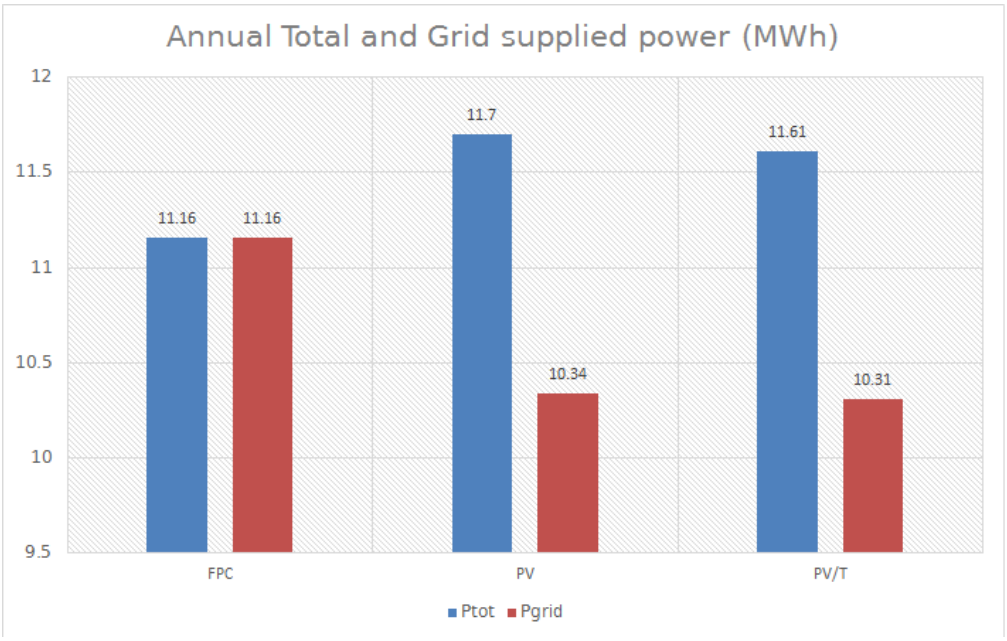

Fig. 4.9: Total and grid-supplied power

By analyzing the annual power profile of the SAGSHPs, the following conclusion can be drawn: The greatest difference in grid power draw is found in the month of June, which is cooling season. That is because the FPC system does not contribute to the cooling loads in any way. That monthly difference alone drops the overall performance of the FPC system compared to the other two. The small differences during heating season can reduced with a larger solar field. Simulations with a 100 m^2 field minimize the winter difference bringing the performance level on par with the others. To combat the cooling season challenge, a hot water fired absorption chiller could be installed, that provides cooling utilizing the hot water produced by the FPCs. This would of course drive up the costs and the complexity of the SAGSHP system.

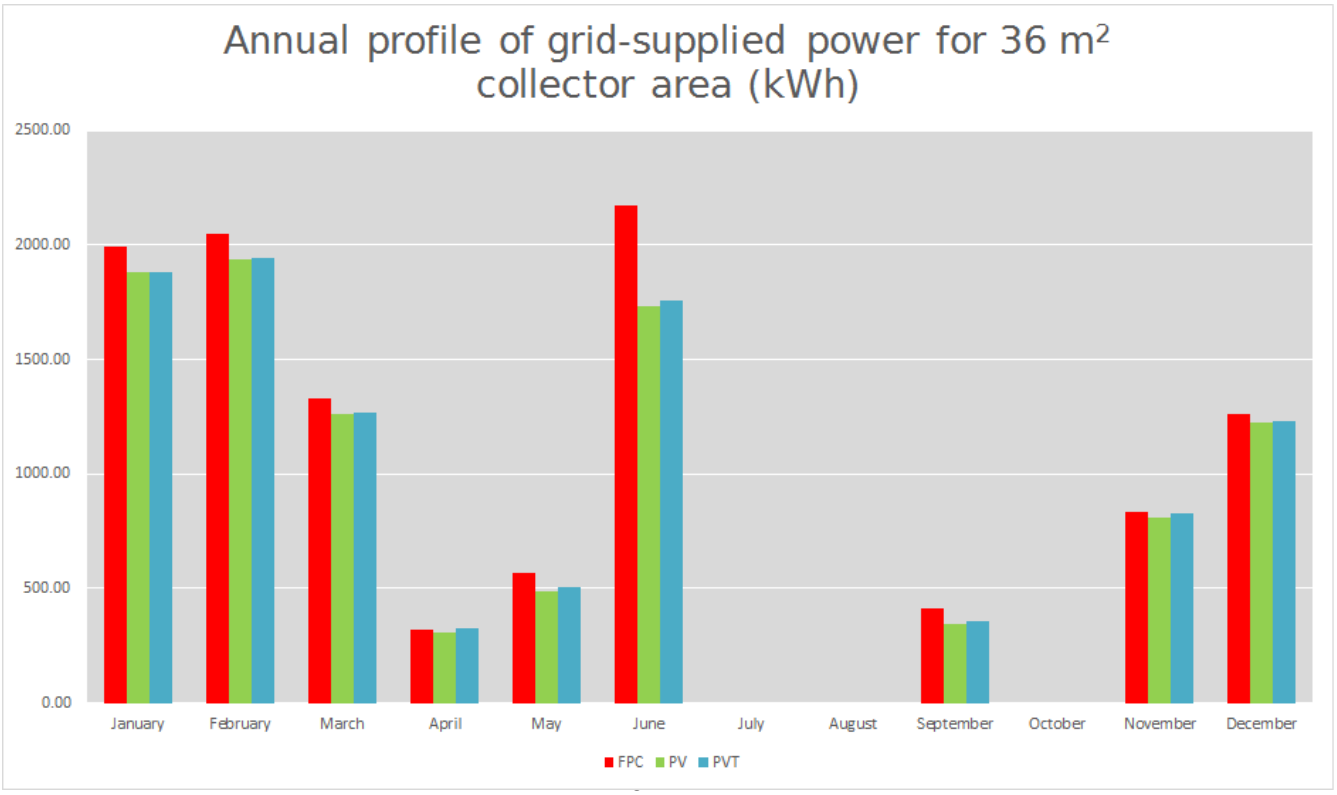

As for the environmental aspect, because the excess power output of the PV, PV/T configurations to the grid is being accounted for, their net emissions are far better that the FPC one. Negative values of emissions have been explained previously but unfortunately, although being feasible and attractive solutions, are not permitted with current legislation [This could change should the net metering scheme take also into account the rest of the energy needs of the buildings, but that is a too complex analysis to be conducted by this study]. Out of all systems the PV/T system has the lowest carbon emissions, with PV being only slightly behind.

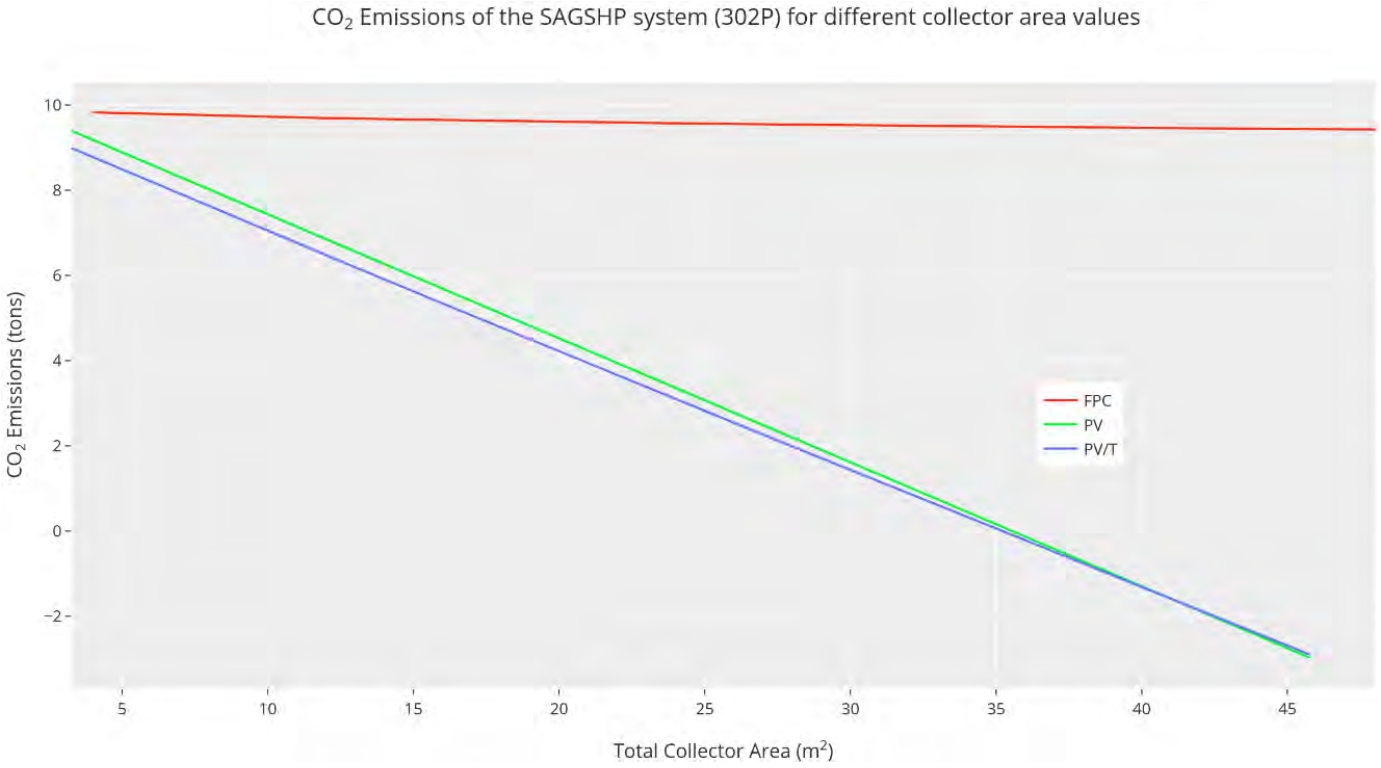

Fig. 4.10: CO_2 Emissions

4.5 Economic Analysis

A simple economic analysis was performed. For the total cost, the initial capital and the operation cost were taken into account. Workforce, installation and maintenance were neglected as they would be the same for these systems that are of very similar nature.

$$C_{Total} = C_{Initial} + C_{operation}$$

The initial cost is essentially the cost of the equipment. Neglecting all costs that are present in all systems, costs are only accounted for when they are special to the configuration. Those are:

$$C_{In.\ FPC} = C_{Panels} + C_{Tank}$$
$$C_{In.\ PV} = C_{Panels} + C_{Inverter}$$
$$C_{In.\ PV/T} = C_{Panels} + C_{Tank} + C_{Inverter}$$

After surveying the Greek market [68], the following average values were found:

FPC panels	100 € per m^2
PV panels	200 € per m^2
Storage tank	150 € per m^3
Inverter	1500 €

PV/Ts have not yet penetrated into the mainstream greek market so the average value of the panels was taken from a survey of all available PV/Ts in Europe by de Keizer et al. [69] as 300 € per m^2.

The operational cost is the electricity cost by the power draw of the SAGSHPs. In Greece, educational institutions belong to the bill rate group for professionals and businesses. As of 2020, that is 0.14 €/kWh [70]. The life cycle of 20 years for the SAGSHP systems and a discount factor of 4% has been decided upon. Thus the cost of operation after 20 years is:

$$C_{operation,Tot} = C_{1\ year\ of\ op.} * \frac{1-(1+r)^{-n}}{r} = C_{1\ year\ of\ op.} * 13.59$$

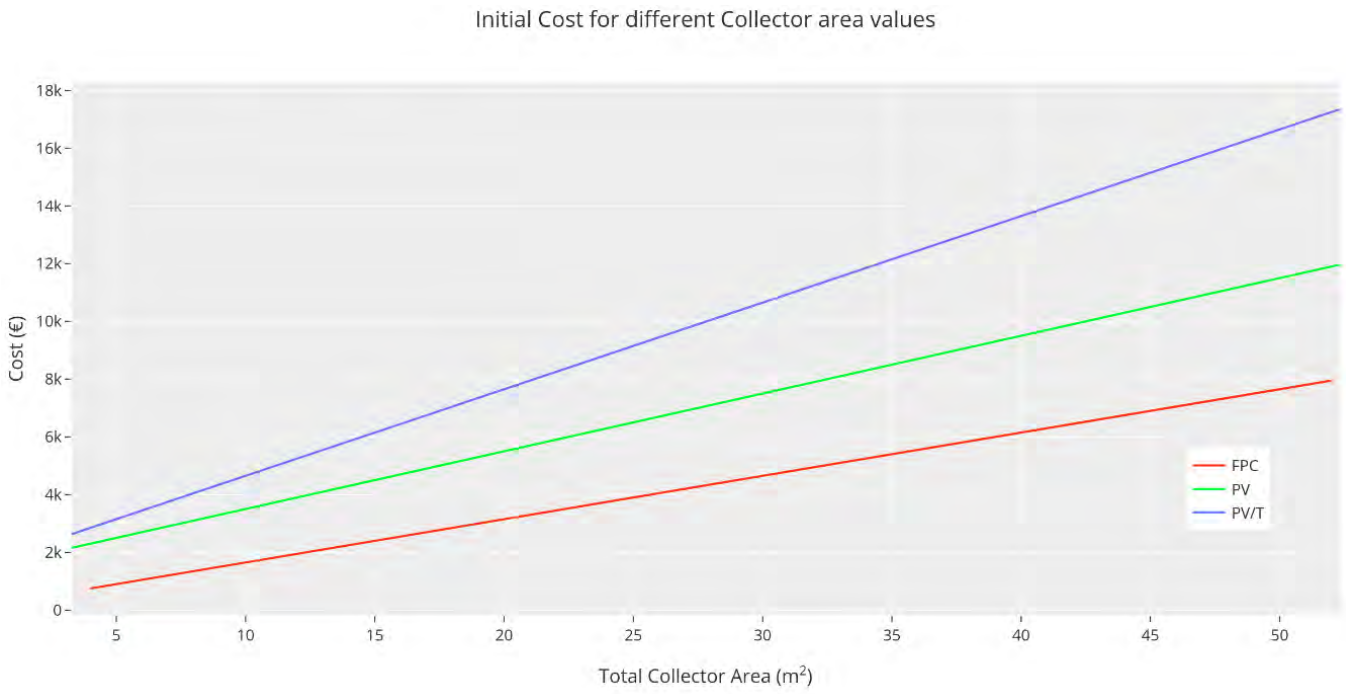

Fig. 4.11: Initial capital

FPC is the most affordable solution, being a simple and well established technology. PV is somewhat more expensive, although their costs drop rapidly year by year. PV/T is a novel technology with a limited market, hence its higher cost.

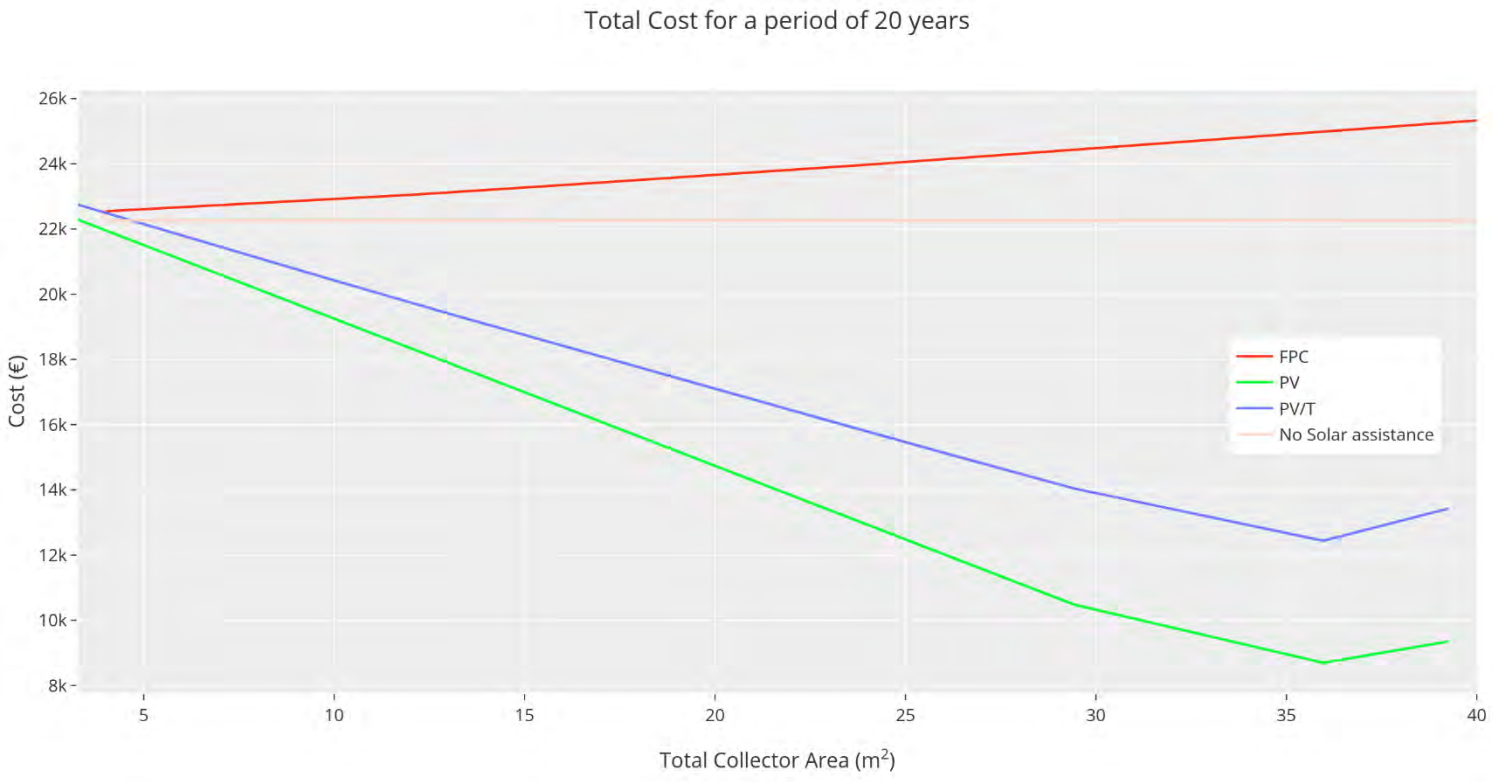

Fig. 4.12: Total cost for a 20 year period

The comparison between the total cost of the SAGSHPs for a period of 20 years is presented. Unexpectedly, the cost of an FPC is so high, that it even surpasses the base cost of a non-solar configuration. The cost saved by the reduction of the power consumed is not enough to even achieve net balance with the initial capital invested. PV has the lowest cost overall, with quite a significant difference to next cost effective configuration of PV/Ts. This is attributed to the almost identical electrical power output of the two systems but the PV has a lower cost per panel, therefore achieving a better net difference. This too is unexpected, as one would assume that the PV/T is more efficient, in terms of both increasing the COP and generating more power. These assumptions are true, but as noted before, the energy savings caused by the higher COP values and the higher power output were minimal and not enough to bring the net difference below that of the PV configuration. The rise in cost located between 35 and 40 m^2 for the PV and PV/T systems is due to the fact that in the net metering scheme, power provided to the grid that exceeds the net balance agreed upon, is not counted for and cannot be sold. This is insignificant though, as these collector area values are over the limit of solar f = 1 and therefore illegal according to current legislation.

5. CONCLUSIONS

Three different Solar Assisted Ground Source Heat Pump systems are proposed as upgrades to the GSHPs installed in a university building complex in Volos, Greece, in order to reduce its carbon footprint. This study investigates the energy and financial performance of the three proposed SAGSHP configurations. Systems connected to a Flat Plate Collector, a Photovoltaic and a hybrid Photovoltaic/Thermal solar field respectively have been simulated using TRNSYS, with multiple variables. The simulations were conducted for 8760 hours with a timestep of 3 minutes. Solar radiation data were obtained from the PVGIS database.

The results of the energy analysis indicate that despite the FPC system reducing the total power consumption of the heat pump significantly, it still consumes more power from the grid compared to the PV and PV/T systems which have similar performance. This is mainly because the operation of the FPC solar field is limited to the heating season. This could be resolved by installing a hot water fired absorption chiller, but that would drive up the total cost of the installation. The PV/T configuration consumes the least amount of power from the grid and reduces carbon emissions the most but only marginally compared to the PV equivalent.

For the economic analysis, the costs of the initial capital and the cost of operation were taken into account. For a life cycle period of 20 years, a discount rate of 4% and an electricity price of 0.14 €/kWh, the PV configuration is the most cost-friendly investment due to its lower price per panel and the substantial energy savings, up to the legal limit of f = 1 (up to 40 m^2 solar field). The PV/T alternative is not able to balance its high capital cost with the energy savings accomplished. FPCs despite their low initial cost, fail to reduce the cost of the grid-supplied power and is therefore the least affordable investment. It is worth noting that the 20 year operation of the existing non-solar system is more costly than the operation of a SAGSHP system with either PVs or PV/Ts installed. Installation and maintenance costs have not been included, yet these can be covered by the large net difference.

Taking all the previous results into account, it can be confidently stated that the optimal configuration is that of the SAGSHP coupled to PVs because it combines excellent energy performance with the lowest cost possible. Solar Assisted Ground Source Heat Pumps seem very promising in reducing or eliminating the carbon footprint of buildings in a cost-friendly, sustainable manner.

6. REFERENCES

[1] Rousselot. (2018), Energy efficiency trends in buildings. Odyssee-Mure project[European Union. [Available from: https://www.odyssee-mure.eu. cited 2020 July 1st]

[2] Prindle. (2009), Energy Efficiency as a Low-Cost Resource for Achieving Carbon Emissions Reductions. National Action Plan for Energy Efficiency[Environmental Protection Agency. [Available from: http://www.epa.gov/eeactionplan.

[3] Eurostat, (2020), *SHARES Data*, European Commission.

[4] Nouri, Noorollahi, and Yousefi (2019) Solar assisted ground source heat pump systems – A review. *Applied Thermal Engineering*. **163**: p. 114351.

[5] (2020), Climate Change. Ministry of Environment and Energy, Greece [Available from: http://www.ypeka.gr.

[6] Ministry of Environment and Energy, (2019), *Greece – National Inventory Report 2019*, in *United Nations Framework Convention on Climate Change*.

[7] Moomaw, (2011), *Renewable Energy Sources and Climate Change Mitigation: Special Report of the Intergovernmental Panel on Climate Change*, in *Renewable Energy and Climate Change*, Cambridge University Press: Cambridge.

[8] (2020), Atmospheric concentration of CO2. National Oceanic and Atmospheric Association (NOAA)

[Available from: https://www.esrl.noaa.gov/gmd/ccgg/trends/weekly.html. cited 2020 May 15]

[9] Manzella, Allansdottir, and Pellizzone, *Geothermal energy and society*. Lecture Notes in Energy.

[10] Sarbu and Sebarchievici, *Solar Heating and Cooling Systems : Fundamentals, Experiments and Applications*.

[11] (2017), International Energy Association IEA. [Available from: https://www.iea.org/. cited 2020 June 10th]

[12] (2020), European environment agency. [Available from: https://www.eea.europa.eu/. cited 2020 June 10th]

[13] Sarbu and Sebarchievici, *Solar heating and cooling systems fundamentals, experiments and applications*.

[14] Refrigereration Overview. Science Direct [Available from: https://www.sciencedirect.com. cited 2020 July 5th]

[15] Malamatenios, *Geothermal energy - Solar thermal energy*, ΓΣΕΒΒΕ – Ινστιτούτο Μικρών Επιχειρήσεων, 2014.

[16] CodeCalculation. Heat Pump. [Available from: www.codecalculation.com. cited 2020

[17] Bayer, et al. (2012) Greenhouse gas emission savings of ground source heat pump systems in Europe: A review. *Renewable and Sustainable Energy Reviews*. **16**(2): p. 1256-1267.

[18] Air source Heat Pump. [Available from: www.nialls.co.uk. cited 2020 May 1st]

[19] Barbier (2002) Geothermal energy technology and current status: An overview. *Renewable and Sustainable Energy Reviews*. **6**: p. 3-65.

[20] Arndt, *Geothermal Gradient*, in *Encyclopedia of Astrobiology*, M. Gargaud, et al., Editors., Springer Berlin Heidelberg: Berlin, Heidelberg. p. 662-662,2011

[21] CRES, *TESSe2b Training Material*, European Commission, 2018.
[22] American Society of Heating and Engineers, *ASHRAE Handbook, HVAC Applications*, American Society of Heating, Atlanta, 2015.
[23] Ground source heat pump, closed loop illustration. [Available from: https://basix.nsw.gov.au. cited 2020 April 20th]
[24] Slinky system illustration. [Available from: www.nhbcfoundation.org. cited 2020 July 10th]
[25] Chiasson, *Geothermal Heat Pump and Heat Engine Systems: Theory and Practice*, Wiley, 2016.
[26] Sebarchievici (2016) Using Ground-Source Heat Pump Systems for Heating/Cooling of Buildings. *Advances in Geothermal Energy*.
[27] Glassley, *Geothermal energy : renewable energy and the environment*. Energy and the environment, CRC Press, Boca Raton, 2010.
[28] Lund and Boyd (2016) Direct utilization of geothermal energy 2015 worldwide review. *Geothermics*. **60**: p. 66-93.
[29] Papachristou, et al., *Geothermal Energy Use, Country Update for Greece*, 2016.
[30] Andritsos, et al. (2011) Characteristics of low-enthalpy geothermal applications in Greece. *Renewable Energy*. **36**(4): p. 1298-1305.
[31] Karytsas, Polyzou, and Karytsas, *Social Aspects of Geothermal Energy in Greece*. p. 123-144,2019
[32] [Available from: https://calpak.gr. cited 2020 July 5th]
[33] Regenerative Energien für Gebäude 1, *Evacuated Tube Collector*.
[34] Kalogirou, *Solar energy engineering : processes and systems*, Elsevier/Academic Press, Burlington, MA, 2009.
[35] Tiberiu and Kreindler (2010) Design of a Solar Tracker System for PV Power Plants. *Acta Polytechnica Hungarica*. **7**.
[36] Hasan and Sumathy (2010) Photovoltaic thermal module concepts and their performance analysis: A review. *Renewable and Sustainable Energy Reviews*. **14**(7): p. 1845-1859.
[37] Prakash (1994) Transient analysis of a photovoltaic-thermal solar collector for co-generation of electricity and hot air/water. *Energy Conversion and Management*. **35**(11): p. 967-972.
[38] F.D.E Solar. [Available from: www.fdesolar.com. cited 2020 May 15th]
[39] Solar Power. European Comission. [Available from: https://ec.europa.eu/energy/topics/renewable-energy/solar-power_en. cited 2020 June 5th]
[40] EurObserv'ER. [Available from: https://www.eurobserv-er.org/. cited 2020 June 5th]
[41] (2020), Statistics of the Photovoltaic market for 2019 (In Greek). Hellenic Association Of Photovoltaic Companies HELAPCO. [Available from: https://helapco.gr/. cited 2020 July 1st]
[42] Solar resource map. Solar GIS. [Available from: https://solargis.com.
[43] Eicker, *Energy efficient buildings with solar and geothermal resources*, Wiley, Chichester, 2014.
[44] Kouremenos, Antonopoulos, and Domazakis (1985) Solar radiation correlations for the Athens, Greece, area. *Solar Energy*. **35**(3): p. 259-269.

[45] Pärisch, et al. (2014) Investigations and model validation of a ground-coupled heat pump for the combination with solar collectors. *Applied Thermal Engineering*. **62**: p. 375–381.
[46] Fang, Hu, and Liu (2010) Experimental investigation on the photovoltaic–thermal solar heat pump air-conditioning system on water-heating mode. *Experimental Thermal and Fluid Science - EXP THERM FLUID SCI*. **34**: p. 736-743.
[47] Li, Sun, and Zhang (2014) Performance investigation of a combined solar thermal heat pump heating system. *Applied Thermal Engineering*. **71**(1): p. 460-468.
[48] Calise, et al. (2016) Thermoeconomic optimization of a solar-assisted heat pump based on transient simulations and computer Design of Experiments. *Energy Conversion and Management*. **125**: p. 166-184.
[49] Ozgener and Hepbasli (2005) An Economical Analysis on a Solar Greenhouse Integrated Solar Assisted Geothermal Heat Pump System. *Journal of Energy Resources Technology*. **128**(1): p. 28-34.
[50] Ozgener and Hepbasli (2005) Exergoeconomic analysis of a solar assisted ground-source heat pump greenhouse heating system. *Applied Thermal Engineering*. **25**(10): p. 1459-1471.
[51] Franco and Fantozzi (2016) Experimental analysis of a self consumption strategy for residential building: The integration of PV system and geothermal heat pump. *Renewable Energy*. **86**: p. 1075-1085.
[52] Plytaria, et al. (2018) Energetic investigation of solar assisted heat pump underfloor heating systems with and without phase change materials. *Energy Conversion and Management*. **173**: p. 626-639.
[53] Banjac (2015) Achieving sustainable work of the heat pump with the support of an underground water tank and solar collectors. *Energy and Buildings*. **98**: p. 19-26.
[54] Thygesen and Karlsson (2013) Economic and energy analysis of three solar assisted heat pump systems in near zero energy buildings. *Energy and Buildings*. **66**: p. 77-87.
[55] Yang, Sun, and Chen (2015) Experimental investigations of the performance of a solar-ground source heat pump system operated in heating modes. *Energy and Buildings*. **89**: p. 97-111.
[56] Thorshaug Andresen and Li (2015) Modelling the Heating of the Green Energy Lab in Shanghai by the Geothermal Heat Pump Combined with the Solar Thermal Energy and Ground Energy Storage. *Energy Procedia*. **70**: p. 155-162.
[57] Bellos, et al. (2016) Energetic and financial evaluation of solar assisted heat pump space heating systems. *Energy Conversion and Management*. **120**: p. 306-319.
[58] K.EN.A.K Regulation for Energy Efficiency in Buildings. T.E.E. [Available from: http://portal.tee.gr/portal/page/portal/SCIENTIFIC_WORK/GR_ENERGEIAS/kenak. cited 2020
[59] National Land Registry of Greece. [Available from: www.ktimatologio.gr. cited 2020
[60] TRNSYS Simulation Tool. [Available from: www.trnsys.com. cited 2020
[61] PVGIS Database and Resource map. Joint Research Lab, European Union. [Available from: https://re.jrc.ec.europa.eu/pvg_tools/en/#TMY.
[62] Perez, et al., (1988), *The development and verification of the Perez diffuse radiation model*: United States.
[63] (2009), *Faethon Test Report*.
[64] Net metering legislation (In Greek). Hellenic Association Of Photovoltaic Companies HELAPCO. [Available from: www.helapco.gr. cited 2020 May 1st]

[65] Net metering example. [Available from: www.georgiasolarpros.com. cited 2020 July 25th]
[66] Florschuetz (1979) Extension of the Hottel-Whillier model to the analysis of combined photovoltaic/thermal flat plate collectors. *Solar Energy*. **22**(4): p. 361-366.
[67] DualSun Website. [Available from: www.dualsun.fr. cited 2020 May 10th]
[68] Various eshops etc. [Available from: www.bestprice.gr, www.skroutz.gr, www.e-shop.gr etc. cited 2020 August 15th]
[69] Keizer, et al., *An Overview of PVT Modules on the European Market and the Barriers and Opportunities for the Dutch Market*, 2018.
[70] Public Power Corporation in Greece. [Available from: www.dei.gr, https://www.dei.gr/Documents/xt.tim.1.7.08.pdf. cited 2020 August 20th]

7. Appendix

RESE IN RAFFREDDAMENTO
KÄLTELEISTUNGEN

COOLING CAPACITY
PUISSANCE FRIGORIFIQUE

MOD.	TEMPERATURA ACQUA USCITA CONDENSATORE °C / *CONDENSER LEAVING WATER TEMPERATURE °C* WASSERTEMPERATUR AM VERFLÜSSIGERAUSTRITT °C / *TEMPERATURE SORTIE EAU CONDENSEUR °C* (Δt in/out=5K)							
		30		**35**		40		45	
	To(°C)	**kWf**	**kWe**	**kWf**	**kWe**	**kWf**	**kWe**	**kWf**	**kWe**
182-P	5	55,6	11,5	51,4	12,8	46,9	14,2	42,0	15,7
	6	57,7	11,5	53,4	12,8	48,7	14,2	43,7	15,8
	7	59,9	11,6	**55,4**	**12,8**	50,6	14,2	45,4	15,8
	8	62,1	11,6	57,5	12,8	52,5	14,2	47,2	15,8
	9	64,4	11,6	59,6	12,8	54,5	14,2	49,0	15,8
	10	66,8	11,6	61,8	12,9	56,6	14,3	50,9	15,8
202-P	5	61,9	13,0	58,1	14,3	53,9	15,8	49,5	17,6
	6	64,3	13,0	60,2	14,3	56,0	15,9	51,4	17,6
	7	66,6	13,1	**62,5**	**14,3**	58,1	15,9	53,4	17,6
	8	69,1	13,1	64,8	14,4	60,3	15,9	55,4	17,7
	9	71,6	13,2	67,2	14,5	62,5	16,0	57,5	17,7
	10	74,1	13,2	69,6	14,5	64,8	16,0	59,7	17,7
242-P	5	71,5	15,0	66,9	16,5	62,1	18,2	57,1	20,2
	6	74,2	15,0	69,5	16,6	64,5	18,3	59,3	20,2
	7	76,9	15,1	**72,1**	**16,6**	67,0	18,3	61,6	20,3
	8	79,8	15,1	74,8	16,6	69,5	18,4	64,0	20,3
	9	82,7	15,2	77,5	16,7	72,1	18,4	66,4	20,3
	10	85,7	15,2	80,4	16,7	74,8	18,4	68,9	20,4
262-P	5	83,0	16,8	76,6	18,7	69,6	21,0	62,1	23,6
	6	86,1	16,9	79,5	18,7	72,3	21,0	64,5	23,6
	7	89,3	16,9	**82,5**	**18,7**	75,1	21,0	67,1	23,6
	8	92,6	16,9	85,6	18,8	77,9	21,0	69,7	23,6
	9	96,0	16,9	88,7	18,8	80,9	21,0	72,4	23,7
	10	99,4	16,9	92,0	18,8	83,9	21,0	75,1	23,7
302-P	5	96,5	19,7	90,2	21,8	83,6	24,2	76,8	27,1
	6	100	19,7	93,6	21,8	86,9	24,2	79,9	27,1
	7	104	19,7	**97,2**	**21,8**	90,3	24,2	83,1	27,1
	8	108	19,7	101	21,8	93,8	24,2	86,3	27,1
	9	112	19,7	105	21,8	97,3	24,2	89,7	27,1
	10	116	19,7	108	21,8	101	24,2	93,1	27,2
363-P	5	112	23,3	104	25,7	97,0	28,3	89,0	31,4
	6	116	23,4	108	25,7	101	28,4	92,5	31,4
	7	120	23,4	**112**	**25,7**	105	28,5	96,1	31,5
	8	124	23,5	117	25,9	108	28,5	99,8	31,5
	9	129	23,6	121	25,9	113	28,6	104	31,6
	10	134	23,7	125	26,0	117	28,7	107	31,7
393-P	5	131	25,5	121	28,5	110	31,8	98,2	35,6
	6	136	25,6	126	28,5	114	31,8	102	35,6
	7	141	25,6	**130**	**28,5**	119	31,8	106	35,7
	8	146	25,6	135	28,5	123	31,9	110	35,7
	9	152	25,6	140	28,5	128	31,9	114	35,7
	10	157	25,6	145	28,5	133	31,9	119	35,7
453-P	5	148	29,5	139	32,7	129	36,2	118	40,6
	6	154	29,5	144	32,7	134	36,3	123	40,6
	7	160	29,5	**149**	**32,8**	139	36,3	128	40,6
	8	166	29,5	155	32,8	144	36,3	133	40,6
	9	172	29,5	161	32,8	150	36,3	138	40,7
	10	178	29,5	167	32,8	155	36,3	143	40,7
524-P	5	171	33,7	158	37,6	143	42,1	128	47,2
	6	177	33,7	164	37,6	149	42,1	133	47,2
	7	184	33,7	**170**	**37,7**	155	42,2	138	47,2
	8	191	33,8	176	37,7	161	42,2	143	47,3
	9	198	33,8	183	37,7	167	42,2	149	47,3
	10	205	33,8	189	37,7	173	42,2	155	47,3
604-P	5	194	39,3	181	43,6	168	48,4	154	54,1
	6	201	39,4	188	43,6	175	48,4	160	54,1
	7	209	39,4	**195**	**43,7**	181	48,4	167	54,1
	8	216	39,4	203	43,7	188	48,4	173	54,2
	9	224	39,4	210	43,7	195	48,5	180	54,2
	10	232	39,4	218	43,7	203	48,5	187	54,2

kWf: Potenzialità frigorifera (kW)
kWe: Potenza assorbita (kW)
To: Temperatura acqua in uscita evaporatore (Δt ingr./usc.= 5 K)

kWf: Kälteleistung (kW);

kWf: Cooling capacity (kW)
kWe: Power input (kW)
To: Evaporator leaving water temperature (Δt in./out = 5 K)

kWf: Puissance frigorifique (kW)

RESE IN RISCALDAMENTO

HEIZLEISTUNGEN

HEATING CAPACITY

PUISSANCE CALORIFIQUE

MOD.	To (°C)	TEMPERATURA ACQUA INGRESSO/USCITA CONDENSATORE °C *CONDENSER INLET/OUTLET WATER TEMPERATURE °C* WASSERTEMPERATUR AM VERFLÜSSIGEREIN-AUSTRITT °C *TEMPERATURE DE L'EAU ENTRÉE/SORTIE AU CONDENSEUR °C*					
		30/35		35/40		**40/45**	
		kWt	kWe	kWt	kWe	kWt	kWe
182-P	8	81,9	14,6	74,8	16,2	67,2	18,0
	9	84,9	14,6	77,6	16,2	69,8	18,0
	10	88,1	14,6	80,5	16,2	**72,5**	**18,0**
	11	91,3	14,7	83,5	16,2	75,3	18,0
	12	94,6	14,7	86,6	16,3	78,1	18,0
	13	98,0	14,7	89,8	16,3	81,0	18,1
202-P	8	87,0	16,3	80,9	18,0	74,4	19,9
	9	90,1	16,4	83,9	18,0	77,2	20,0
	10	93,4	16,4	87,0	18,1	**80,1**	**20,0**
	11	96,8	16,5	90,1	18,1	83,1	20,0
	12	100	16,5	93,4	18,2	86,1	20,1
	13	104	16,6	96,7	18,2	89,3	20,1
242-P	8	101	19,0	94,2	20,9	86,6	23,1
	9	105	19,0	97,7	21,0	89,9	23,2
	10	109	19,1	101	21,0	**93,3**	**23,2**
	11	113	19,1	105	21,0	96,8	23,2
	12	117	19,2	109	21,1	100	23,3
	13	121	19,2	113	21,1	104	23,3
262-P	8	120	20,5	109	22,8	97,4	25,7
	9	124	20,5	113	22,9	101	25,7
	10	129	20,5	117	22,9	**105**	**25,7**
	11	133	20,6	122	22,9	109	25,7
	12	138	20,6	126	22,9	113	25,7
	13	143	20,6	131	22,9	117	25,7
302-P	8	131	23,2	122	25,8	112	28,8
	9	136	23,3	126	25,8	117	28,8
	10	141	23,3	131	25,8	**121**	**28,8**
	11	146	23,3	136	25,8	126	28,8
	12	151	23,3	141	25,8	130	28,8
	13	157	23,3	146	25,8	135	28,8
363-P	8	152	27,1	141	29,9	130	33,1
	9	158	27,2	147	30,0	135	33,1
	10	163	27,3	152	30,0	**140**	**33,2**
	11	169	27,3	158	30,1	145	33,3
	12	175	27,4	163	30,2	151	33,3
	13	182	27,5	169	30,2	156	33,4
393-P	8	181	30,7	165	34,2	148	38,4
	9	188	30,7	171	34,3	153	38,4
	10	195	30,7	178	34,3	**159**	**38,4**
	11	202	30,7	184	34,3	165	38,4
	12	209	30,7	191	34,3	171	38,4
	13	216	30,8	198	34,4	178	38,5
453-P	8	195	34,5	181	38,2	167	42,6
	9	202	34,5	188	38,2	173	42,7
	10	210	34,5	195	38,3	**180**	**42,7**
	11	217	34,5	202	38,3	187	42,7
	12	225	34,5	210	38,3	194	42,7
	13	233	34,5	218	38,3	201	42,7
524-P	8	234	41,3	213	46,2	190	51,6
	9	242	41,3	221	46,2	197	51,7
	10	251	41,3	229	46,2	**205**	**51,7**
	11	260	41,4	237	46,2	213	51,7
	12	270	41,4	246	46,3	221	51,7
	13	279	41,4	255	46,3	229	51,8
604-P	8	257	45,8	239	50,7	220	56,6
	9	266	45,8	248	50,7	228	56,7
	10	276	45,8	257	50,8	**237**	**56,7**
	11	286	45,8	267	50,8	246	56,7
	12	297	45,8	276	50,8	255	56,7
	13	307	45,8	287	50,8	265	56,8

To : Temp. acqua in uscita evaporatore (Δt ingresso/uscita = 5 K)
kWt : Potenzialità termica (kW)
kWe : Potenza assorbita (kW)

To : Wassertemperatur am Verdampferaustritt (Δt Ein/Austritt = 5 K)
kWt : Heizleistung (kW)
kWe : Leistungsaufnahme (kW)

To :Evaporator leaving water temperature (Δt in/out = 5 K)
kWt : Heating capacity (kW)
kWe : Power input (kW)

To : Temperature sortie eau èvaporateur (Δt in/out = 5 K)

Α.2.5 ΚΑΜΠΥΛΗ ΣΤΙΓΜΙΑΙΑΣ ΑΠΟΔΟΣΗΣ, βασιζόμενη στην ολική επιφάνεια και στην μέση θερμοκρασία του ρευστού μεταφοράς θερμότητας.

INSTANTANEOUS EFFICIENCY CURVE, based on gross area and mean temperature of heat transfer fluid.

Α.2.5.1 Εξίσωση γραμμική / Lineal fit to data

Η στιγμιαία απόδοση ορίζεται από τη σχέση / ***The instantaneous efficiency*** η ***is defined by*** :

$$\overline{\eta}_G = \hat{Q} / (A_G\, G)$$

Συνολική επιφάνεια που χρησιμοποιείται για την καμπύλη: ..... 1.99 m^2
Gross area used for curve

Παροχή ρευστού που χρησιμοποιήθηκε στις δοκιμές: .....0.039 kg/s
Fluid flowrate used for the tests

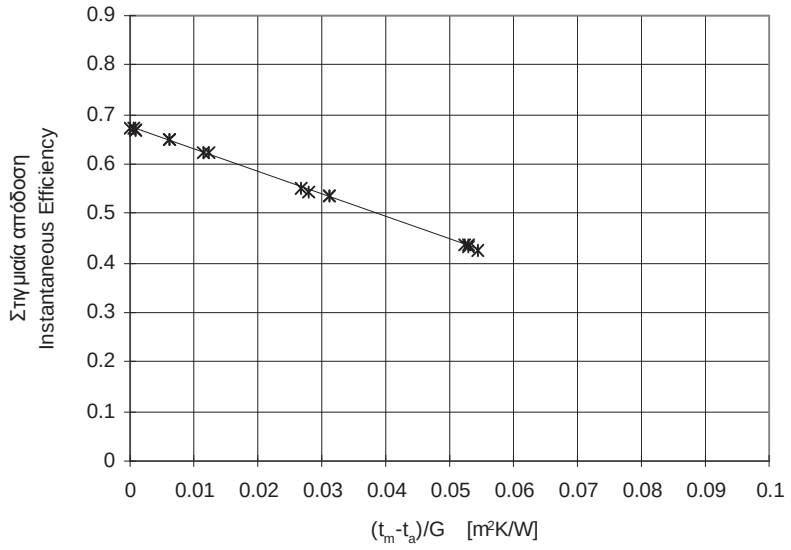

Εξίσωση γραμμική: $\overline{\eta}_G = \overline{\eta}_{0G} - \overline{U}_G \dfrac{t_m - t_a}{G}$

Linear fit to data:

$\overline{\eta}_{0G}$ **= **0.67

$\overline{U}_G$ **=.....** 4.54 W/(m^2 K)

TECHNICAL DATA

GENERAL DATA		
Length	1650 mm	
Width	991 mm	
Frame width	35 mm	
Frame color / Backsheet	Black / Black	
Maximum load	5400 Pa (snow) / 2400 Pa (wind)	
	Spring NI*	Spring I*
Weight empty / filled	24,3 / 29,3 kg	25,1 / 30,1 kg

* NI = Non-Insulated, I = Insulated

PHOTOVOLTAIC DATA		
Number of cells per module	60	
Cell type	PERC Monocrystalline	
Nominal power (P_{mpp})	300 Wp	310 Wp
Module efficiency	18,3 %	19,1 %
Rated voltage (V_{mpp})	32,6 V	33,2 V
Rated current (I_{mpp})	9,19 A	9,31 A
Open circuit voltage (V_{oc})	39,9 V	40,3 V
Short circuit current (I_{sc})	9,77 A	9,88 A
Power output tolerance	0 / +5W	
Maximum system voltage	1000 V DC	
Reverse current load	20 A	
NOCT	45 ± 2°C	
Connectors	MC4 / MC4 compatible	
Application class	Classe II	
Voltage temperature coefficient (μV_{oc})	-0,29 %/°C	
Current temperature coefficient (μI_{sc})	0,05 %/°C	
Power temperature coefficient (μP_{mpp})	-0,39 %/°C	

Power measurement tolerance : +/- 3%

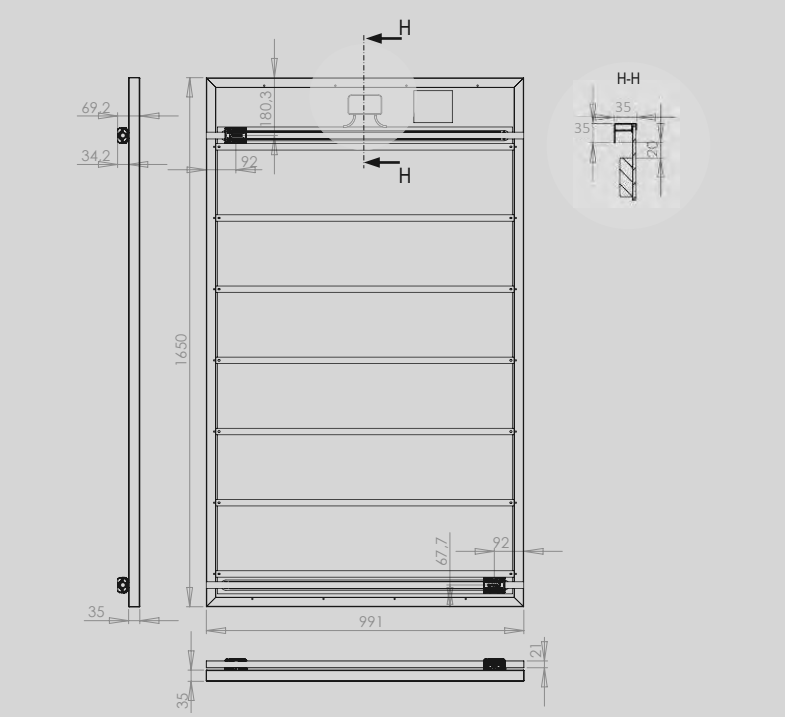

Non-insulated version of the Spring panel with DN15 DualQuickfit® fitting

THERMAL DATA			
Gross area	1,635 m²		
Volume of heat transfer liquid	5 L		
Maximum operating pressure	1,5 bar		
Pressure loss per panel (Pa | *mmWS*)	Portrait	Landscape	
	59 | 6	167 | 17	at 32 L/h
	461 | 47	961 | 98	at 100 L/h
Hydraulic input/output	DualQuickfit® fittings		
	Non-Insulated	Insulated	
Maximum temperature	70 °C	75,6 °C	
Optical efficiency a_0	58,9 % *	58,2 % *	
Heat loss coefficient a_1	16,0 W/K/m² *	10,8 W/K/m² *	
Heat loss coefficient a_2	0 W/(m²,K²) *		

* The a_0, a_1 et a_2 coefficients are the measured values from testing during EN 9806:2017 certification at KIWA for unglazed collectors with a **windspeed u = 1m/s : $a_0 = n_0 - c_6{}^*u'$; $a_1 = c_1 + c_3{}^*u'$; $u' = u - 3$.**

Power output as a function of the temperature of the water in the panel (by application)

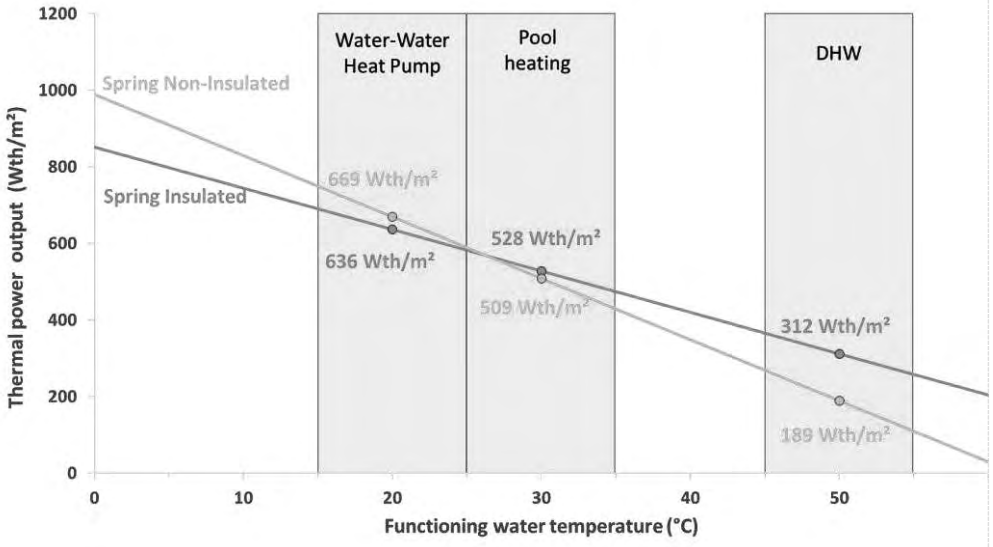

Power values are calculated using a0 and a1 coefficients (windspeed=1m/s) in STC conditions (Text = 25°C, G = 1000 W/m²)